MASTER THESIS

Reconstructed 3D-models of the digestive organs of ballan wrasse (*Labrus bergylta)* during ontogeny

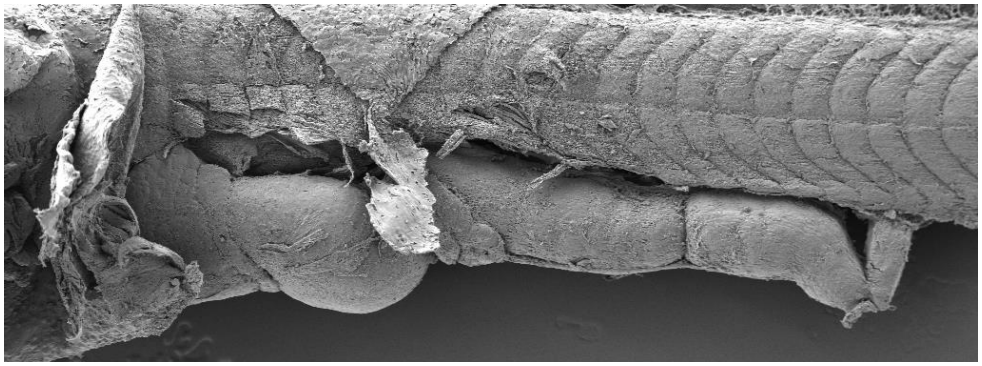

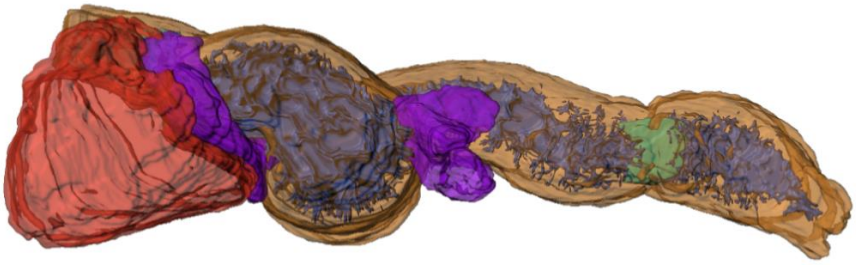

For the fulfillment of Master of Science in Developmental Biology and Physiology

Sissel Norland

Department of Biology

University of Bergen, Norway

August 2017

Front page: Ballan wrasse larvae (Stage 3; 18 days post hatching). Upper: Scanning electron micrograph of the left side of outer surface of the digestive system and urinary bladder. Lower: 3D reconstruction of the digestive system including the outer surface (serosa and adventitia, *transparent orange*), liver (*transparent red*), exocrine pancreas (*transparent purple*), intestinal lumen (*blue*) and valve between midgut and hindgut (*turquoise*).

ACKNOWLEDGEMENT

First, I would like to thank my supervisor Professor Ivar Rønnestad at Marine Developmental Biology group at the University of Bergen. I really appreciate this opportunity given to me to work with fish anatomy and physiology, and the fascinating ballan wrasse in a very interesting project. Thank you for all the support, insights and feedbacks throughout the whole process. A big thank you goes to all the staff at Marine Developmental Biology group for making the days very enjoyable, and support through this process. Especially Nina Ellingsen and Teresa Cieplinska for excellent help with the lab work and methodical discussions and Prof Emeritus Harald Kryvi for help with dissections of my larva, sharing his knowledge of histology and the insightful discussions together with Hege Hellberg (FishVet group).

This study is part of a larger project on ballan wrasse- no Guts no Glory. Thank you, Dr. Øystein Sæle at NIFES for helping me at the first sampling of larvae, and providing many useful insights during this process together with Hoang Le. The samplings were done at Marine Harvest Labrus. Thank you for the cooperation, especially Anette Lekva for letting me sample fish larva and answering all my questions!

Critical point-drying and sputter-coating with gold-paladium (Au/Pd) was performed by Irene Heggstad (Elektronmikroskopisk felleslaboratorium, University of Bergen). Thank you for all the help preparing the samples for scanning electron microscopy and teaching me to use the microscope along with Egil S. Erichsen. Thank you to Erik Von Stedingk in the support team at Bitplane for the answering all of my questions regarding Autoaligner and Imaris.

Lastly, I would like to thank my fellow students for five amazing years, my friends and my family for your support and belief in me. And Alex, this would never be possible without you. Thank you for your patience and all the support!

TABLE OF CONTENT

ABSTRACT

This study describe the ontogeny of the digestive tract and it's associated glands of ballan wrasse at six reference stages from yolk sac larva (Stage 1; 4 DPH) until juvenile phase (Stage 6; 102 DPH). Reconstructed 3D-models based on histological sections were made by Imaris 3D rendering software. Statistical data from the 3D-models were retrieved to study morphometric scaling of the digestive organs and relate the scaling to functional capacity of digestion and processing. Finally, the data were used to explore morphological and histological evidence for the possible presence of an intestinal bulb in the proximal midgut in the agastric ballan wrasse.

At Stage 1; 4 DPH the larva had a straight incipient gut located dorsally for the yolk sac along with liver, gallbladder and exocrine pancreas containing few zymogen granules, demonstrating a functional digestive system ready for onset of exogenous feeding. All organs had a strong growth in both surface areas and volumes until Stage 2; 10 DPH. At this stage, an intestinal bulb was observed as an expansion in diameter in the proximal midgut. In addition, there were folding of the intestinal epithelium (villi) and a valve between distal midgut and hindgut was clearly differentiated, as was an endocrine pancreas. The beginning of intestinal rotation (into one loop) were seen at Stage 3; 18 DPH. At this stage, the exocrine pancreas had become more scattered. The ducts from the gallbladder and exocrine pancreas terminated in the anterior part of the bulbus. The bulbus may increase the residence time of ingested food in this segment and thus increase the efficiency of mixing feed with bile and pancreatic secretions. As the larvae grew (Stages 4 to 6; 29-102 DPH), the intestinal bulb persisted only as a slight enlargement of the proximal midgut. The intestinal villi became larger concurrent with elongated liver and formation of hepatopancreas from Stage 5; 71 DPH. The digestive tract of this agastric fish did not show consistent evidence of a functional bulbus with presence of a distinct narrowing of the luminal diameter with an increased muscle layer at the end of the bulbus.

The morphometric scaling demonstrated allometric growth of the digestive organs. The relative volume (mass) of gut tissue decreased compared to the other organs during ontogeny; gut tissue declined from 79% to 62%, liver and exocrine pancreas increased from 21% to 38 from Stage 1 to 6. During this time, intestinal mucosal surface area-to-volume ratio decreased from 0.33 (incipient, straight intestine) to 0.02 μm^{-1}(highly folded). The relative increase in growth of the

liver and exocrine pancreas indicate an increased digestive capacity by pancreatic secretions and capacity for post-prandial metabolism by the liver.

The specific growth rate of the endocrine pancreas was higher compared to the other tissues and organs; 16.94% day^{-1} for endocrine pancreas, 6.18-7.12% day^{-1} for gut tissue, liver and exocrine pancreas, respectively. This may suggest an altered capacity for postabsorptive hormonal and metabolic handling of absorbed nutrients as the ballan wrasse goes through ontogeny.

1. INTRODUCTION

1.1 Sea lice issue opens up for the use of host-cleaner fish symbiosis

Research on the ballan wrasse (*Labrus bergylta*) has been the subject of growing interest over the last few years, due to the use of wrasses (*Labridae*) in the Atlantic salmon (*Salmo salar*) farming industry as an aid to reducing fish disease caused by salmon lice (*Lepeophtheirus salmonis*) in open sea cages (Bjordal, 1991). The salmon louse is a host-specific, marine, crustacean ectoparasite on salmonids such as the Atlantic salmon, sea trout (*Salmo trutta*), rainbow trout (*Oncorhynchus mykiss*) and Arctic char *(Salvelinus alpinus*) (Boxaspen, 2009, Costello, 2009, Skiftesvik et al., 2013). Sea lice have been a growing problem from the pioneering days of fish farming in Norway since the mid-1970s, and are currently one of the most serious problems for the industry, with immense economic cost to producers (Costello, 2006, Ottesen et al., 2008, Boxaspen, 2009, Hamre and Sæle, 2011). The UN Fisheries and Agriculture Organization reported in 2008 an economic loss due to sea lice in the salmonid aquaculture industry of 305 million euros worldwide, of which 131 million euros in Norway alone (Costello, 2009). The total costs in Norway is estimated to increase to over 532 million euros in 2017 (Barstad, 2017).

Sea lice infections involve various complications (Wagner et al., 2008). The louse attaches to the host and feeds on its mucus and skin, leaving the wounded tissue at risk of necrosis and vulnerable to secondary infections by bacteria and fungi. The louse also feeds on the host's blood and increases the likelihood of the host becoming anemic. An infected salmon displays elevated levels of stress in terms of behavioral changes and other physiological symptoms, such as elevated plasma levels of catecholamines, the stress hormone cortisol and elevated plasma glucose levels (primary and secondary stress responses). Tertiary responses to stress causes osmoregulatory problems, reduced immune response to bacterial infections, inhibited growth, reduced swimming performance, reduced reproductive success and at worst, death of the fish (Costello, 2006, Iwama et al., 2006, Wagner et al., 2008).

The number of sea lice infections rose with the spread of salmon farming, which represent a strong host abundance within a small area, which is an optimal setting for lice expansion (Heuch et al., 2005). Thus, the fish farms need to keep the level of sea lice to a minimum due to animal welfare regulations, and to minimise the spread of sea lice to wild populations. Several established and emerging approaches are used to combat the sea lice problem in salmon

farming, whereas some of them causes significant stress to the fish, with elevated post-treatment mortality. The chemicals that have been the prevalent method for many years have a significant effect on the immediate environment of the cages, and may also have an impact on farm employees' health. In addition, sea lice have been shown to rapidly develop resistance to chemical delousing medications such as organophosphates and pyrethroids, thus stronger chemical treatments are continuously needed. Other methods for coping with sea louse include the use of hydrogen peroxidase, lice skirts, lasers, the use of functional fish feed to prevent the sea lice from infesting the host and mechanical removal by spraying the salmon in temperate or saline water (Costello, 1993, Boxaspen, 2009, Barstad, 2017, Hjeltnes et al., 2017). In contrast to several of the methods described above, the use of cohabiting cleaner fish has been introduced as a natural way of delousing farmed salmon.

Several species display cleaner fish behavior in systems with farmed Atlantic salmon. The ballan wrasse together with other species of wrasse (goldsinny wrasse *Ctenolabrus rupestris*, corkwing wrasse *Symphodus melops* and rock cook *Centrolabrus exoletus*), and the lumpfish (*Cyclopterus lumpus*) are important contributors to reducing sea lice infections either alone or in combination with chemical treatment (Bjordal, 1988, 1991, Ottesen et al., 2008, Skiftesvik et al., 2013).

Norwegian fish farms produces 214 million salmonid smolts in 2006, and by 2015 this number had increased to 312 million, while 682 000 wild and farmed cleaner fish were set out in salmonid cages in 2006, which increased to 26.4 million fish in 2015 (Fiskeridirektoratet, 2017a, 2017b, Hjeltnes et al., 2017). To avoid overfishing of wild wrasse populations, and to provide for the increasing demands for wrasse in the salmon industry, attempts to farm wrasses started in the late 1980s (Costello, 2006, Hamre et al., 2013, Skiftesvik et al., 2013). The Institute of Marine Research (IMR) research station at Austevoll outside Bergen, Norway started wrasse farming trials and studied their cleaning symbiosis with salmon (Bjordal, 1988, 1991, 1992). Marine Harvest Labrus started large-scale production of ballan wrasse in 2009 (Espeland et al., 2010). Today, ballan wrasse are an important tool for dealing with salmon louse infections in the Norwegian aquaculture industry.

Ballan wrasse is the largest of the wrasses that occur on the Norwegian coast, and Skiftesvik et al. (2013) concluded that this species was, overall, the most suitable cleaner fish. As an efficient and robust delouser, they have become the most valuable of the wrasse species used in aquaculture, and only lumpfish are more widely used in the sea cages due to their preference

for lower water temperatures (Skiftesvik and Bjelland, 2003, Espeland et al., 2010, Skiftesvik et al., 2013, Fiskeridirektoratet, 2017b). The production of ballan wrasse starts by inducing spawning in wild-caught adults by means of light and temperature manipulation. The fertilized eggs are collected and reared through the larval and juvenile stages in indoor tanks until the age of about 12 months, when they are released into the salmon cages. Today, cages for on-growing salmon are often large sea cages with a circumference of 120-140 m. These appear to work well for co-culture of salmon and cleaner fish. The most successful results in keeping down the number of lice has been seen when the cages are stocked with 1-5% wrasse (species- and size-dependent) compared to the salmon stock (Fiskeridirektoratet and Mattilsynet, 2010, Lusedata, 2017).

Commercial production of wrasse is relatively new, and knowledge of several key aspects of their feeding biology is limited. Fish farmers therefore utilised information from Atlantic cod aquaculture in the start-up phase, with some success but also some technical and biological problems such as low growth rate and high mortality (Hamre et al., 2013). Since wrasse are reared to be released into the sea cages, most research on nutritional physiology and digestion has targeted the early stages, from first feeding through weaning with formulated feed as the first bottleneck in the production. However, rearing juveniles from 0.5 g to 25-50 g body weight, when they are typically released into the sea cages also tends to be difficult (Kousoulaki et al., 2015, Øie et al., 2017).

There is a lack of knowledge about the nutritional requirements, feeding behavior and digestive system of wrasse larvae (Hamre and Sæle, 2011, Hamre et al., 2013, Rønnestad et al., 2013). All wrasses lack stomach and pyloric caeca, and have a very short intestine though the larval and adult life stage. Both the live and formulated feeds and feeding protocols needs to be optimized and adapted to the wrasse at different developmental stages. It is thus essential to describe and understand the digestive function and processing capacity of the digestive system, and how it change during development. This includes providing a description of the morphology of the developing digestive tract and its associated organs from larva to the juvenile phase.

1.2. Life history of wild ballan wrasse

1.2.1 Life cycle from adult to larvae

The ballan wrasse is a marine fish that lives in the Atlantic along the coastline from Morocco to Trondheimsfjorden in mid-Norway (Espeland et al., 2010, Froese and Pauly, 2017). Species characteristics include large lips, marbling pattern on the operculum, large scales**,** and highly coloured pigmentation. There are two different morphotypes based on skin colour; red spotted and plain green colour (**Figure 1.1**). This may represent genetic differences and different life strategies within the species, rather than being sex-related as in the hermaphroditic cuckoo wrasse (*Labrus mixtus*) (Almada et al., 2016, Quintela et al., 2016). Spotted individuals display a higher investment in somatic growth (length-weight ratio, age-at-size, otolith size, weight and total length) compared to non-spotted individuals (Villegas-Rios et al., 2013). As a protogynous hermaphrodite, the fish start their life as females and transform into males around the age of 6-10 years (Skiftesvik and Bjelland, 2003, Froese and Pauly, 2017). Ballan wrasse are found inshore in the temperate littoral zones, where they can feed and spawn (Artüz, 2005). It is a carnivorous species whose diet consists mainly of molluscs, crustaceans, gastropods and echinoderms (Dipper et al., 1977, Figueiredo et al., 2005).

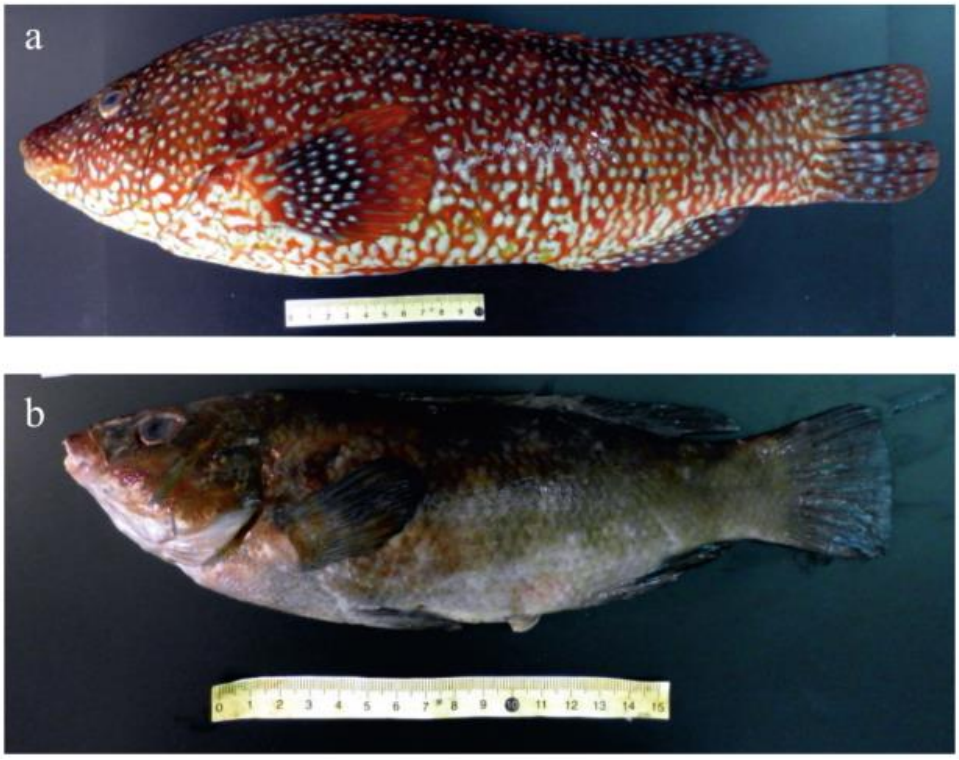

Figure 1.1: Ballan wrasse morphotypes as (a) red spotted and (b) plain with variable green color. Retrieved from Quintela *et al.*, 2016.

During spawning from June to July, the dominant males display aggressive territorial behaviour over a harem of females. The females build nests of algae and lay eggs around 1 mm in diameter (Artüz, 2005, Ottesen et al., 2012) that are fertilized by the male. The eggs are sticky and demersal. The male shows paternal care by guarding the nest until the eggs hatch, after which they move to new harems and repeat the spawning ritual (Espeland et al., 2010). For all teleosts that are ectotherm conformers, the embryonic developmental rate, including time of hatching, is temperature-dependent (Hunter, 1981). The zygote goes through cleavage (becoming an embryo), blastula period, gastrulation with germ ring migration and segmentation before the larvae hatches at 74.0 ± 12.4 degree days (mean ± S.D;˚C day) (Darwall et al., 1992, Dunaevskaya, 2010, D'Arcy et al., 2012).

Like many marine fish larvae living in temperate waters, the ballan wrasse larvae hatch when they are relatively small compared to the freshwater species (Osse and van den Boogaart, 1995, Falk-Petersen, 2005). A larva at hatching is 2.7 to 3.6 mm in length (Artüz, 2005, Dunaevskaya, 2010). The larvae rely entirely on the nutrition stored in the yolk-sac until it starts exogenous feeding. From the onset of first feeding and until metamorphosis, the larvae feed mainly on zooplankton and larval feeding success increases gradually over time (Darwall et al., 1992, Hunter, 1981).

1.2.2 Systematization of larval development

When describing the development of fish larvae, and particularly when describing a wide range of functional attributes, there is a challenge related to the age and length of the fish. Length alone is a poor characterization of larval development, since larvae display allometric growth (Heath, 1992). It is very common to refer to the age of the fish in terms of days post fertilization or days post hatching (DPH). However, since developmental rates depends strongly on the temperature, several authors prefer the use of day degrees, species-specific temperature coefficient (Q_{10}) (Fuiman et al., 1998) or temperature optimum (Rombough, 1997, Otterlei et al., 1999). An alternative is to class larval development into stages, with detailed description of the morphology and with additional characteristics such as size, bone development, cranial ossification and myotome height (Sæle and Pittman, 2010).

No published classification of the larval development into defined ontogenetic stages for the ballan wrasse is currently available, as in Atlantic cod and Atlantic halibut (Sæle et al., 2004,

Sæle et al., 2017). A preliminary categorization for ballan wrasse that is correlated to standard length (**Table 1.1)** has been suggested by Ottesen *et al*., (2012).

Table 1.1 Main developmental stages in ballan wrasse larvae. Modified from Ottesen et al. (2012) for Stages 1-4.

Stage	Developmental stage	DPH	SL (mm, mean ± S.D.)
1	Yolk sac larva	0-9	4.28 ± 0.11
2	Preflexion larva	10-25	5.35 ± 0.30
3	Flexion larva	26-33	5.90 ± 0.78
4	Postflexion larva	34-49	10.52 ± 0.82

The yolk-sac larvae (**Stage 1**) lasts from 0-9 days post-hatching (DPH). The larvae are dependent on endogenous feeding (lecitotrophic) until the larvae are lecitoexotrophic from 7-9 DPH (Dunaevskaya, 2012). The larval body is transparent with some pigments (melanophores). The preflexion larva (**Stage 2**) is characterized by being fully dependent on exogenous feeding, the start of inflation of the swim bladder, caudal fin ray anlagen and a heavily pigmented body (Ottesen et al., 2012). Flexion larve (**Stage 3**) display an upwardly inclined urostyle, incipient rays in the anal fin, partly resorbed primordial fin fold, partly defined dorsal fin from the caudal fin and small pelvic fins. Postflexion larvae (**Stage 4**) have separated fins with fin rays and a fully pigmented body except from the urostyle.

Artüz (2005) described the ontogeny of ballan wrasse, but without any classification into developmental stages. He described a post-larval individual (17.8 mm SL) that resembled an adult. The body was pigmented, but with sparse pigmentation in the abdomen and with an unpigmented urostyle. Juvenile (19.1 mm SL) had adult-shaped lips and fins and separated dorsal fin rays (Artüz, 2005). The end of metamorphosis in ballan wrasse (15-17 mm SL) takes place when the juvenile body is fully pigmented. The vertebrae and scales are ossified, the hepatopancreas is present and the general growth pattern goes from allometric to isometric and larval characteristics are completely replaced for an adult appearance (Osse and van den Boogaart, 1995, Dunaevskaya, 2010, Gagnat et al., 2016).

Ø. Sæle (Nifes, Bergen, Norway, pers. comm.) has suggested a new, extended classification of ballan wrasse development from Stage 1 yolk sac larvae until Stage 6 juvenile stage. The

present study will further support this classification system to include the development of the digestive system for Stages 1-6.

1.3 Development of the digestive system

The ontogeny of the digestive system of the ballan wrasse follow the general pattern of teleost larvae (Kjørsvik et al., 1991, Gisbert et al., 2004, Falk-Petersen, 2005, Sala et al., 2005, Kamisaka and Rønnestad, 2011, Gomes et al., 2014b), but with species-specific characteristics and adaptations in morphology and physiology. The digestive tract develops from an epithelial tract originating from the endoderm during embryonic development. The anterior end of the digestive tract gives rise to primordial buds, which develop into the associated digestive glands (pancreas, liver and gallbladder). The embryo develops the three germ layers ectoderm, mesoderm and endoderm during the gastrulation period, when the germ ring becomes established. This consists of two layers; the outer epiblast (future ectoderm) and inner hypoblast, giving rise to the mesoderm and endoderm (Gilbert, 2014).

The endodermal progenitor cells that gives rise to the digestive tract involute to form an epithelial tube that is surrounded by mesenchymal cells derived from the lateral plate mesoderm (Wallace and Pack, 2003, Wallace et al., 2005, Gilbert, 2014). Like most other marine fish species, a hatched ballan wrasse larva has an incipient gut located dorsally to the yolk-sac, and the mouth and anus are closed (Govoni et al., 1986, Falk-Petersen, 2005, Zambonino Infante et al., 2008, Dunaevskaya, 2010).

Prior to the onset of exogenous feeding and throughout the larval period and juvenile metamorphosis, the digestive system goes through large morphological and possibly significant physiological changes (Krogdahl, 2001, Wallace et al., 2005, Yúfera and Darías, 2007b, Zambonino Infante et al., 2008, Rønnestad et al., 2013). The incipient gut of a fish larva becomes segmented into foregut that will become the future esophagus (and stomach if present), midgut (future proximal, middle and distal midgut) and hindgut, typically with a valve separating the midgut and hindgut, ending with the rectal valve, and importantly, the opening of mouth and anus (Govoni et al., 1986, Rønnestad et al., 2003). The digestive tract becomes histologically divided into layers (*tunicae*) comprising of the *mucosa, submucosa, muscularis externa* and *serosa* (*serosa* is sometimes referred to *adventitia* when outside the abdominal

cavity i.e. the esophagus). Goblet cells appear in the esophagus, and intestinal diameter increases and becomes more folded, although there might be some remnant of the yolk (Kamisaka et al., 2003, Falk-Petersen, 2005, Zambonino Infante et al., 2008).

The incipient gut of ballan wrasse larvae differentiates into esophagus, midgut and hindgut separated by a valve (Dunaevskaya, 2010, Gagnat, 2012). The intestine of a larva that have started exogenous feeding is modified with villi, the midgut holds no goblet cells and is separated from the hindgut with cells supranuclear vesicles (Dunaevskaya, 2010, Gagnat et al., 2016). The intestine develops from being a straight tube into a curled tube with one loop (Gagnat, 2012, Krogdahl et al., 2014, Gagnat et al., 2016).

Endodermal progenitor cells of the digestive tract give rise to the pancreas, liver, and gallbladder, as well as swim bladder and thymus and even the lungs in terrestrial vertebrates (Smith et al., 2000, Wallace and Pack, 2003, Ng et al., 2005, Gilbert, 2014). Therefore, there is a conserved pattern of the development of the digestive organs throughout vertebrate evolution (Smith et al., 2000). Liver, gallbladder and the exocrine pancreas (and the endocrine pancreas in some larvae) are present in the ballan wrasse larvae at 4 DPH (Gagnat, 2012, Gagnat et al., 2016). These organs are functional at the onset of exogenous feeding and continues to growth in size throughout the development (Yúfera and Darías, 2007b, Gagnat, 2012, Gagnat et al., 2016).

The pancreas is a unique gland that comprises both endocrine and exocrine cells. In healthy humans, there is a ratio of less than 5% endocrine and 95% exocrine cells (Das et al., 2014), which may be hypothesised to be similar in a healthy developing fish larva. The "classic" model of pancreatic organogenesis in fish is where pancreas develops from an endodermal origin where the digestive tract forms buds in the anterior midgut; two buds in zebrafish, *Danio rerio* (Field et al., 2003a), three buds in medaka *Oryzias latipes* (Assouline et al., 2002). These buds merge to form a solid, tubuloalveolar pancreas (Yee et al., 2005). The exocrine pancreas produces digestive enzymes and bicarbonate. Some bicarbonate production also occurs in the intestinal epithelium (Wilson et al., 2002).

During the organogenesis of the pancreas, one specific bud gives rise to the endocrine pancreatic cells (Islam, 2010, Kryvi and Poppe, 2016), while the other bud(s) give rise to the acinar- and centroacinar cells of the exocrine pancreas, and the network of duct systems draining into the pancreatic duct (*ductus pancreaticus*) (Field et al., 2003a). Functional

endocrine cells are scattered among exocrine alveoles as Islets of Langerhans or packed into one cluster of cells; Brockmans body (Kryvi and Poppe, 2016). The pancreatic duct drains into the proximal midgut together with the bile duct (*ductus choledochus*) with a sphincter system (Gartner and Hiatt, 2007). The exocrine pancreatic tissue with islets of Langerhans in 4 DPH ballan wrasse larvae is initially a compact organ located posterior to the liver, but becomes scattered along the abdominal cavity, while small pockets of exocrine pancreas have been observed within the liver tissue; hepatopancreas at 55 DPH (Gagnat et al., 2016).

The liver is a large organ located anteriorly in the fish abdomen. An outgrowth from the anterior midgut endoderm gives rise to the hepatocytes and the hepatic duct (*ductus hepaticus)*. The liver develops through a primary budding stage (from the endodermal anlagen to a duct-form) and goes through a second growth stage to increase the size (Field et al., 2003b) while a part of the anlagen develops into the gallbladder (Gilbert, 2014). The hepatocytes are organized into tubules with bile capillaries (*bile canaliculi*). The intracellular space within the hepatocytes consists of fat deposits in vacuoles and the granular endoplasmatic reticulum. The amount of fat vacuoles varies with age, sex, nutritional status and species. For example, Atlantic salmon have low-fat livers, while Atlantic cod have fatty livers with large fat deposits in the hepatocytes (Kryvi and Poppe, 2016).

Bile produced in the liver is transported by the common hepatic duct *ductus hepaticus* into the cystic duct *ductus cysticus,* ending in the gallbladder, where it is stored until use. The gallbladder is sack-like in form, often irregular shape with some trabecula (Kryvi and Poppe, 2016). Trabecula are irregular growths in the wall of the gallbladder, creating pockets of various sizes; they can increase the surface area, perhaps helping to concentrate the bile (H. Kryvi, University of Bergen, Norway, *pers.comm.*). The gallbladder empties the bile through the *ductus cysticus* into the common bile duct *ductus choledochus* that ends in the lumen of the proximal midgut next to the pancreatic duct.

The liver of 3 DPH ballan wrasse larvae, if present, is undeveloped and matures at the start of exogenous feeding. The hepatocytes show low levels of vesicles containing accumulated glycogen, rough endoplasmatic reticulum (ER) and mitochondria (Romundstad, 2015). The gallbladder is present in 4 DPH larva and located between the liver and the pancreas (Gagnat, 2012).

1.4. Growth pattern and digestion

1.4.1 Comparative growth patterns of digestive organs

A growing larva will prioritise development of the most important organs first, although growth and shape-change are often associated with the evolution (Zelditch et al., 2012). The development is not continuous, but is rather a periodised process. Isometric growth means that there is an increased size, but the shape remains unchanged. Fish ontogeny includes periods of allometric growth, when the different organs and organ systems develop at different rates. For example, the head and tail regions of fish larvae develop first, which is advantageous for feeding, locomotion and escaping (Osse and van den Boogaart, 1995, Yúfera and Darías, 2007b).

Data on allometric growth patterns and the morphometric scaling of organs and tissues can help provide useful information about the biology of larval development and physiology. The volume and area of organs are interspecific and display ontogenetic variations. Several allometric studies have been performed on outer morphology (see Osse and van den Boogart (1995) and Gagnat et al., (2016) for further reviews), but few studies have focused on the internal organs of the larvae.

It has been suggested that the differentiation and strong growth of the digestive system are crucial to enabling digestion to support nutritional and metabolic requirements (Yúfera and Darías, 2007b). Growth of the digestive organs in the common dentex, *Dentex dentex* and turbot, *Psetta maxima* shows strong positive allometric growth before the larvae become completely dependent on exogenous feeding. Growth in older larvae indicates a trend towards isometric growth of the digestive tract and the liver, and even negative allometric growth for the pancreas (Sala et al., 2005). Gagnat et al., (2016) observed a similar pattern in their study of the growth of different organs in ballan wrasse larvae from hatching until 60 DPH. Their data suggested that the digestive tract, pancreas and liver, all displayed positive allometric growth until a change in growth pattern into negative allometric growth took place around 6.0 mm SL (Gagnat et al., 2016). Positive allometric growth of the digestive tract, pancreas and skeletal muscles has also been shown in carp (*Cyprinus caprio*) (Alami-Durante, 1990).

1.4.2 Digestive capacity

The high growth rate of fish larvae requires a high rate of ingested proteins and lipids, and smaller amounts of other nutrients including minerals and micronutrients. Hamre and colleagues (2013) attempted to establish basic guidelines for the composition of macronutrients in formulated feed for juvenile ballan wrasse. Their study showed that a diet ratio of 10-12 % lipids, 12.5-16.0 % carbohydrates and 65-70 % proteins resulted in the best growth rate (in weight and length) in the juveniles. The bioavailability depends on the efficiency of digestion and absorption of dietary nutrients. The digestive efficiency however differs greatly between species and depends on parameters such as the developmental stage of the fish and feed type (Rønnestad et al., 2007).

Lipids are an important energy source, a structural component of cell membranes and a signalling molecule (in post-transcriptional regulation of proteins and as messenger molecules) for the fish larvae and adults (Rønnestad et al., 2013). Fish require lipids in their diet, especially the essential n-3 and n-6 fatty acids, which must be supplied through the diet (Torstensen et al., 2001). Lipids have been suggested to be digested in fish larvae in a similar way to adult fish with bile salts, pancreatic lipases and bile-activated lipases (BAL). In general, lipids (mostly triacylglycerols and phospholipids) are emulsified into lipid droplets by bile salts and BAL, while lipases and co-lipases breaks the ester bonds. The micelles of free fatty acids and glycerols are absorbed and resynthesized in the enterocytes and packed in chylomicrons. The chylomicrons are transported to the liver for storage and further transport to tissues, packed in lipoproteins. Cholesterol in the mammalian liver is converted to bile acid by Cyp7 biosynthesis, where Cyp7 A1 activity have been measured in fish such as ballan wrasse larvae (Hansen et al., 2013). Fish feed with low levels of fat and high amounts of carbohydrates or proteins causes the fish to store excess energy as fat (Torstensen et al., 2001).

The role played by carbohydrates in fish larval development is not clear, and the amount of carbohydrates in fish feed for larva is low, although it beneficial in formulated feed for its capacity to bind water (Rønnestad and Hamre, 2001). Carbohydrates such as starch and oligosaccharides are hydrolysed by pancreatic amylases and glucosidases. Brush-border enzymes such as isomaltase and maltase hydrolyze disaccharides into monosaccharides, which are absorbed by the enterocytes and transported to the liver by the portal vein. Pancreatic amylase is expressed in the ballan wrasse yolk-stage larvae and other fish larvae such as the walleye pollock *Theragra chalcogramma*, gilthead seabream *Sparus aurata* and Senegalese

sole *Solea senegalensis* (Hansen et al., 2013, Rønnestad et al., 2013). The level decreases throughout the larval stage due to gastric and/or pancreatic maturation (Cahu et al., 2004, Rønnestad et al., 2013). The presence of amylase in early development may indicate the importance of an optimised amount of carbohydrates in the diet as an energy source from the start of exogenous feeding, and for triggering the digestion process through ingestion of microalgae by engulfing water and plankton (Hansen et al., 2013, Rønnestad et al., 2013). The effects of carbohydrates on the gut flora have been reviewed by Hansen et al. (2013).

It is well known that increased protein intake is correlated with increased protein synthesis (Espe et al., 2001). Exocrine pancreatic enzymes play a major role in protein digestion through enzyme production. A greater relative volume of the exocrine pancreatic enzymes compared to the gut could indicate an increased capacity for nutrient digestion through higher enzyme secretion. The liver is the major organ of metabolism in fish. Assuming that the capacity for nutrient absorption and post-prandial modification is proportional to the volume of the liver; a higher relative volume of the liver could increase digestive capacity and enable the organ to modify proteins and lipids to a greater extent than at earlier stages.

The enzyme glucokinase in the liver phosphorylates glucose to glucose-1(6)-phosphate, which can be further modified by glycolysis. The enzyme activity is regulated by insulin and glucagon secreted by the endocrine pancreas (Hamre, 2001). Insulin, glucagon and glucagon-like peptide (Glp) are only a few of the hormones necessary for homeostasis and energy metabolism in both fish and mammals (Rønnestad et al., 2017). Insulin stimulates glucose uptake as well as protein synthesis and lipogenesis in the cells. Glucagon is the antagonist of insulin and stimulates glucose release from cells (Hamre, 2001).

Proteins and amino acids supply the body with key building components. It is also an important energy source and plays an important role in antibody activity. Digested proteins are broken down by endopeptidases and exopeptidases into polypeptides. Proteolytic enzymes are secreted by the stomach (pepsin together with acid denaturation by hydrochloric acid) and from the exocrine pancreas (trypsin, chymotrypsin, elastase and carboxypeptidase A and B). Enzymes are also present in the brush border of the intestine (enterokinase, aminopeptidase, tripeptidase and dipeptidase) to hydrolyse the polypeptides into absorptive units (tri- and dipeptides and free AA), which are taken up by the enterocytes and becomes transported in the portal vein to the liver and incorporated in the body's protein turnover (Espe et al., 2001).

Trypsin is regarded as the most important protease in an alkaline environment in the gut until gastric glands in the stomach appear during the transition from larva to juvenile (Zambonino Infante and Cahu, 1994, Yúfera and Darías, 2007b). The less efficient alkaline digestion of protein increases with gastric digestion through acid denaturation and pepsin hydrolysis (Mazurais et al., 2011). A functional stomach in fish develops during metamorphosis and the time at which larvae start to weaning onto formulated feed simultaneously with the development of the pyloric caeca to increase the surface area for digestion and absorption (Rønnestad et al., 2013). Acidic and proteolytic gastric digestion is observed from climax-metamorphosis in the Japanese flounder *Paralichthys olivaceus* (Rønnestad et al., 2000a), Asian seabass *Lates calcarifer* (Walford and Lam, 1993) and Atlantic halibut (Gomes et al., 2014b). Until recently, most of the experience of Norwegian fish farmers were with altricial-gastric species such as Atlantic cod, Atlantic halibut and turbot, all of which develop their stomach during metamorphosis, and weaning during or after the time the stomach becomes functional. The lack of stomach and pyloric caeca in the ballan wrasse demonstrates the need for basic knowledge of the development of digestion in agastric fish.

1.4.3 Role of the stomach – compensatory solutions in agastric fish?

The stomach is an expansion of the distal foregut. The distal end of the stomach is the called pylorus; it ends in a pyloric constriction and is regulated by a pyloric sphincter, which administrates the flow of chyme (partly digested food) downstream into the intestine. The shape of the stomach displays a wide range of variations, from tubular to asymmetric (Kryvi and Poppe, 2016), and serves a range of physiological purposes, mainly related to digestion.

The stomach plays a role in the storage and retention of ingested food, enabling the fish to ingest fewer and larger meals. This capacity depends on a pronounced relaxation of the smooth muscle layer of *m. externa* in combination with an effective pyloric sphincter (Smith and Tabin, 1999, Smith et al., 2000). The stomach also releases gastric acid, which promotes the digestion of proteins and decalcifies bony tissue (Koelz, 2009). The low pH of the gastric acid act as a barrier against pathogens such as bacteria (Martinsen et al., 2005). The secretion of pepsin from the oxyontopeptic cells is an important contribution to digestion of proteins (Koelz, 2009). The stomach also provides a steady supply of partly digested feed (chyme) to the anterior midgut to optimise the digestion and absorption of nutrients such as proteins and lipids (Smith et al., 2000,

Rønnestad et al., 2013). Finally, the stomach plays a role in osmo- and ion regulation and also facilitates the absorption of micronutrients, e.g. Fe^{3+}, Ca^{2+}, and B_{12} (Koelz, 2009). These vital functions must also be adequately performed by the fish to meet their nutritional requirements.

In the evolution of vertebrates, only the most primitive classes of fish (e.g. Cyclostomes) and few of the advanced vertebrates lack a stomach [e.g. some teleosts, the egg-laying s monotreme mammals and the duck-billed platypus (Koelz, 2009)]. The ballan wrasse, Chinese sucker (*Myxocyprinus asiaticus*), gobies, scarids, blennids, cyprinids (e.g. zebrafish and other families) are all agastric throughout their life-cycle (Jobling, 1994, Smith et al., 2000, Ng et al., 2005, Liu et al., 2013). On the other hand, the Senegalese sole *Solea senegalensis* develops a stomach, but lacks acidification and proteolysis by the stomach, and rather maintains a neutral pH throughout the intestine (Yúfera and Darías, 2007a). The lack of a stomach is functional in the wild, but may give rise to problems in the context of aquaculture. The reason why some species have lost their stomach during evolution can only be speculated over, but one possible explanation is that a calcium carbonate-rich diet (i.e. corals and mollusc shells) can possibly neutralize the gastric acid, leading to the loss of peptic digestion (Lobel, 1981, Bakke et al., 2010).

There are differences in the ontogeny of a functional stomach in fish (Rønnestad et al., 2013). Precocial fish have a functional stomach at the onset of feeding (e.g. Atlantic salmon). Altricial larvae develop a functional stomach during the larval phase and metamorphosis (e.g. Atlantic cod and halibut), while agastric species do not possess a stomach in either the larval or adult stages (e.g. wrasses). The variations in the digestive tract often reflect their feeding habits and food preferences regardless of the presence or absence of a functional stomach (Ray and Ringø, 2014). Most fish, including the Atlantic salmon and the gudgeon (*Gobio gobio*), are carnivores, and have a shorter digestive tract than omnivores like the roach (*Rutilus rutilus*). The mirror carp (*Cyprinus caprio*) is a herbivore and has a longer digestive tract than omnivores (Al-Hussaini, 1949). Herbivores represent only 7% of all fish species (Bone, 2008).

Since most marine fish larvae, including the ballan wrasse, do not have a stomach at first-feeding, they have a reduced ability to digest conventional formulated diets and are therefore given live feed. The larvae are gradually weaned from live feed (e.g. enriched rotifers and co-fed with brine shrimp [*Artemia* spp.]) onto formulated feed.

The altricial-gastric Atlantic cod and Atlantic halibut, possesses a bulb-like form in the proximal midgut, with a sphincter before metamorphosis, which develops into the functional stomach (Kamisaka and Rønnestad, 2011, Gomes et al., 2014a). The bulb may act as a temporary storage compartment and /or complement pancreatic secretions in proteolytic digestion before the development of a functional stomach (Gomes et al., 2014b).

1.4.4 Intestinal bulb

Several studies support the idea that agastric fishes have some ability to retain food in the anterior part of the intestine. This upper part, known as the intestinal swelling (Al-Hussaini, 1949), pseudogaster (Kalat and Shabanipour, 2010) or intestinal bulb (Jobling, 1994, Ng et al., 2005); have been suggested to be capable of retaining ingested food, prolonging its residence time in the digestive tract and thus assisting lipid and protein digestion (Rombout et al., 1985, Kamisaka et al., 2003, Gomes et al., 2015).

The establishment of a functional intestinal bulb with a functional sphincter requires a larger layer of muscle and nerves (Gomes et al., 2014b). The autonomic nervous system regulates the action of the sphincter: parasympathetic nerves inhibit the sphincter muscle, while the sympathetic system activates the sphincter muscles (Gartner and Hiatt, 2007). A sphincter (e.g. pyloric- and ileorectal sphincter) is characterized by a thicker *m. externa* (both circular and longitudinal smooth muscle) than the *m. externa* layer in the rest of the digestive tract (Luizi et al., 1999). It is therefore to be expected that all functional sphincters can be identified histologically. However, *in vivo* studies of Atlantic halibut have shown that strong and sustained contractions (3-5 waves min^{-1}) can also occur in areas that are not characterized by muscle bundles, i.e. in the pyloric caeca (Rønnestad et al., 2000b). Unfed zebrafish also display similar intestinal contractions, although at a lower rate, which may be due to different feeding modes compared to the Atlantic halibut (Holmberg et al., 2003).

It may be difficult for agastric fish larva to digest complex proteins without the help of proteolytic and acid secretion in the stomach, so enzyme secretions from the exocrine pancreas play a central role in digestion (Rønnestad et al., 2007, Hansen et al., 2013, Gomes et al., 2014b). In agastric species, the food particles move directly from the esophagus to the intestine (Smith et al., 2000) at the site where the common bile duct *ductus choledochus* and hepatic duct *ductus pancreaticus* end in the lumen of the intestine. If the ingested food enters a functional

bulbus at the site where bile and pancreatic secretes are released, this could help to efficiently mix the food with digestive enzymes to improve absorption.

Glycogen, fatty acids and proteins are mainly digested in the anterior segments of the intestine in ballan wrasse juveniles (Shao, 2016). The intestine of ballan wrasse is divided into four segments, from the anterior to posterior end of the digestive tract. The 1st segment is the proximal midgut with the bulbus, the second and third segments are the middle and distal midgut, while the fourth is the hindgut (Krogdahl et al., 2014).

1.5 3D rendering and analysis

Virtually all studies of the ontogeny of the digestive system in fish are based on 2D imaging and drawings. It can be difficult to conceptualize the spatial distribution of the digestive organs and limit an overview of a three-dimensional bulbus in a 2D image, along with the elongation of the liver and scattered pancreatic tissue.

A three dimensional representation of the digestive organs has previously been developed for visualisation of the ontogeny of the digestive system of Atlantic cod (Kamisaka and Rønnestad, 2011) and Atlantic halibut (Gomes et al., 2014b). This thesis describes and discusses a 3D visualisation of the digestive system of six developmental stages of the ballan wrasse. 3D rendering of the digestive system permits rotation and zooming of the model from all angles while adding or removing irrelevant organs in studies of the exterior and interior of the model. The software performs statistical analysis automatically to allow a more accurate analysis than a mathematical approach alone would permit. Statistical analysis can be incorporated in morphometric studies of volume and surface area of the digestive system, while the morphometric scaling can also provide an indication of the functional capacity and processing of the digestive system. The present study extends and develops the work of Kamisaka and Rønnestad (2011) Gomes et al. (2014b) to the ballan wrasse, in the light of the importance of the development of its gut anatomy and physiology to the successful rearing of this species.

1.6 Aims of the study

This study will describe the development of the digestive tract and associated glands in ballan wrasse using reconstructed 3D models combined with anatomical and histological descriptions, by light- and scanning electron microscopy, based on six developmental stages.

Aims of the study:

1. Establish 3D models of the digestive system of the ballan wrasse in six developmental reference stages.
2. Describe the ontogeny of the digestive system in ballan wrasse from larva until juvenile.
3. Describe the growth of the digestive tract and associated organs in terms of surface areas and volume.
4. Relate morphometric scaling of the intestine and associated glands to functional capacity for digestion and processing.
5. Determine whether an intestinal bulbus[1] is present in the ballan wrasse.

[1] To simplify the terminology in this thesis the proximal midgut is referred to as bulbus to permit easier identification of the section where this function is explored.

2. MATERIALS AND METHODS

2.1 Material

Ballan wrasse larvae were collected from the commercial hatchery of Marine Harvest Labrus (MHL) at Naturgassparken, Øygarden, Norway. Broodstock of natural spawning fish were distributed into eight tanks (9000 L) with approximately 30 females and 5 males in each tank. The bottoms of the tanks were covered with green mats to collect the fertilized eggs.

The larvae originated from two batches containing a mix of fertilized eggs that had been spawned between 21-22. and 27-28. August 2015, respectively. The mats with fertilized eggs were collected and incubated in tanks (900-1000 L) until hatching (9-10 days at 11.3˚C) under a 12/12 hour light/dark regime.

Newly hatched larvae (0 DPH) were transferred to feeding tanks (9000 L; initial stock density of 1.0-1.3 mill larvae). These tanks were kept in 24h darkness with no feed added until 4 DPH. From 4 DPH live feed was added and light was kept continuously on. The temperature in the feeding tanks was 13.7˚C at 0 DPH, and slowly raised to 16.0˚C at 24 DPH from which point it was stable t throughout development. Oxygen saturation was maintained above 80 %, and the water flow was initially 45 l/m, rising to 60 l/m from 22 DPH. At 102 DPH, the larvae were transferred from first feeding tanks to larger rearing tanks (27 000 L).

The larvae were fed cooled live feed four times a day (08:00, 14:00, 20:00 and 02:00) until they were weaned on to a formulated feed. In the first period, they were fed enriched rotifers; *Brachionus* spp. [Aquafarms, Florida, USA]) from 4 DPH until 25-30 DPH. From 20-25 until 57 DPH the larvae were co-fed with enriched brine shrimp *Artemia* (INVE Aquaculture Inc, Salt Lake City, USA). Both rotifers and *Artemia* were enriched with Multigrain (BioMar, Norway).

An experimental formulated feed (Nofima, Norway) containing high quality shrimp and cod meal to improve palatability (A. Lekva, MHL, pers. comm) was introduced from 47 DPH in a co-feeding protocol (live *Artemia* and formulated feed) for 10 days (until 57 DPH). From 57-60 DPH the larvae were fed only formulated feed from Otohime (Otohime B1 and B2 at first, followed up with Otohime C1, Marubeni Nisshin Feed Co. Ltd, Japan).

2.2 Sampling of larvae

Larvae were sampled between September and December 2015. At each sampling 8-11 larvae were collected. The first sampling took place on the day the larvae started exogenous feeding (4 DPH), and the last at 102 DPH when the SL were 25 mm in length. Each sampling was planned to collect larvae at a specific developmental Stage (**Table 2.1**; Ø. Sæle, Nifes, Bergen, Norway, *pers. comm*, 04.09.15) with a correlating standard length (SL). Only larvae of the specific SL for each developmental Stage was used for further analysis, and larvae that were too large or too small were excluded.

All the larvae sampled were fed at the time of sampling to ensure that the gut was in an active digestive state with functional physiological processes and corresponding active tissues. When a fed fish is studied, morphometric changes from starvation can be excluded i.e. proteolysis in the intestine, reduced lipid storage in the hepatocytes and regenerated of exocrine pancreas (and zymogen granules).

Table 2.1: Larvae collected and used in the study. Dr. Ø. Sæle, Nifes, Bergen, Norway, *pers. comm.*, provided the description of the stages.

Developmental stage	**1**	**2**	**3**	**4**	**5**	**6**
Target SL (mm)	4	5	7	10	15	25
Sampled SL Mean ± SEM (mm)	5.19 ± 0.17	6.12 ± 1.16	7.07 ± 1.30	9.05 ± 0.91	16.46 ± 1.10	25.85 ± 2.90
Sampled age (DPH)	4	10	18	29	71	102
Age-related stages:	Yolk sac larva	Yolk sac/ Preflexion larva	Preflexion larva	Flexion larvae	Post flexion larvae/ Juvenile	Juvenile

The smaller larvae (Stages 1- 4; 4-10 mm SL) were captured with a 1 m-long plastic tube (1 cm inner diameter) that was lowered into the tank and then closed off with the thumb to collect the water column with the larvae trapped inside. This vertical transect sampling also prevented weak or sick larvae from being sampled at the surface. The larger larvae (Stages 5 and 6; >15 mm SL) were sampled individually using a fine-mesh net, but also here, larvae swimming on the surface were not captured. Only larvae of visually confirmed high quality were used.

Immediately after sampling, the larvae were sedated with Metacain and photographed under a microscope using a Canon IXUS camera and graph paper in the background for scale. These photos were used to measure the standard length (SL) of the larvae and to verify that they were of good quality. The photos of the larvae were uploaded into *ImageJ* software (NIH, USA) and the SL was measured from the tip of the dorsal lip to the beginning of the tail fin.

After photography, the larvae were transferred to teleost fixative (**Appendix A.1**) using dram glasses and Falcon tubes for the smaller (Stages 1-4) and larger (Stages 5-6) larvae, respectively. They were then brought to the Department of Biology (HIB, University of Bergen, Norway) and stored in fixative for 24 h in a refrigerator. After 24 hours, the larvae were rinsed for 1x10 min in PBS and transferred to 70% ethanol before storage in 70% ethanol in a refrigerator until further use.

Further larvae were sampled during spring and summer 2017 in order to document the outer morphology of the developmental stages. They were sedated with Metacain at Marine Harvest Labrus before transport to HIB stored on ice. Larvae were put on agar gel (**Appendix A.3**), covered completely with sedative and photographed with an RS Photometric CoolSNAP-PRO color camera attached to a Leica M420 macroscope with 6:1 Leica Apozoom objective with Image-Pro Plus software (Media Cybernetics, USA) for Stages 1-4. A Nikon D3000 digital camera with AF-S DX Zoom-Nikkor 18-55 mm f/3.5-5.6G ED II lens was used to photograph Stages 5 and 6.

2.3 Light microscopy

One larva from each Stage (1-6) was prepared for light microscopy. The larvae stored in 70% ethanol were dehydrated (2x15 min in 96% ethanol), and embedded in glycolmethacrylate resin (Technovit ® 7100 (Heraeus Kulzer GmbH & Co, Germany; **Appendix A.3**). The three smallest

larvae (Stages 1-3) were embedded whole with no dissection. The largest larvae (Stages 4-6) were dissected before embedding to fit into the embedding casts. The head (posterior to the operculum), tail, pectoral and pelvic fins, skin and skeletal muscles surrounding the abdomen were carefully dissected away. The two largest stages were also decalcified in formic acid (23h) and rinsed in PBS (1x10 min) before dehydration, dissection and embedding.

All stages of the larvae were cut into semi-thin (2 μm) longitudinal serial sections using a Leica RM 2155 microtome. All sections were placed on glass slides (three sections per slide), air dried under heat (<50.0˚C) and stained with toluidine blue for 60 seconds (Philpott, 1966) (**Appendix A.4**) before excessive staining was rinsed off with warm water. The slides were air dried before cover slips were mounted using DPX New (Merck KGaA, Darmstadt, Germany).

Light micrographs of the serial sections were used to prepare image stacks for the reconstructed 3D models and to study details of the histology of specific tissues. Image stacks for Stages 1-4 used in the 3D models were scanned using RS Photometric CoolSNAP-PRO color camera connected to a Leica M420 macroscope with a 6:1 Leica Apozoom objective with Image-Pro Plus software (Media Cybernetics, USA). For histological studies and preparation of the image stacks for Stages 5 and 6, the RS Photometric CoolSNAP-PRO colour camera was mounted on a Leica DMLB microscope using Live tiling settings in Image-Pro plus. Image editing (color to grey tones and contrast) were performed in Adobe Photoshop CC2015 (Adobe System Incorporated, USA).

2.4 3D reconstruction of the digestive organs

To create the reconstructions in the 3D rendering software (Imaris, 8.4; Bitplane AG, Switzerland); image stacks were made from the serial sections (explained in the section above). The image stacks were modified (image converted and aligned) before they were uploaded into Imaris. The 3D reconstructions were based on manual drawings of the contours of the individual digestive system organs, and the Imaris software rendered the 3D models based on the contours drawn. The volume and area of all the organs in the 3D models were automatically calculated by the 3D rendering software (Imaris MeasurementPro) and separately saved and downloaded in MS Excel for each developmental stage.

The ideal image stack involves every serial section with the tissues or organs of interest. The building of the 3D models using the current approach was demanding of both the hardware and the software resources. In order to limit the time involved in the rendering process, preliminary tests showed that a number of sections used in the reconstruction below 95 gave an adequate workflow. In addition, the alignment software had an upper threshold at 100 images in a stack. For Stage 1 every second section cut was used in the stack, giving an image stack of 60 slides. For the other developmental stages, the number ranged between every three to 13 sections, resulting in stacks of 80-90 images. All the reconstructions were thus made with image stacks of approximately the same number of images.

The alignment software is developed for scanning electron micrographs and workes very well for gray-scale images, though the image stacks used in this study were created from light micrographs (RGB), which were therefore batch-converted to grey-scale micrographs. The micrographs also needed a simpler filename (image 00#) to upload in their correct order in the alignment software. Image stacks were batch-converted and batch-renamed to simpler filenames in IrfanView (Irfan Skiljan, Austria). To align the images, the stacks were uploaded into AutoAligner 6.1 (Bitplane AG). The head (if present) and proximal part of the abdomen (the liver, villi of the intestine and the swim bladder) were set as the region of interest (ROI) for automatic alignment. A manual fine adjustment was performed before the alignment was applied to the whole image stack (**Figure 2.1**).

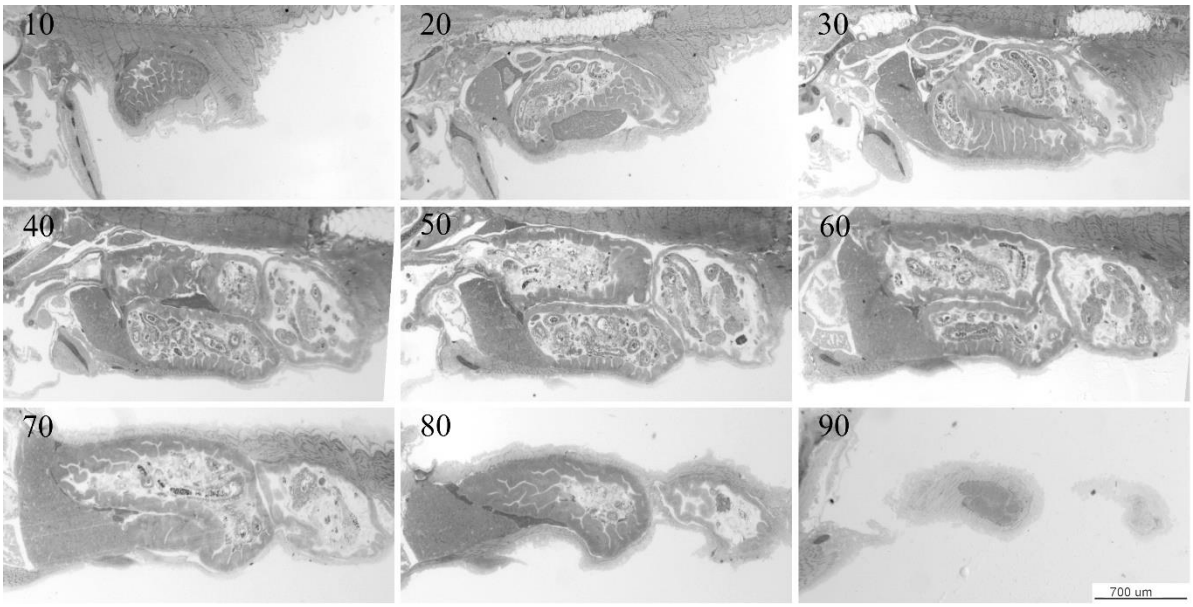

Figure 2.1 Example of image stack of Stage 4 (29 dph) ballan wrasse larvae. Number in upper left show slide number in AutoAligner and Imaris (section thickness 2 µm, every 4th section used in the model). The image stack is numbered from right (image 001) to left side (last image).

The aligned image stacks were next uploaded to Imaris 8.4 (Bitplane AG) to produce the 3D reconstruction of the digestive organs. The image properties (voxel sizes) were set before the surfaces were drawn, to retrieve correct dimension of the 3D reconstruction and statistical measurements of the organs of interest. While a pixel represents a 2D image, a voxel is volumetric and represents the 3D image by taking the X- and Y pixel sizes (complementary to X- and Y voxel size) of the image and adding the distance between the images in the stack (the Z-voxel size) in the same scientific notation (µm is used in this study).

Since the image acquisition system using RS Photometric CoolSNAP-PRO colour camera and Image-Pro plus software did not measure the X- and Y pixel size of the images, this was set manually in Imaris, depending on the magnification used for the micrographs. The Z-voxel size was set on the basis of the distance between the serial sections in the image stacks. For example, every second section used for Stage 1 at 2 µm thickness gives a 4 µm Z-voxel size; and every 13th section used for Stage 6 at 2 µm gives a Z-voxel size of 26 µm (**Appendix C, Table C.1**).

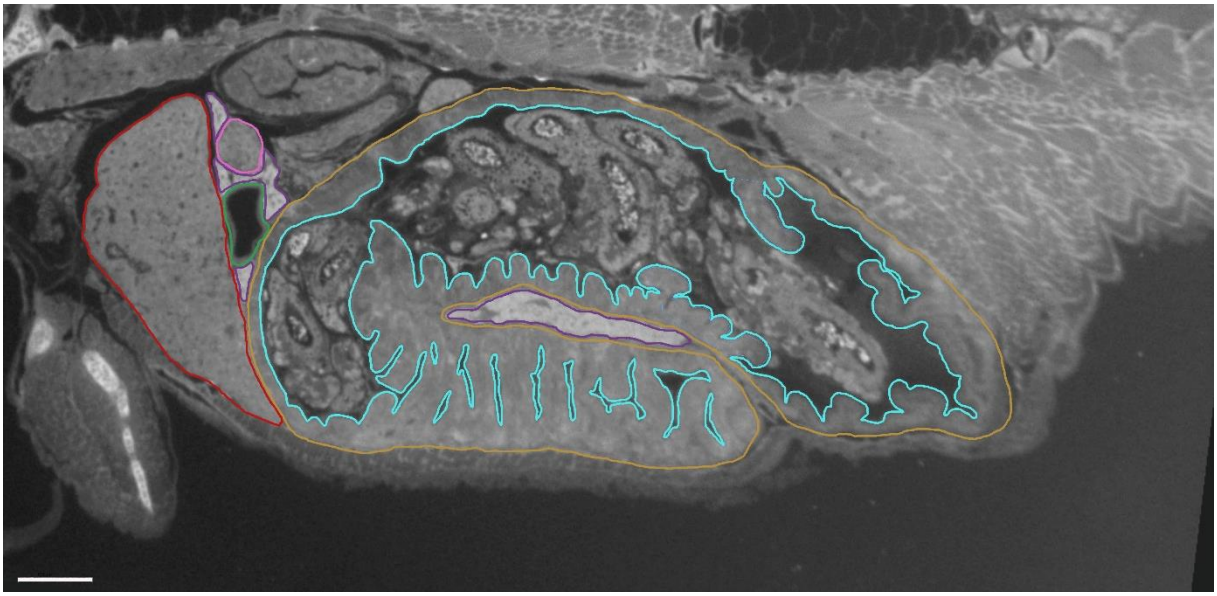

Figure 2.2 The manual drawing process in Stage 4 (29 dph) of a ballan wrasse larvae. The image shows slide #28 displayed in Imaris (Bitplane AG.), equivalent to 224 µm in from the right side of the digestive system (section thickness 2 µm, every 4th section used in the model). Each organ was drawn and traced separately and with different colour codes. *Orange:* outer surface of the digestive tract. *Blue:* lumen of the intestine. *Red:* liver. *Green:* gallbladder. *Purple:* exocrine pancreas. *Pink:* primary Islet of Langerhans. Scale bar (white, in lower left) 100 µm.

The 3D models were made from contour surfaces (polygons with nodes) that were manually drawn using the 'Surface' tool in the Surpass mode in Imaris. Each surface was created and identified with a specific colour code that was repeated in all the Stages (**Figure 2.2**). Up to

nine surfaces were created in each model: 1) Outer surface of the digestive tract. 2) Lumen of oesophagus. 3) Lumen of intestine. 4*) Valve between midgut and hindgut. 5) Exocrine pancreas. 6*) Endocrine pancreas. 7*) Pancreatic duct. 8) Liver. 9) Gall bladder. Surfaces marked with an asterisk [*] were not generated for all the developmental stages, because these structures were not always observed in the micrographs or were not present at the developmental stage. The surfaces created in the dataset were duplicated and given their colour code for visualisation in the grey-scale images in three dimensions (X-Y, X-Z and Y-Z) 2D images in Slice mode in Imaris. After manually drawing the surfaces, Imaris generated reconstructed 3D models from the surfaces, which were displayed on the computer screen and saved in the .ims file format (**Figure 2.3**).

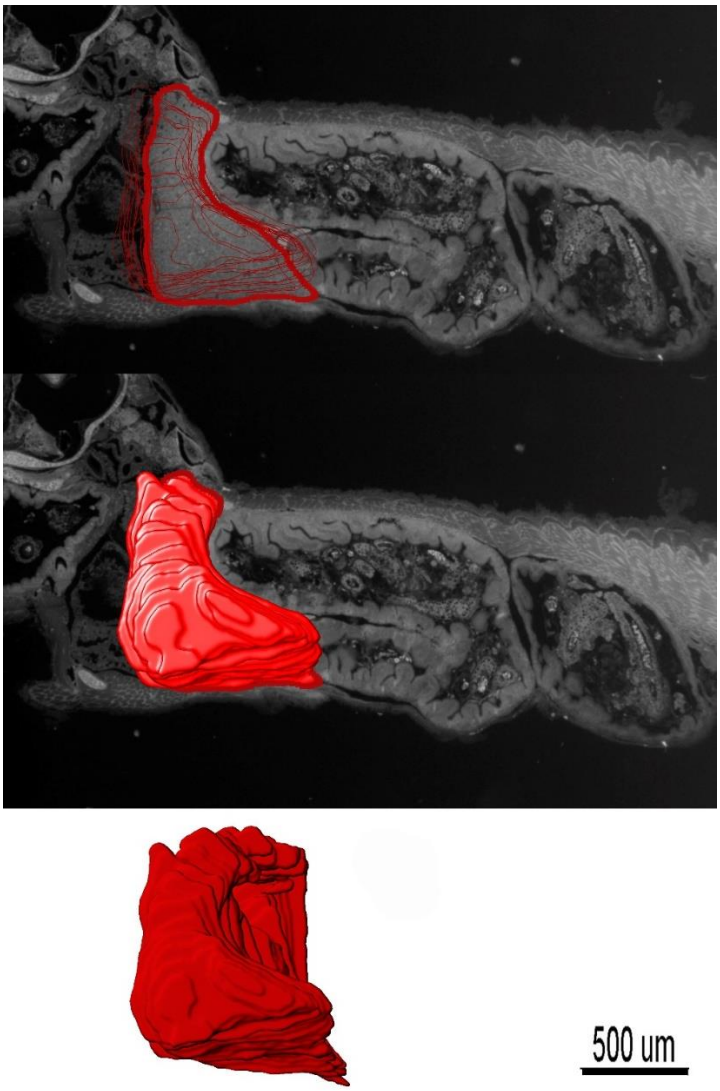

Figure 2.3 3D rendering of the liver tissue in Stage 4 of the ballan wrasse larva. Upper: The drawn surfaces (polygons with nodes) with 'Surface' tool in Imaris of the liver. The thick red line indicates the drawn surface of the liver on the slide, while the thin lines are drawn surfaces prior to (to the left of) this slide. Middle: 3D reconstruction of the liver created by Imaris on the slide and surfaces drawn prior to this slide. Lower: The whole liver as a rendered 3D reconstruction.

The beginning of the esophagus was set from the constriction at the posterior end of the pharynx where the pharyngeal pad and skeletal muscle of the *muscularis externa* was observed, or as close to this area as could be observed visually. The end of the esophageal lumen was set where the epithelial sheet changed into the simple columnar epithelial cells with microvilli of the gut, and the end of prominent circular muscle layer of *muscularis externa* of the esophagus. The outer surface of the digestive tract was set at the serosa and adventitia.

The images of the 3D models used in this thesis were captured using the "Snapshot" function in Imaris and saved in the .tiff file format.

Imaris MeasurementPro, an extension of Imaris 3D rendering software, provided the statistical measurements (surface areas and volumes). A reconstructed 3D model of an organ, e.g. the liver, was represented by a network of small triangles (a triangle mesh). The surface area of the organ is automatically calculated by the total number of triangles x the triangle surface area. The volumetric data is based how much space the triangular mesh occupies in a grid defined by the voxel size.

2.5 Scanning electron microscopy (SEM)

Two larvae from each Stage (1-6) were prepared for SEM. The first series (one larvae from Stages 1-6) was investigated for the outer morphology of the digestive system. Except for Stage 1 (where the larvae were too small for dissection), the skin and muscle tissue surrounding the abdominal cavity were dissected away before SEM. In Stages 2 to 4, only the skin surrounding the abdominal cavity was removed. For Stages 5 and 6, the head, the tail and muscle dorsal and lateral to the abdominal cavity were also removed. The second series (the second larva from each Stage) were prepared to study details of the internal morphology of the gut. Larvae in Stage 1-3 were cut in transverse. Stage 4-6 were cut sagittally (both left and right side were investigated in the SEM), and the head and tail were dissected away.

After dissection, the larvae were hydrated in 50% ethanol for 10 min (since they had been fixated and stored on 70% EtOH) and rinsed in PBS (2x10 min) before they were secondarily fixated in 1% osmium tetraoxide for 60 min (**Appendix A.5**). After fixation, the larvae were rinsed in distilled water (2x10 min) and rehydrated in an acetone series (50 % acetone for 2x10 min), and stored in 70 % acetone before critical point-dried. The larvae were mounted on a stub

with double-sided tape before becoming sputter-coated with gold-palladium (Au/Pd) using a Polaron SC502 Sputter Coater (Quorum Technologies, East Sussex, England). The larvae were examined and photographed using a ZEISS Supra 55VP field-emission scanning electron microscope (Carl Zeiss AG, Oberkochen, Germany).

2.6 Calculations

Tissue volume and area of all the organs in the 3D models were automatically calculated by the 3D rendering software (Imaris MeasurementPro) and downloaded as Ms Excel sheets for each developmental stage. The specific growth rate (SGR) of each organ was calculated from the volume data using the following equation.

$$SGR = (\ln V_2 - \ln V_1)\,(t_2 - t_1)^{-1}$$

$\ln V_2$ is the natural logarithm of the volume of a given organ at time t_2, and $\ln V_1$ is the natural logarithm of the initial volume of the same organ at initial time t_1.

3. RESULTS

3.1. Larval development

The larvae were sampled in the course of five visits from September to December 2015, and from two different tanks (Tank 2 and Tank 7). Generally speaking, larval quality and growth were within production standards, but tank 7 showed some increased mortality (A. Lekva, Marine Harvest, Norway, *pers. comm.*).

On the first visit, larvae for Stages 1 and 2 were collected (from tanks 2 and 7 respectively). On later sampling visits, larvae from either tank 2 or tank 7 with suitable SL were used for further analyses by microscope and 3D rendering of the digestive system in Imaris. Three samples were taken when the larvae were fed enriched rotifers, one during the *Artemia* feeding period, and two while the fish were being fed formulated feed (**Figure 3.1**).

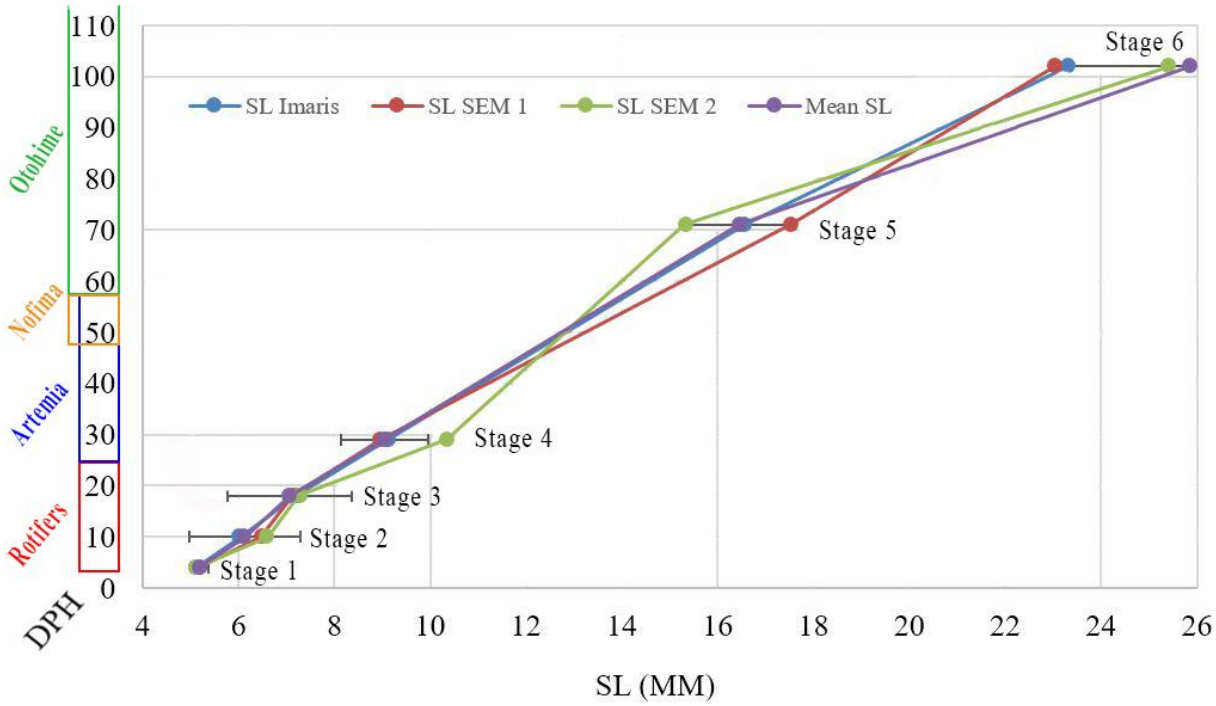

Figure 3.1 Stage-related size (mm SL) of selectively sampled larvae at 4, 10, 18, 29, 71 and 102 DPH with food type (Rotifers, *Artemia* and formulated feed). *Purple line:* mean ± SEM mm SL of all sampled fish after selection. *Blue line:* SL of larvae prepared for light microscopy and 3D reconstruction. *Red line:* SL of the first series of larvae prepared for scanning EM (external morphology). *Green line:* SL of larvae prepared for second series of scanning EM for sagittal cut tissues.

3.2 Stage 1 – 5.1 mm (SL)

Stage 1 yolk-sac larvae were collected at 4 DPH, which was the first day live feed (enriched rotifers) was added to the tanks (**Figure 3.4**). The SL of all the sampled fish was 5.19 ± 0.17 mm (mean ± SEM; n=10). The larva selected for reconstruction in Imaris was 5.12 mm in length. At this stage, the digestive tract was a straight incipient gut located dorsally to the yolk (**Figure 3.5, 3.6)**. No food was observed in the intestine in this specimen. The length of the digestive tract, analysed from the start of the esophagus to the anus, was 2.15 mm. This represented a ratio of 0.41 of the SL, i.e. 41% of the SL of the larva.

The esophagus was a cylindrical, hollow tube with no folding (**Figure 3.6, 3.9**). It started from the constriction of the pharynx, and followed dorsally to the liver and ended with a constriction before entering the intestine (**Figure 3.10**). No goblet cells were observed in the esophageal mucosa. The external muscle layer of the esophagus was unstriated and thin.

No bulbus or intestinal swelling was observed at this stage. The layers in the digestive tract were tightly packed where the *m. externa* was thin (**Figure 3.11**). The mucosal cell type were enterocytes of simple columnar epithelium (height 15.92 ± 0.74 µm, width 2.80 ± 0.53 µm). The apical end of the enterocytes consisted of microvilli (height 0.97. ± 0.07 µm) throughout the gut and was observed in both the micrographs and scanning EM (**Figure 3.11, 3.12**). No goblet cells were identified in the intestine. An ileorectal valve could not be observed and there were no histological differences between the anterior and posterior intestine. There was a slight luminal constriction between the posterior midgut and the future hindgut where the ileorectal valve would be visible in later stages (**Figure 3.6**), but there were no increased muscular tissues resembling a valve or sphincter at this stage.

The liver was located cranially in the abdominal cavity and covered the anterior part of the gallbladder (**Figure 3.7**). The liver histology showed a clear structure of hepatocytes and sinusoids, coherent with a tubular-like gland. Some small fat deposits were observed within the hepatocytes (**Figure 3.13**).

The gallbladder was located between the liver and the exocrine pancreas, ventral to the intestine and dorsal to the yolk-sac, consisting of simple cuboidal cells and lacking visible connective tissue or a muscle layer. The *ductus choledochus* ended in the lumen of the intestine shortly

behind the constriction between the esophagus and the intestine from the ventral side (**Figure 3.8**).

The exocrine pancreas was located posterior to the liver, to the left and right side of the digestive tract. The pancreatic tissue was not as compact as the liver, but the left and right lobes were connected ventral to the intestine, making a compact pancreas (not diffuse, **Figure 3.8**). A few zymogen granules were observed in the acinar cells at this stage (**Figure 3.13b**).

Neither endocrine pancreas nor *ductus pancreaticus* were observed in the serial sections at this stage.

3.3 Stage 2 – 6.0 mm (SL)

Stage 2 larvae were collected at 10 DPH and had been feeding on enriched rotifers for six days since Stage 1 (4 DPH). The SL of the sampled larvae were 6.12 ± 1.16 mm (mean ± SEM, n= 10). The larva reconstructed in Imaris was 6.02 mm long. The digestive tract was still a straight tube, but one of the obvious changes were a widening of the intestine and almost complete consumption of the yolk (**Figure 3.5, 3.6, 3.14**). Food was present in the gut, unlike the specimen in Stage 1. The length of the digestive tract was 3.12 mm, giving a relationship between gut length and SL of 0.50; i.e. 50 % of the SL of the larva.

The esophagus was still relative long and with a few goblet cells in the esophageal mucosa proximal to the pharynx, but no goblet cells were observed in the distal region (**Figure 3.15**). The layers of the esophagus could be distinguished in the micrographs with *mucosa*, *submucosa*, *muscularis externa* and *adventitia*, where the *m. externa* was very prominent, with striations close to the pharynx (**Figure 3.16**).

At this stage, the anterior midgut expanded laterally in diameter immediately after the constriction between the esophagus and the intestine (**Figure 3.6**). This expansion resembled the shape of a bulbus and narrowed just anterior to the ileorectal valve. The ileorectal valve was clearly visible and separated the midgut and hindgut (**Figure 3.17, 3.18a, 3.18c**). The only cell type that could be observed throughout the intestinal mucosa was enterocytes with microvilli; no goblet cells were observed. A thin external muscle layer (the direction of the fibres could

not be distinguished) enclosed the intestine, and was covered by the serosa (**Figure 3.18c**). No increased muscle layer around or after the bulbus were present.

There was folding (villi) of the intestine, with a leaf-like structure in the bulbus and a stronger folding in the post-bulbus region and anterior to the valve between the midgut and hindgut (**Figure 3.6, 3.18b, 3.19**).

The liver was located anteriorly in the abdominal cavity, with left and right lobes connected ventral for the digestive tract (**Figure 3.7**). Accumulation of fat was observed in the hepatocytes, as in Stage 1 (**Figure 3.19**). The gallbladder was located between the liver and exocrine pancreas on the right side of the intestine and the *ductus choledochus* entered the bulbus ventrally, similar as in Stage 1 (**Figure 3.8**).

The shape of the exocrine pancreas was similar as in Stage 1, with left and right lobes connected ventrally and a few zymogen granules present. One primary islet of Langerhans (endocrine pancreas) was observed close to the gall bladder (**Figure 3.8, 3.19**). At this stage, no *ductus pancreaticus* could be observed.

3.4 Stage 3 - 7.2 mm (SL)

Stage 3 larvae were collected 18 DPH and had been feeding on enriched rotifers since Stage 1 (4 DPH). The SL of the sampled fish were 7.07 ± 1.30 mm (mean ± SEM, n= 10). Larvae at 7.20 mm were reconstructed in Imaris. A clear change that was observed at this stage was the initiation of gut rotation (down, forward and up on the right side of the digestive tract) in one loop. This rotation affected the whole tract, i.e. there were both a luminal rotation and a rotation of the outer surface of the intestine (**Figure 3.5, 3.6, 3.20, 3.21**). A second change at this stage was the pronounced presence of villi throughout the intestine, although these decreased in length and number towards the anus (**Figure 3.6**). The yolk was completely absorbed, and the larvae were thus fully dependent on exogenous feeding for survival. The length of the digestive tract was 4.11 mm. This represents 57% of the larval SL.

The esophagus was shorter and folded (longitudinal villi from the pharynx until the constriction prior to the intestine; **Figure 3.22**). A few goblet cells were present in the mucosa proximal to the pharynx, as in Stage 2, and the esophageal *m. externa* was striated until the midgut. The

anterior midgut did not appear to have a pronounced extended diameter compared to Stage 2, but rather a diameter more similar to the rest of the midgut. Thus, the proximal midgut did not resemble a distinct functional bulbus with increased *m.externa*. The diameter of the middle- and posterior midgut gradually decreased towards the valve. The curl of the midgut showed a right-handed orientation as a V-shape (**Figure 3.6**). The intestinal mucosa consisted of simple columnar cells with microvilli. No goblet cells were observed in either the midgut or the hindgut. Folded mucosa of the bulbus consisted of tall longitudinal villi, and their length and number decreased towards the hindgut.

The only distinct narrow passage in the intestine were the ileorectal valve (**Figure 3.24**). The ileorectal valve separated the midgut and hindgut, as it had been seen in Stage 2. The valve was seen on the mucosal surface (a narrow passage) and on the outer surface of the intestine (narrowing of the surface; **Figure 3.5, 3.6, 3.21**). There was no increase in the muscle bundle at the base of the valve (**Figure 3.24**). The hindgut had a similar diameter to that of the posterior midgut, before a narrow anus.

The liver was located anteriorly and to the left and right of the intestine. The two parts were connected ventrally to the esophagus, similar to Stages 1 and 2 (**Figure 3.7**). Compared to the exocrine pancreatic tissue, the liver was a compact organ (**Figure 3.13, 3.22**). The gall bladder seems to have a permanent location on the right side of the intestine between the liver and exocrine pancreas (**Figure 3.8**).

Exocrine pancreatic tissue was more scattered along the intestine than before in earlier stages (**Figure 3.8**). It was located posterior to the liver, and scattered on both the left and right sides of the digestive tract. Exocrine pancreatic tissue was also observed between the intestinal loop, filling the empty spaces. One primary Islet of Langerhans (endocrine pancreas) was present within the exocrine pancreas, located close to the gall bladder, as in Stage 2.

The *ductus pancreaticus* was observed for the first time and it terminated in the lumen of the bulbus along with the *ductus choledochus* from the gallbladder, in the form of two separate openings (**Figure 3.23**). The two types of duct were separated by following them through the serial sections, where the origin of the pancreatic duct started somewhat diffused in the exocrine pancreas and its connective tissue, and the bile duct started from the enlargement of the gallbladder (*ductus cysticus* and *ductus choledochus* could not be differentiated).

3.4 Stage 4 – 9.1 mm (SL)

Stage 4 larvae were collected at 29 DPH. They had recently ended the period during which they were fed enriched rotifers and had been feeding on *Artemia* for the previous five days. The SL of the sampled fish were 9.05 ± 0.91 mm (mean ± SEM, n= 9). The larva reconstructed in Imaris had an SL of 9.13 mm.

No new tissues or organs were observed at this stage or any later stages in the study. The organs and structures that were present in Stage 3 will either increased in length, surface area and volume [e.g. intestine, liver and exocrine pancreas], number [Islets of Langerhans]) or mature (e.g. enterocytes of the intestine; **Figure 3.25**). However, the most obvious distinct trait at this stage was the lengthening of the intestinal loop and growth of the gut tissue. The curl of the intestine followed the pattern from left to right in one loop, and the coil had grown larger since Stage 3 (**Figure 3.5, 3.26**). The length of the digestive tract was 5.30 mm, equal to 58% of the SL of the larva.

The esophagus was short, but with some fewer longitudinal folds than at Stage 3, and was surrounded by prominent circular skeletal muscle (**Figure 3.25, 3.27**). Goblet cells were dominant close to the pharynx, but absent in the distal esophagus and in the bulbus. The bulbus ended when the gut bent ventrally, forming a narrow passage in the post-bulbus region (**Figure 3.6**). The rotation of the gut had increased in length and the middle midgut followed the length of the bulbus in the cranial direction until the midgut met the posterior end of the liver and bent dorsally and then ventrally again into the posterior midgut in a Z-shape (**Figure 3.5, 3.26**). The intestinal mucosa of the bulbus had longitudinal villi as in Stage 3, and the villi decreased in number towards the hindgut (**Figure 3.6, 3.28**). The posterior midgut and the hindgut were separated by a valve. The hindgut had a wider diameter than the posterior midgut, with a few goblet cells spread among the epithelium, and ended with the anus (**Figure 3.28**).

The liver maintained its shape as a compact organ located anteriorly in the abdominal cavity, ventral to the esophagus, as seen in all the previous stages (**Figure 3.7**). The gallbladder was located on the right side of the digestive tract and between the liver and exocrine pancreas (**Figure 3.8**).

Exocrine pancreas was located along the posterior end of the liver and between the loop of the intestine scattered within the connective tissue outside of the serosa, further developing the

trend from Stage 3 (**Figure 3.8**). Also in Stage 4, only one primary islet of Langerhans (endocrine pancreas) was identified, and as in earlier stages, it was located close to the gallbladder on the right side of the digestive tract. The pancreatic duct terminated in the lumen of the bulbus together with the duct from the gallbladder, just as in Stage 3 (**Figure 3.8**).

3.5 Stage 5 - 16.5 mm (SL)

Stage 5 were collected 71 DPH, when they were being fed a formulated feed from Otohime. They had been weaned from *Artemia* starting 15 days before sampling, with a transition period during which they were co-fed with both *Artemia* and formulated feed from Nofima for 10 days. The external morphology of the specimens was similar for an adult, suggesting a post-metamophosis juvenile (**Figure 3.4**) resembled Stage 4, but with an elongated liver (**Figure 3.5, 3.30**). The SL of the sampled fish was 16.46 ± 1.10 mm (mean ± SEM, n= 7). The individual reconstructed in Imaris was 16.56 mm long (SL). The length of the digestive tract was measured to 10.89 mm, equivalent to represent 66% of the SL.

Goblet cells and teeth (data not shown) were observed in the mucosa of the mouth close to the pharynx. The esophagus was relatively short, folded, and with a high density of goblet cells, especially at the cranial end of the esophagus, as in Stage 4 (**Figure 3.29, 3.31**). The *m. externa* of the esophagus was striated skeletal muscle at both the anterior and posterior ends.

The intestinal mucosa was highly folded, with numerous villi, particularly in the bulbus where they were tall and longitudinally oriented (**Figure 3.6, 3.31**). The intestinal rotation was a single loop with a shape similar to that of Stage 4 (**Figure 3.5, 3.6**). Only a few goblet cells were present in the bulbus, but the number of goblet cells increased posteriorly towards the hindgut, with the highest density in the hindgut along with the smallest villi (**Figure 3.32**).

The liver was located posterior to the *septum transversum*, surrounding the gallbladder, and was located mainly to the left of the digestive tract, unlike in Stages 1-4 (**Figure 3.7, 3.30**). The liver had increased in size, with elongations on the ventral side of the midgut all the way to the hindgut. In addition to the elongations, the left and right sides of the liver were connected both dorsally and ventrally to the esophagus, whereas in earlier stages this was limited to only the ventral side of the esophagus.

The exocrine pancreatic tissue was located unsystematically in the abdominal cavity and "filled in the empty spaces" between liver, gallbladder and the digestive tract, as in earlier stages (Stages 3 and 4), but more prominently now (**Figure 3.8**). However, at Stage 5 there were parts of exocrine pancreas within the liver tissue (hepatopancreas) distributed along larger blood vessels (**Figure 3.33**).

This was the first stage at which several islets of Langerhans were observed; there was one primary islet (the largest, in the same region as in Stages 2-4) located dorsally to the gallbladder that was surrounded by several smaller islets located close to the large primary islet (**Figure 3.8, 3.34**). The pancreatic duct terminated in the lumen of the bulbus next to the duct from the gallbladder, as seen in Stages 3 and 4 (**Figure 3.8, 3.34**).

3.6 Stage 6 - 23.3 mm (SL)

Stage 6 were 102 DPH juvenile ballan wrasse. At this time, they had been feeding exclusively on formulated feed since the previous sampling (Stage 5). The SL of the sampled fish was 25.85 ± 2.90 mm (mean ± SEM, n= 8). The overall contour of the digestive tract followed the same pattern as observed in Stage 5 (**Figure 3.5, 3.35**). One specimen of 23.31 mm-long (SL) was reconstructed in Imaris. The length of the digestive tract was 16.3 mm, which was 0.69 of the larval SL, i.e. 69% of the SL.

The esophagus was short and straight, and the mucosa were folded with a high density of goblet cells until the bulbus (**Figure 3.6, 3.35, 3.36**). The *m. externa* consisted of an inner longitudinal layer and an outer circular layer of skeletal muscle (**Figure 3.36**). The esophagus terminated in the constriction prior to the bulbus, as seen since Stage 1 and throughout the development (**Figure 3.6**). While the outer esophageal circular muscle layer of *m. externa* disappeared at the constriction, the inner longitudinal layer continued beyond the constriction and became the outer longitudinal layer of the midgut (**Figure 3.36**).

The bulbus, unlike the esophagus, had only a few goblet cells located between the mucosal columnar epithelium, as seen in Stage 5 (**Figure 3.36**). Goblet cells appeared further down the digestive tract, particularly in the hindgut, although the highest density of goblet cells in the digestive tract was in the esophagus. The epithelium of the intestine had matured compared to 4 DPH (Stage 1), with a taller columnar cell height of 22.12 ± 2.22 μm and a diameter of 3.19

± 0.64 μm with microvilli (height 0.72. ± 0.16 μm) throughout the intestine (**Figure 3.37**). Otherwise, the intestinal mucosa showed less symmetry of tall longitudinal villi, but rather circular villi throughout the intestine. The mucosa of the hindgut was also highly folded, but not as strong as the midgut (**Figure 3.6**).

The bulbus had a wider diameter and narrowed prior to the rotation of the digestive tract, as seen in earlier stages (**Figure 3.6**), but no prominent *m.externa* were observed around or after the bulbus. This was rather similar to the muscle layer in other parts of the intestine except for the ileorectal sphincter. The bulbus followed the whole length of the abdominal cavity before descending to a right-sided Z-curl. The bulbus narrowed in at the site where the midgut bent down into the middle and bent upwards into the distal midgut, which was separated from the hindgut by the ileorectal sphincter with increased *m. externa*. The hindgut ended with the anus (**Figure 3.36, 3.38)**.

At this stage, several narrow passages (constrictions) were observed on the luminal surface of the midgut in addition to the previously described narrow passage defining the "end" of the bulbus (**Figure 3.35, 3.39**). A second narrow passage was present in the middle midgut after the descending loop, a third in the middle midgut ahead of the ascending loop, and a 4th on the dorsal side of the ascending loop of the midgut (**Figure 3.39**). There was a hint of larger muscle bundles, but these did not resemble the structure of the ileorectal sphincter separating the distal midgut from the hindgut.

The liver surrounded the esophagus and was elongated ventral to the digestive tract mainly on the left side, as seen in Stage 5 (**Figure 3.7**). The liver contained small vesicles of glycogen and a few macrophages. The liver and the exocrine pancreas were well vasculated tissues. The exocrine pancreas with zymogen granules was located between the liver and the digestive tract and within the empty space of the loop for the midgut as in Stages 3-5 (**Figure 3.8, 3.36**). Exocrine pancreatic tissue was regularly present within the liver around the larger blood vessels (hepatopancreas) as seen in Stage 5 (**Figure 3.33**). What had changed at this stage was that the connective tissue within the exocrine pancreas included large populations of immune cells, in particular eosinophilic granular cells (**Figure 3.40**). Some eosinophilic granular cells were also present in the submucosa and the serosa of the digestive tract, but not as prominently as in the exocrine pancreas.

Endocrine pancreas was observed within the exocrine tissue. Again, one large primary islet was located close to the gallbladder and several smaller islets close to the larger one as seen in Stage 5 (**Figure 3.8**). The gallbladder and the pancreatic duct ended in the lumen of the bulbus together, similar pattern as seen for Stages 3-5.

3.7 Size and growth of the organs

The surface areas and volumes of all organs were retrieved from the 3D rendering software. The outer surface area of the digestive tract (*adventitia* and *serosa*) increased 58 times between Stages 1 and 6; 0.99 mm^2 and 58.40 mm^2 at Stage 1 and Stage 6, respectively (**Table 3.1, Figure 3.2**). The *mucosa* of the esophagus and intestine displayed a major increase in surface area between Stages 1 and 2 compared to the other tissues. Moreover, while there was substantial and increasing growth of the surface area of the intestinal *mucosa* throughout the development process, the rate of growth of the esophageal *mucosa* decreased. The esophageal mucosal surface area grew gradually from 0.02 to 3.64 mm^2 from Stage 1 to 6. The intestinal *mucosa* increased in area from 0.23 mm^2 at Stage 1 to 106.75 mm^2 in Stage 6, which represent a 464-fold increase in the surface area (not including the microvilli). The surface-to-volume ratio of the intestinal *mucosa* fell from 0.33 (incipient gut) to 0.02 μm^{-1} (highly folded) between Stages 1 and 6.

Table 3.1 Surface areas (mm^2) of external surface of the digestive tract (adventitia and serosa), esophageal lumen, intestinal lumen, liver, exocrine and endocrine pancreatic tissue from Stage 1 until Stage 6 in ballan wrasse.

Stage	Adventitia and serosa	Esophageal mucosa	Intestinal mucosa	Liver	Exo pancreas	Endo pancreas
1	0.99	0.02	0.23	0.20	0.15	
2	3.71	0.23	2.52	0.66	0.42	0.025
3	3.88	0.15	3.10	1.37	1.18	0.04
4	12.94	0.43	13.47	5.18	2.29	0.13
5	56.30	3.26	102.86	38.81	30.49	0.88
6	58.40	3.64	106.75	30.67	34.47	0.65

The surface area of the liver increased by a factor of almost 200 from Stage 1 to Stage 5, growing from 0.20 to 38.81 mm^2, and falling to 30.67 mm^2 at Stage 6. The area of the exocrine

pancreas showed a more positive growth than the liver throughout development (Stages 1-6), increasing from 0.15 to 34.47 mm^2. The area occupied by the endocrine pancreas grew from Stage 2 (0.02 mm^2) until Stage 6 (0.65 mm^2).

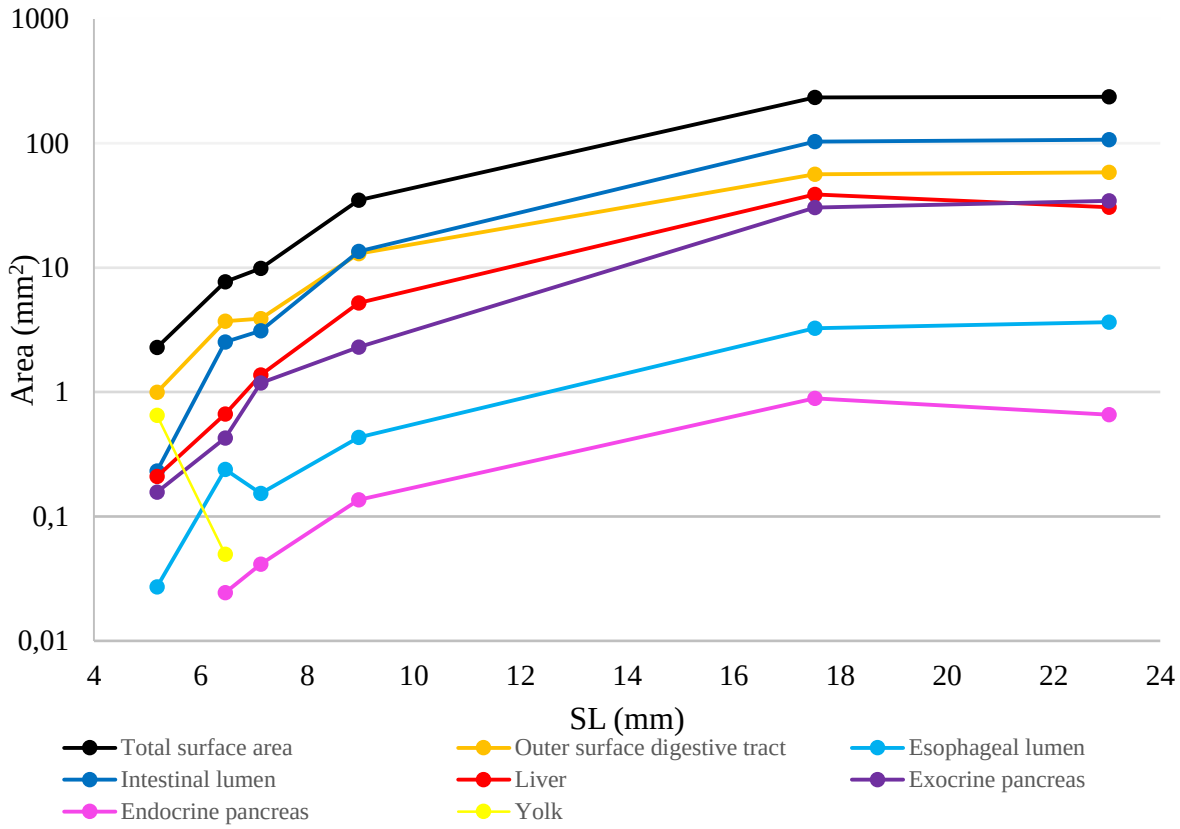

Figure 3.2 Total surface area of all organs (sum of all surfaces) and the area of each organ in ballan wrasse larvae and juveniles. Stage 1 (5.12 mm SL), Stage 2 (6.02 mm SL), Stage 3 (7.20 mm SL), Stage 4 (9.13 mm SL), Stage 5 (16.56 mm SL) and Stage 6 (23.31 mm SL).

The growth in surface area and volume was strong in the earlier stages and levelled out between Stages 5 and 6 (**Figure 3.2, 3.3**). The absolute volumes of all the organs identified at the various stages were measured. The volume (tissue mass) of the outer surface of the digestive tract increased from 0.01 mm^3 in Stage 1 to 8.69 mm^3 in Stage 6. Between Stage 1 and Stage 6, the volumes of the lumen of the esophagus and intestine from grew from 0.00005 to 0.06 mm^3 and from 0.0006 to 3.76 mm^3 respectively (**Figure 3.3**). The yolk volume was 0.008 mm^3 at Stage 1 and was completely absorbed between Stages 2 and 3 (i.e. 0 mm^3; **Figure 3.3**).

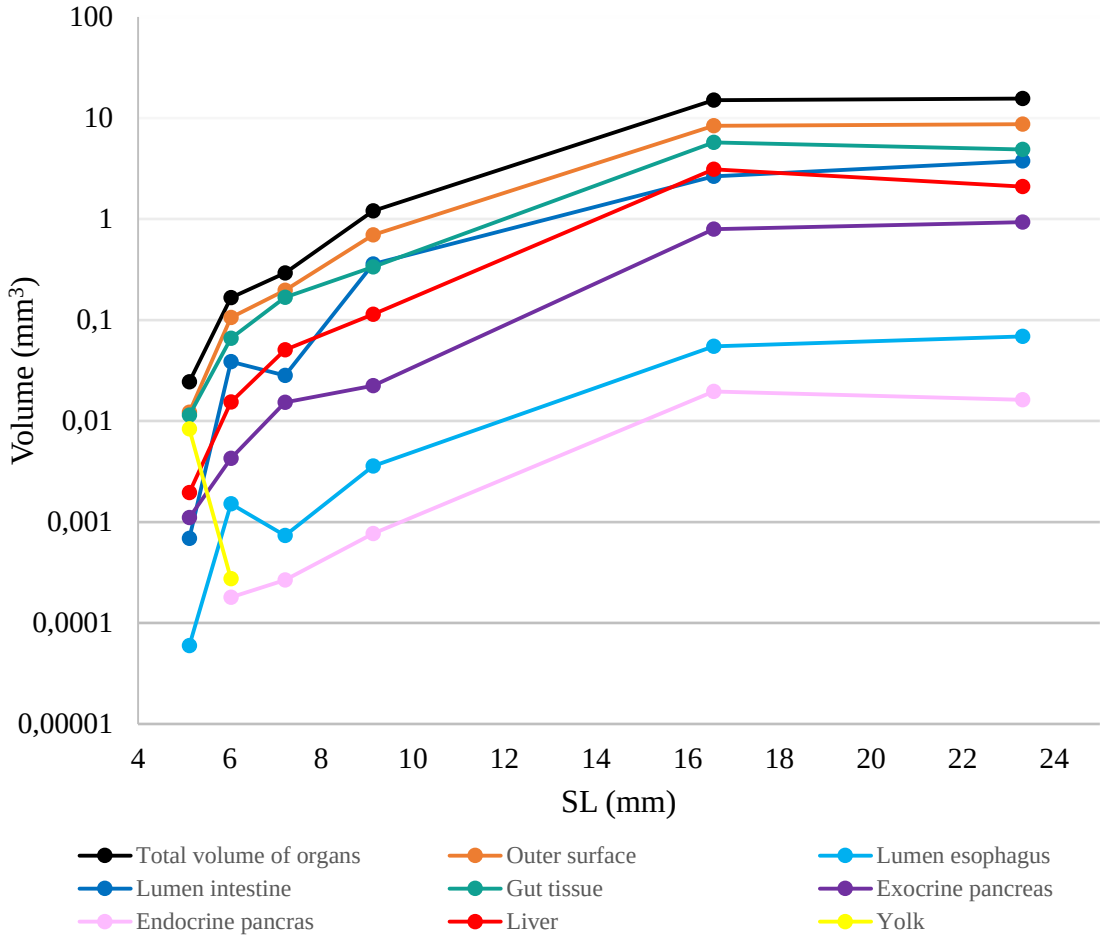

Figure 3.3 Total volume (sum of all volumes) and volume of each organ in ballan wrasse larvae and juveniles. Stage 1 (5.12 mm SL), Stage 2 (6.02 mm SL), Stage 3 (7.20 mm SL), Stage 4 (9.13 mm SL), Stage 5 (16.56 mm SL) and Stage 6 (23.31 mm SL).

The volume of gut tissue was measured as the difference between the volume of the outer surface of the digestive tract subtracted by the volume of intestinal plus esophageal lumen. This volume rose from 0.01 at Stage 1 to 4.87 mm^3 at Stage 6 (**Table 3.2, Figure 3.3**). The liver increased in volume from 0.001 mm^3 at Stage 1 to 3.10 mm^3 at Stage 5 and thereafter decreased to 2.09 mm^3 at Stage 6. The reduction in both surface area and volume of the liver is presumably due to formation of the hepatopancreas, which may compromise the liver's morphometric scaling. The volume of exocrine pancreatic tissue between Stage 1 and Stage 6 was initially at 0.0011 mm^3 and increased to 0.92 mm^3. The endocrine pancreas was observed from Stage 2 (0.0001 mm^3) until Stage 6 (volume 0.01 mm^3).

Table 3.2 Volumes (mm^3) of gut tissue, liver and exocrine and endocrine pancreatic tissue from Stages 1-6. Gut tissue* volumes were calculated as (volume of the outer surface of the digestive tract) minus (sum of volumes of esophageal- and intestinal lumens). Standard length (SL) in mm.

Stage	SL	Gut tissue*	Liver	Exocrine pancreas	Endocrine pancreas
1	5.12	0.01	0.001	0.001	
2	6.03	0.06	0.01	0.004	0.0001
3	7.21	0.16	0.05	0.01	0.0002
4	9.13	0.33	0.11	0.02	0.0007
5	16.57	5.70	3.10	0.79	0.01
6	21.31	4.87	2.09	0.92	0.01

The relative volumes of the digestive organs (gut tissue, liver, exocrine and endocrine pancreas) were calculated in percentages relatives (%) to each other for each stage (**Table 3.3**). The gut tissue always had the highest relative volume. Compared to the liver and pancreatic tissue, the relative volume of gut tissue declined from 78.9 % at Stage 1 to 61.6 % at Stage 6. The relative volume of liver and exocrine pancreas expanded from Stage 1 to 6. The liver increased gradually from 13.5 to 26.5% and the exocrine pancreas from 5-7.5 to 11.7%. The endocrine pancreas remained stable on 0.1-0.2% from Stage 2 and throughout the stages.

Table 3.3 Relative volume (%) of the gut tissue, liver and pancreatic tissue in Stages 1-6. SL in mm.

Stage	SL	Gut tissue	Liver	Exocrine pancreas	Endocrine pancreas
1	5.12	78.9	13.5	7.6	
2	6.03	76.8	18.0	5.0	0.2
3	7.21	71.7	21.6	6.6	0.1
4	9.13	71.0	24.1	4.7	0.2
5	16.57	59.3	32.3	8.2	0.2
6	21.31	61.6	26.5	11.7	0.2

The specific growth rates (SGR) were calculated using the increase of organ and tissue volumes between each stage and from the start to the end of the study (Stages 1-6) to calculate the percentage increase in volume per day (**Table 3.4**). All organs displayed strong growth from Stage 1 to 2, and gradually declined towards Stage 6. The outer surface of the digestive tract, esophageal and intestinal lumen as well the gut tissue (surface subtract the lumens) displayed a daily increase of 6.70, 7.19, 8.78 and 6.17% day^{-1} respectively from Stage 1-6. Liver and

exocrine pancreas grew at the rate of 7.12 and 6.87% day^{-1} from Stages 1-6. The endocrine pancreas (Islets of Langerhans) had a strong SGR of 16.93% day^{-1}. The overall morphometric scaling (surface area and volume) of the digestive system is summarised in **Appendix C**.

Table 3.4 Specific growth rate (SGR) of organs per day (% day^{-1}) in ballan wrasse between each stage (1-2, 2-3, 3-4, 4-5, 5-6) and SGR from Stage 1-6.

Stages	**1 to 2**	**2 to 3**	**3 to 4**	**4 to 5**	**5 to 6**	**1 to 6**
Day difference	6	8	11	42	31	98
Total volume	32.03	7.03	12.81	6.02	0.12	6.59
Outer surface GI-tract	36.08	7.69	11.51	5.92	0.11	6.70
Esophageal mucosa (lumen)	53.81	-9.02	14.37	6.50	0.74	7.19
Intestinal mucosa (lumen)	67.18	-3.89	23.07	4.75	1.14	8.78
Gut tissue (surface – lumen)	29.20	11.64	6.31	6.75	-0.51	6.18
Liver	34.46	14.80	7.35	7.88	-1.27	7.12
Exocrine pancreas	22.59	15.96	3.41	8.50	0.51	6.87
Endocrine pancreas	201.61	4.93	9.64	7.71	-0.63	16.93

The digestive system grew rapidly (in surface area, volume and SGR) in the earliest stages, but came to a halt between Stages 5 and 6, suggesting that the digestive system had matured, and that juveniles redirect their energy towards growth of muscles (**Figure 3.4**).

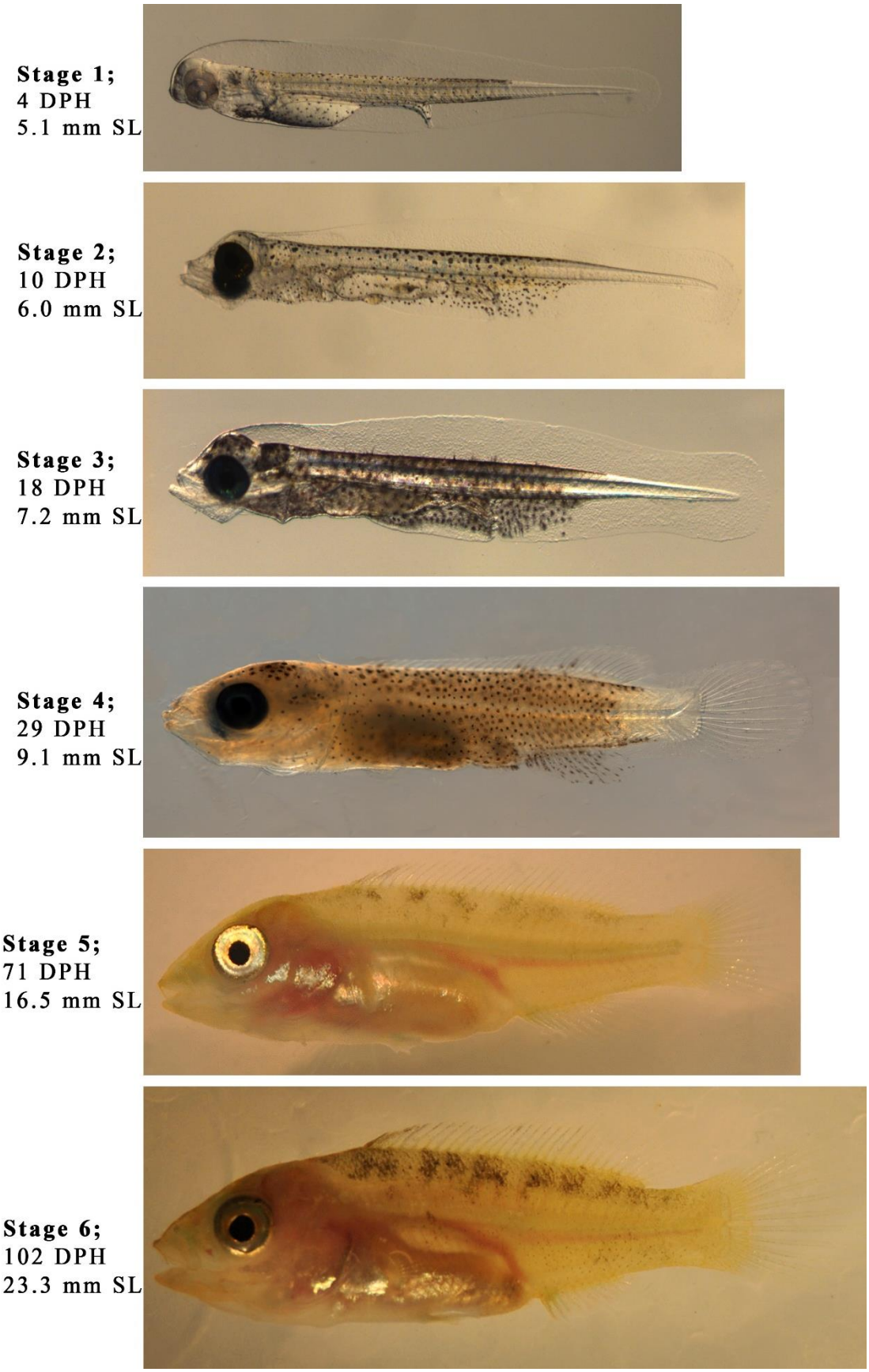

Figure 3.4 External morphological characters of ballan wrasse larvae and juvenile from 4 dph (Stage 1) until 102 dph (Stage 6).

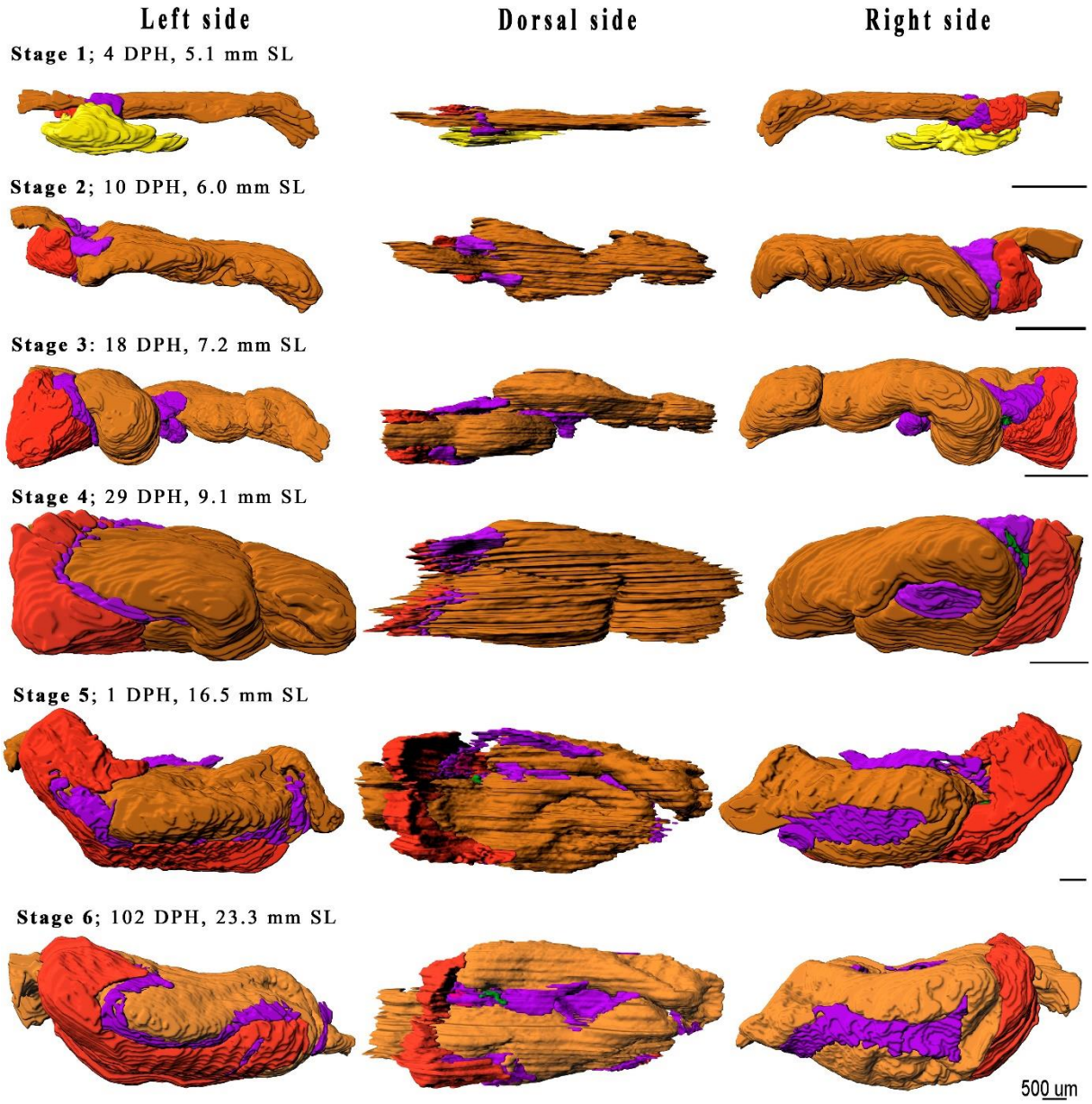

Figure 3.5 Reconstructed 3D models showing the development of the digestive system in ballan wrasse larvae and juvenile from Stage 1 until Stage 6 seen from left, dorsal and right side. *Orange* adventitia and serosa of the digestive tract. *Red* liver. *Purple* exocrine pancreas. *Pink* endocrine pancreas. *Green* gallbladder.

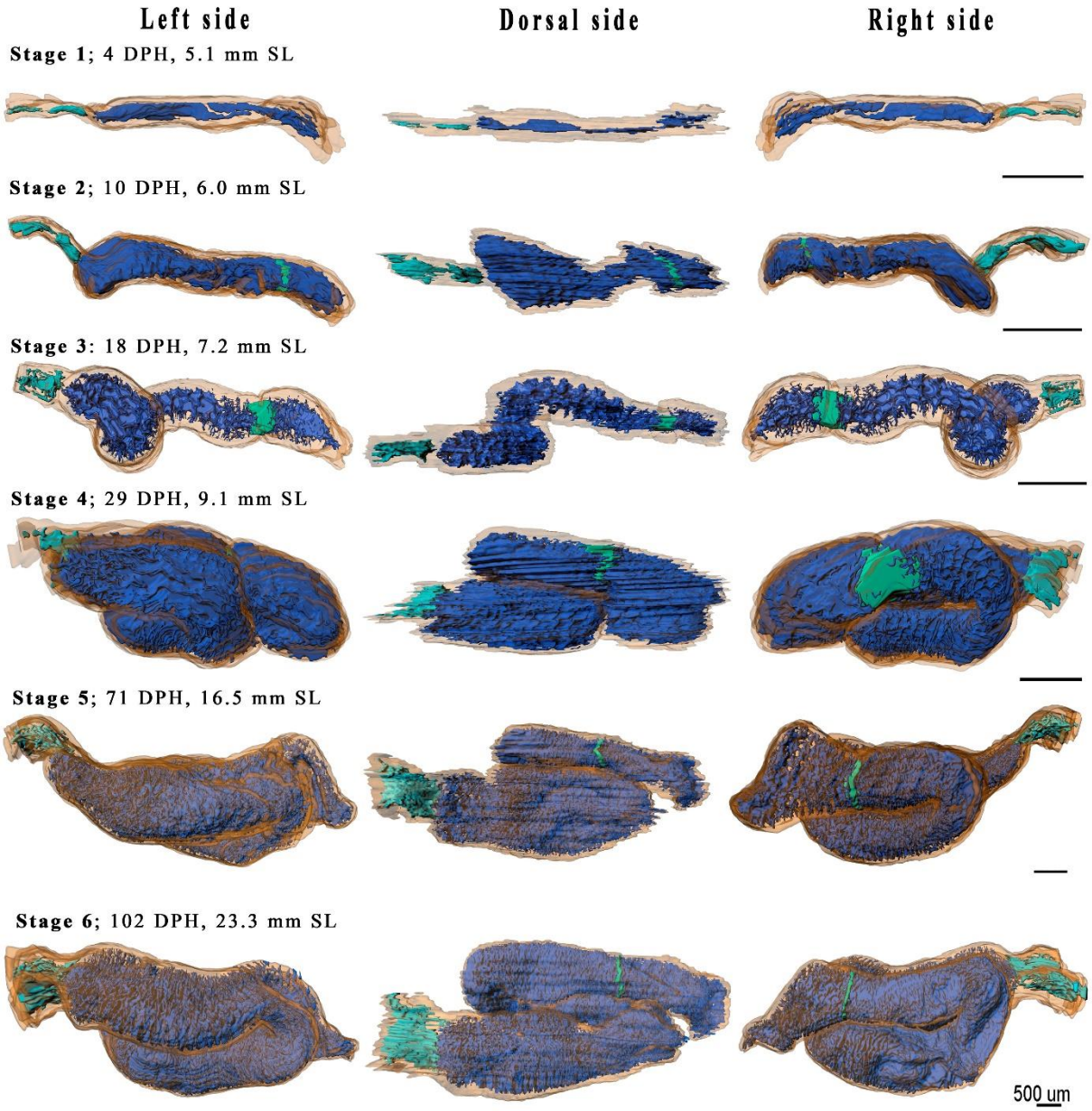

Figure 3.6 Ontogeny of the intestinal lumen in ballan wrasse from Stage 1 larva until Stage 6 juvenile seen from left, dorsal and right side. *Light blue* esophageal lumen. *Dark blue* intestinal lumen. *Turquoise* ileorectal valve. *Orange* adventitia and serosa of the digestive tract (90% transparency).

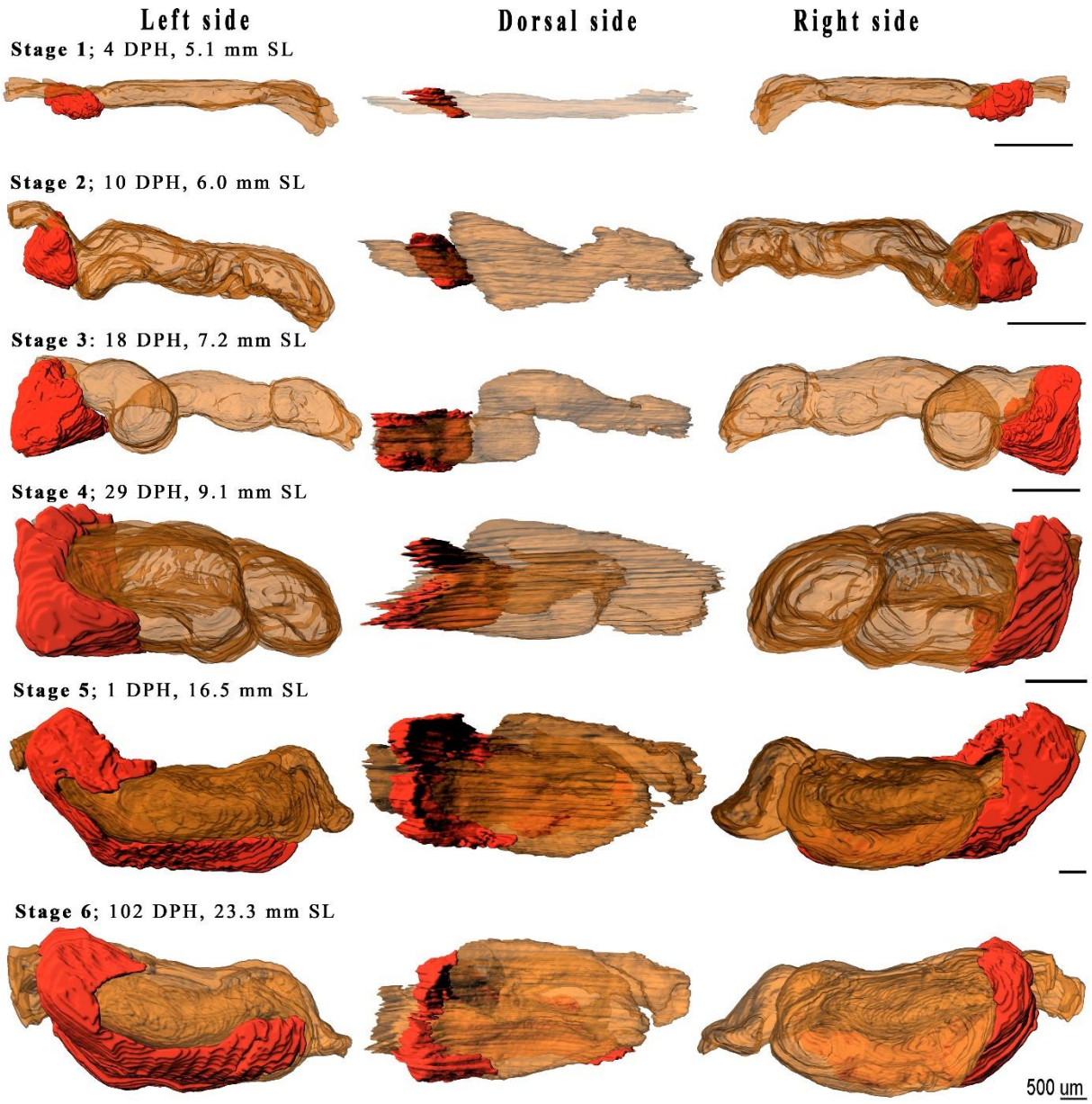

Figure 3.7 3D reconstruction of the ontogeny of the liver in ballan wrasse larvae and juvenile form Stage 1 until Stage 6, studied from the left, dorsal and right side. *Orange* adventitia and serosa of the digestive tract (60 % transparency). *Red* liver.

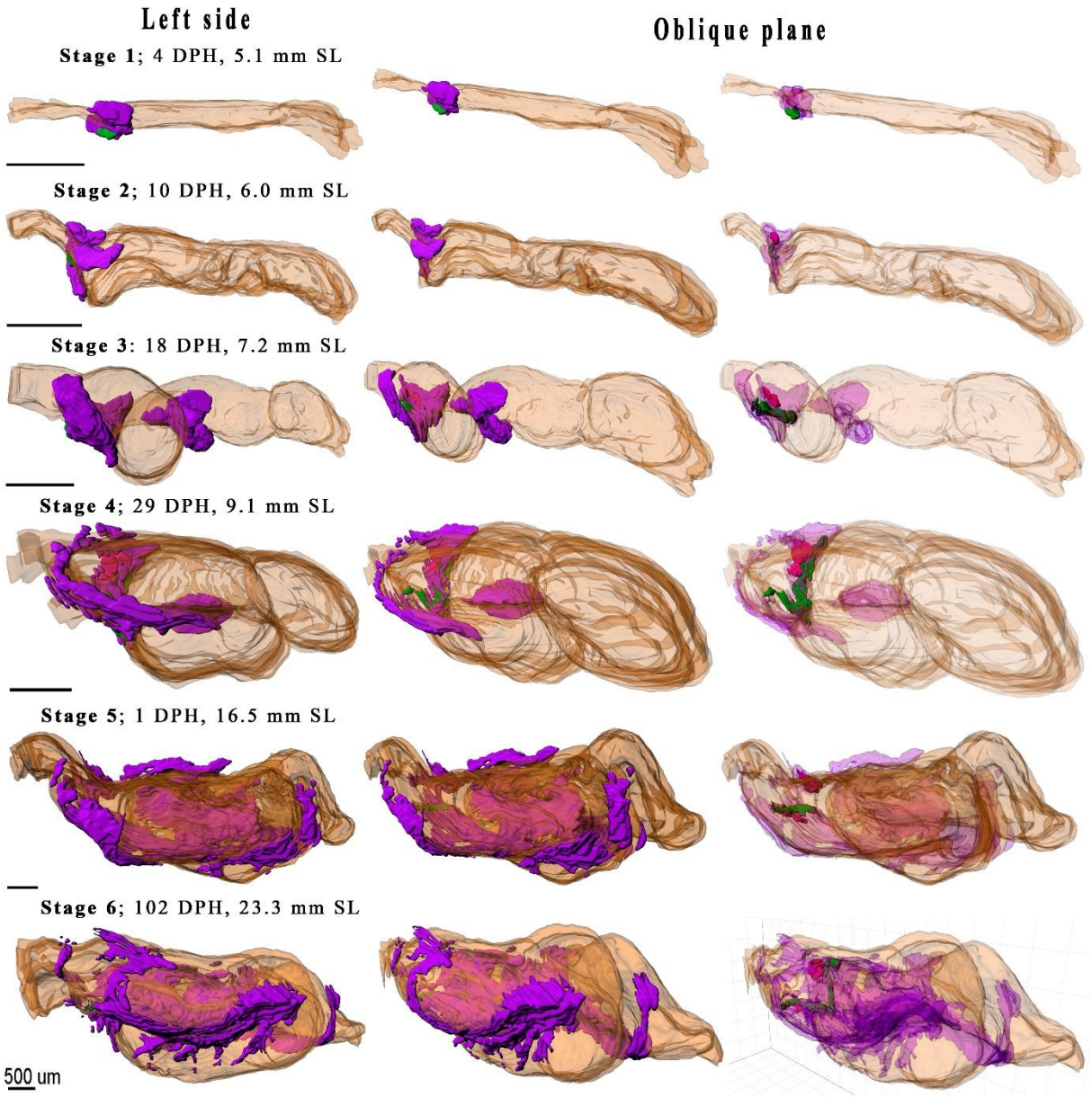

Figure 3.8 Ontogeny and partial distribution of exocrine pancreas (purple), endocrine tissue (dark pink), pancreatic duct (bright pink) and gallbladder (green) in relation to the outer surface of the digestive tract (orange) seen from the left side and oblique plane. The left and middle rows show the outer surface of the digestive tract at 60% transparency. Right row shows the digestive tract at 80 % transparency and exocrine pancreas at 60% transparency.

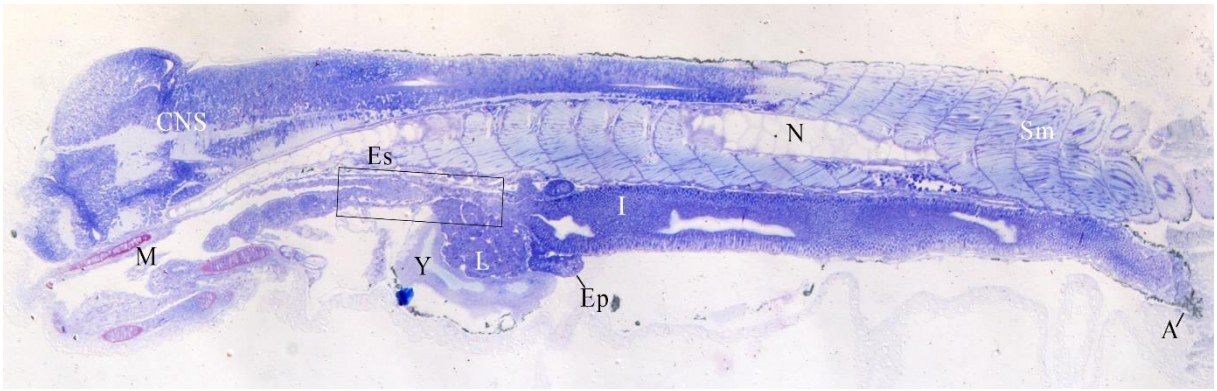

Figure 3.9 Mid-longitudinal section of the digestive system in Stage 1 (4 DPH) ballan wrasse larvae. *A* anus. *CNS* central nervous system. *Ep* endocrine pancreas. *Es* esophagus. *I* incipient intestine. *L* liver. *M* mouth. *N* notochord. *Sm* skeletal muscle. *Y* yolk. Stained toluidine blue, 10x magnification.

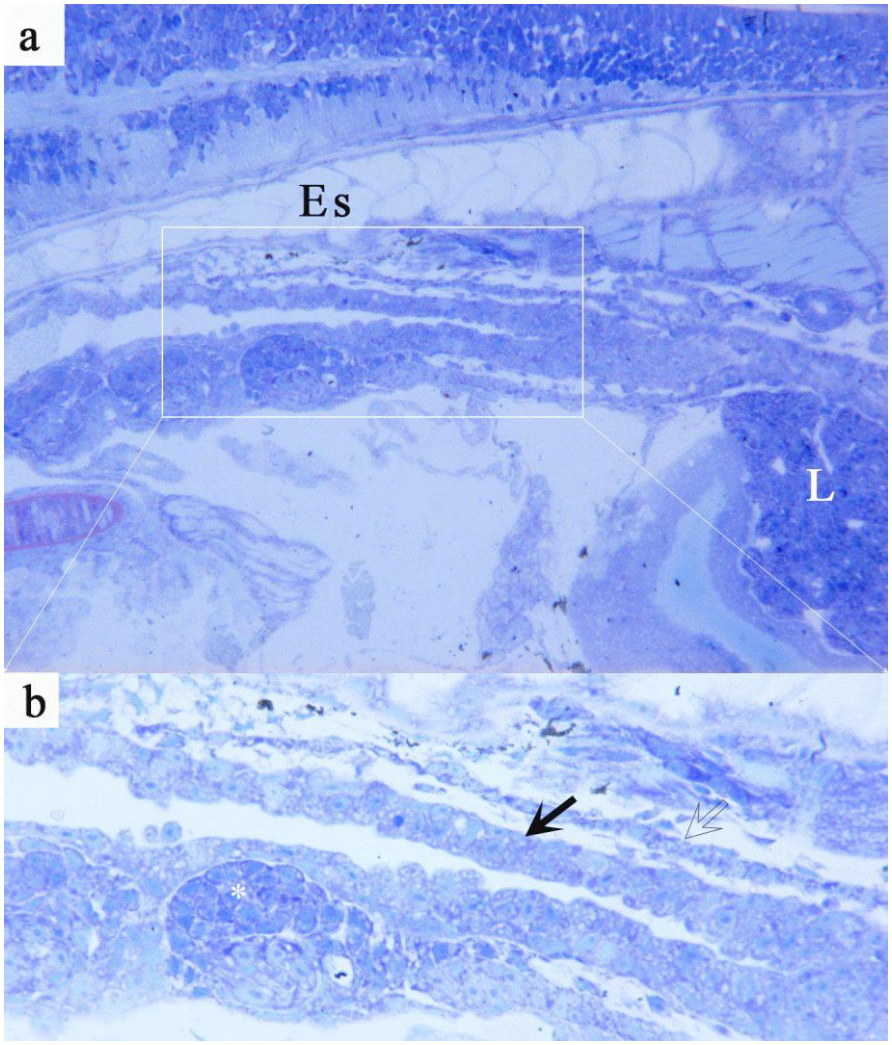

Figure 3.10 Esophagus (*Es*) in Stage 1 ballan wrasse larva. In a) the esophagus is short and located dorsally for the liver (*L*) at 20x magnification. b) 40x magnification of the proximal esophagus with simple cuboidal epithelium (*black arrow*) and very thin external muscle layer (*transparent arrow*). Possibly a taste bud in the lower left (*white asterisk*, *).

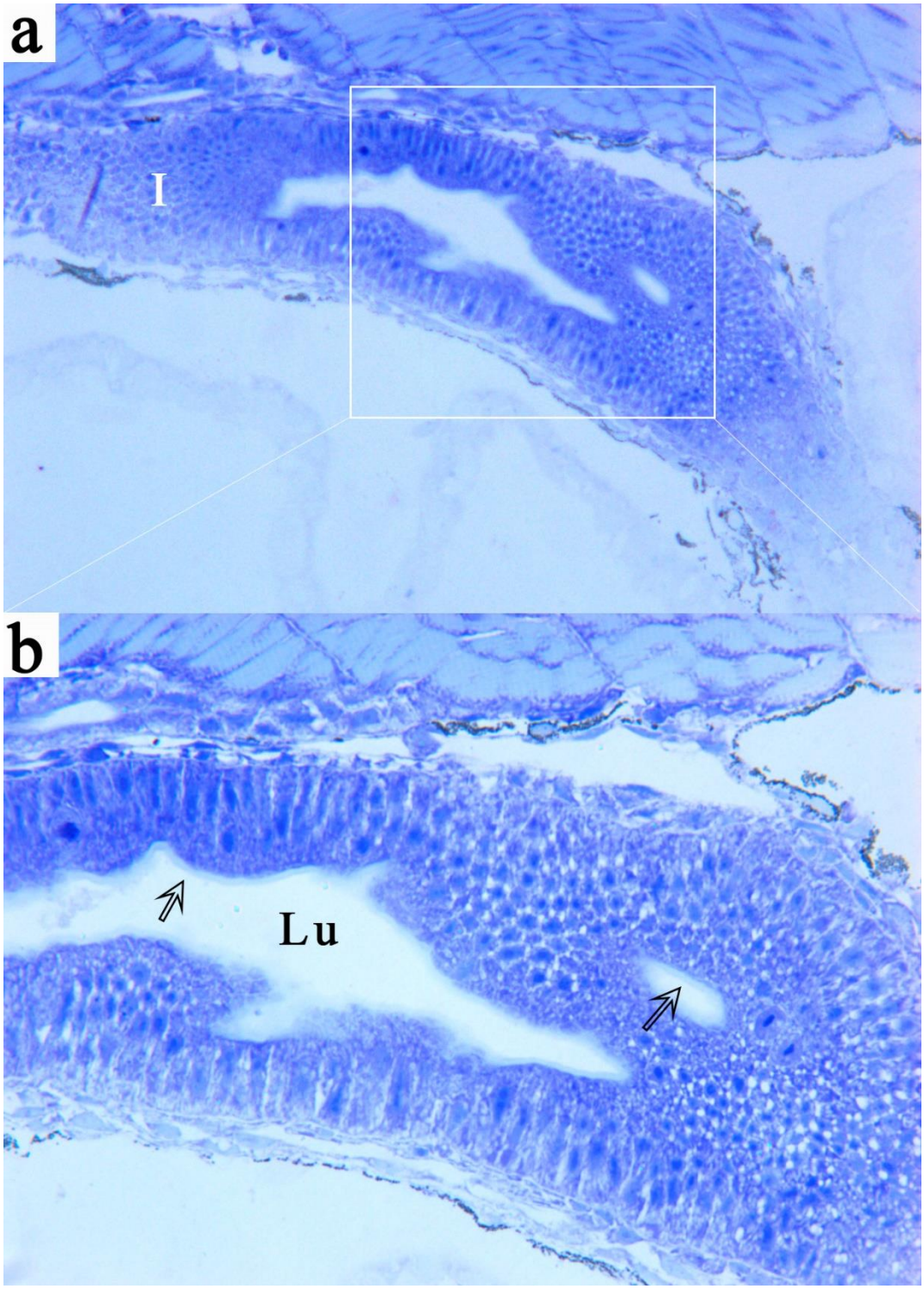

Figure 3.11 Posterior incipient gut in Stage 1 ballan wrasse under a) 20x magnification and b) 40x magnification. The enterocytes creates a simple columnar epithelium with microvilli (*black arrow*) in the apical end of the cell into the lumen (*Lu*) of the incipient intestine. *Submucosa* and *m. externa* in very thin.

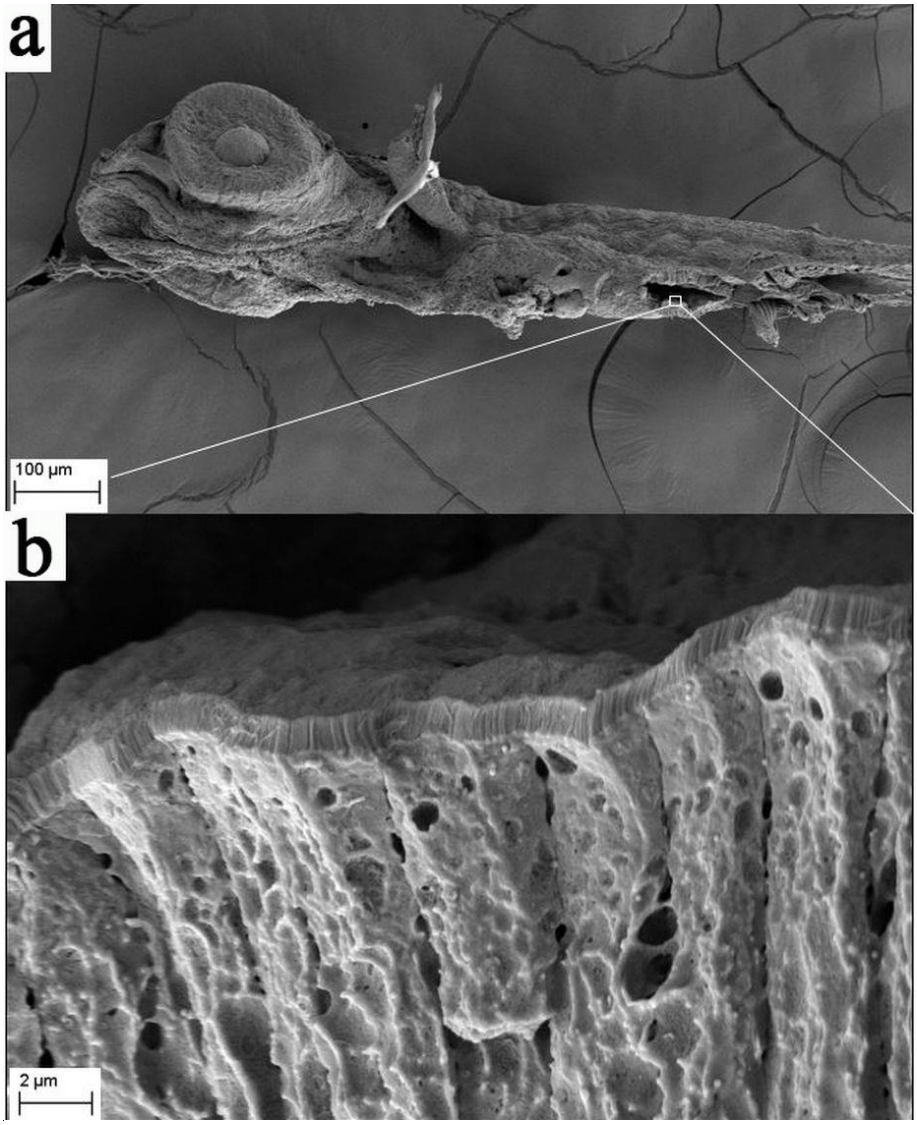

Figure 3.12 Scanning EM of Stage 1 ballan wrasse larva showing clear brush border of the apical end of the enterocytes.

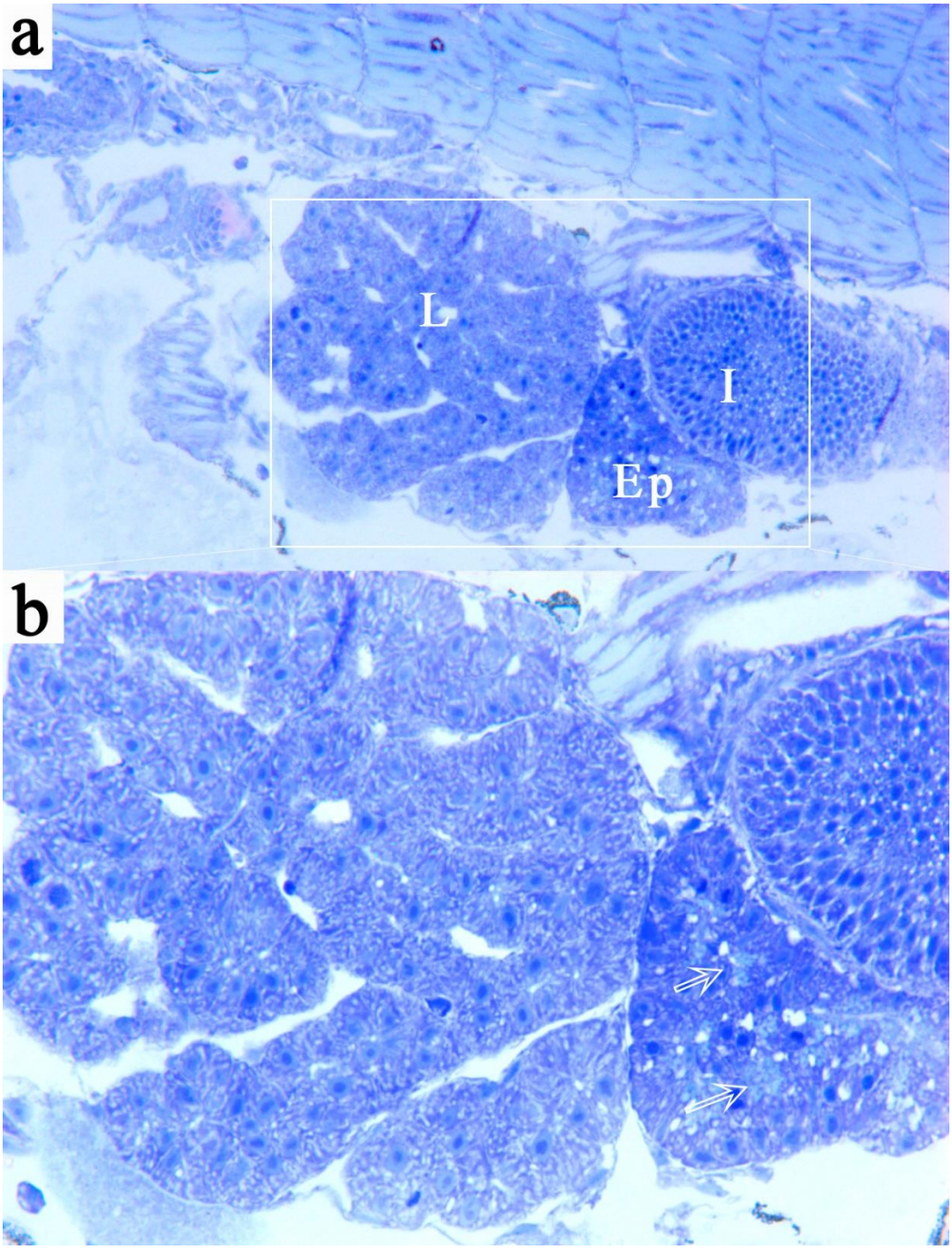

Figure 3.13 Liver (*L*), exocrine pancreas (*Ep*) and incipient gut (*i*) in Stage 1 ballan wrasse larva at a)10x magnification and b) 40x magnification. The structure of the hepatocytes (containing prominent nucleolus and scarce fat deposit) and sinusoids forming a tubular gland. Few zymogen granules (*white arrows*) located within the exocrine pancreas. Stained toluidine blue.

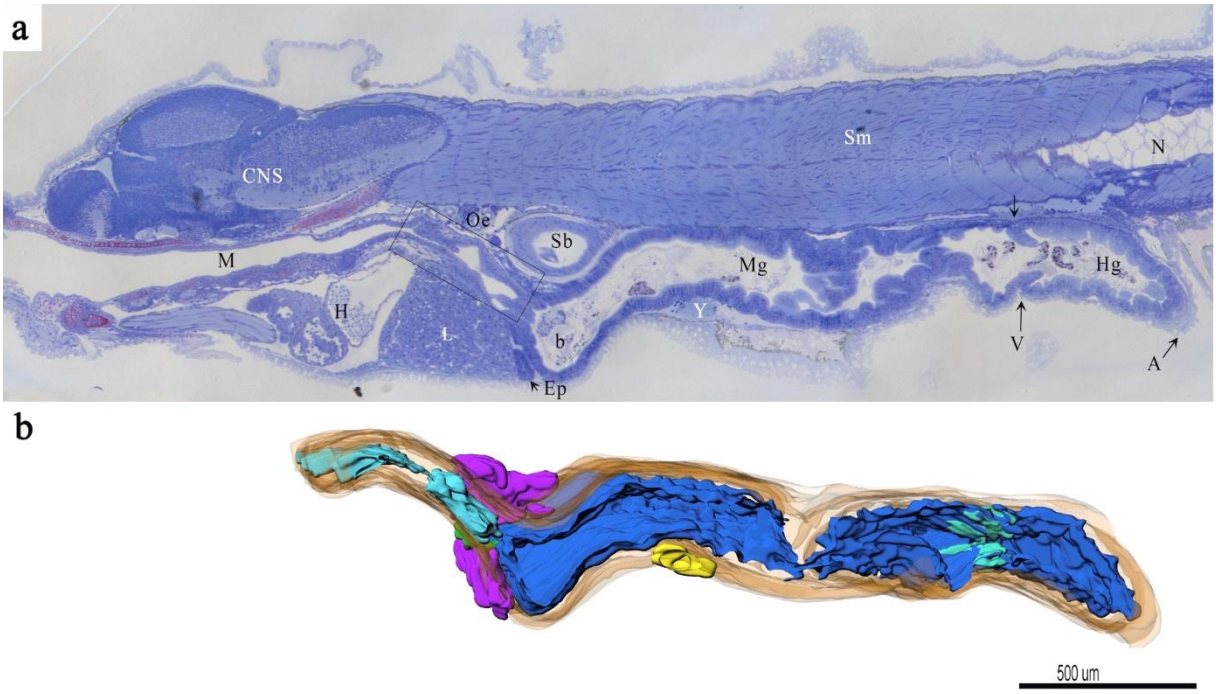

Figure 3.14 a) Mid-longitudinal section of Stage 2 (10 DPH) larvae. The length of the esophagus (*Es*) is marked with a black box; starts at the end of the pharynx and end with a constriction prior to the bulbus (*B*). The intestinal folding increases towards the anus (*A*). *A* anus. *B* bulbus. *CNS* central nervous system. *Ep* exocrine pancreas. *H* heart. *Hg* hindgut. *Oe* esophagus. *L* liver. *M* mouth. *Mg* midgut. *N* notochord. *Sb* swimbladder. *Sm* skeletal muscle. *V* ileoractal valve. *Y* yolk. Stained toulidineblue, 10x magnification. b) Sagittal view of the digestive system in Stage 2 from 3D reconstruction. Note the remnant of yolk (*yellow*) located dorally for the intestine. *Light blue* mucosal surface of the esophagus. *Purple* exocrine pancreas. *Dark blue* mucosal surface of the intestine. *Green* gallbladder. *Turquiose* ileorectal valve. *Organge* outer surface of the digestive tract.

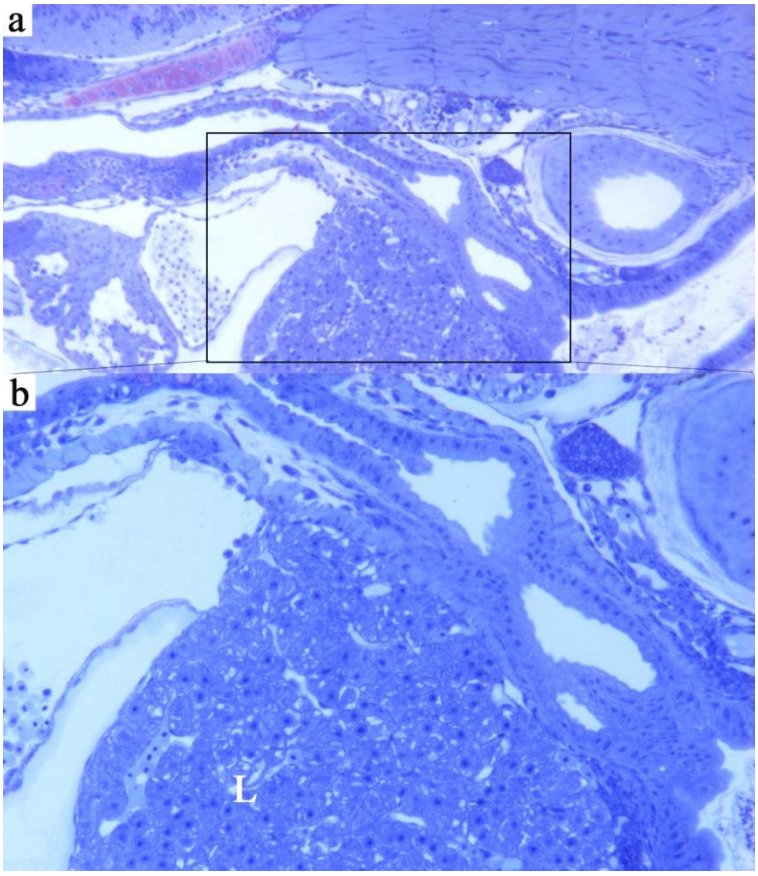

Figure 3.15
The esophageal lumen in Stage 2 under a) 10x magnification with few goblet cells located in the proximal region and prominent *m. externa*, and b) 20x magnification. The esophagus is located dorsally for the vasculated liver (*L*) and ends in a constriction in the transit to intestinal lumen.

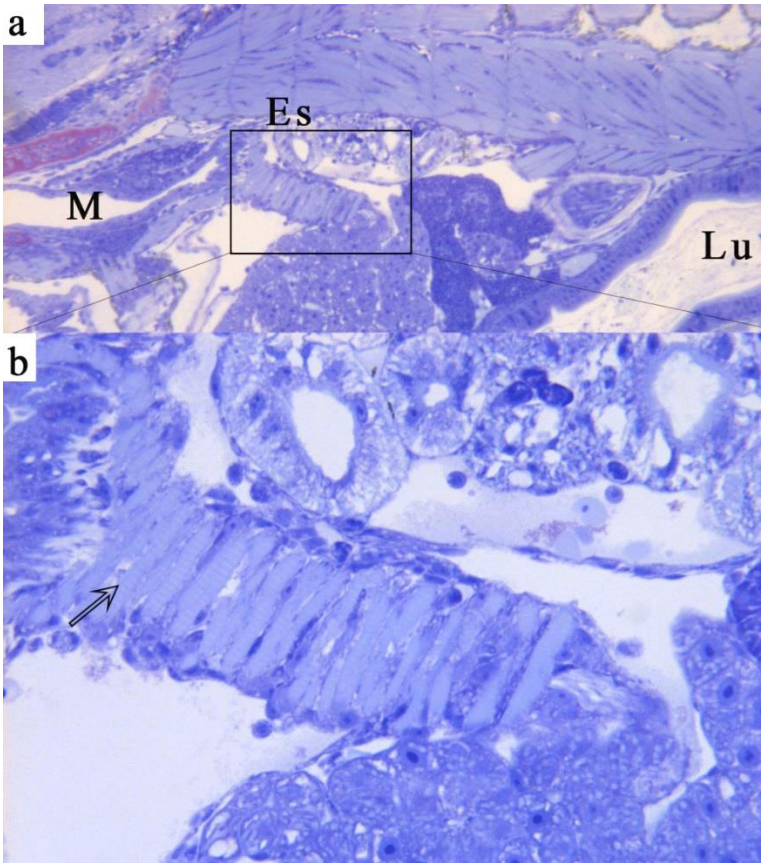

Figure 3.16 External muscle layer, *m. externa* of the esophagus in a) 10x magnification and b) 40x magnification. The proximal region consist of striated muscle fibres (*arrow*). *Es* esophagus. *Lu* lumen of the intestine. *M* mouth.

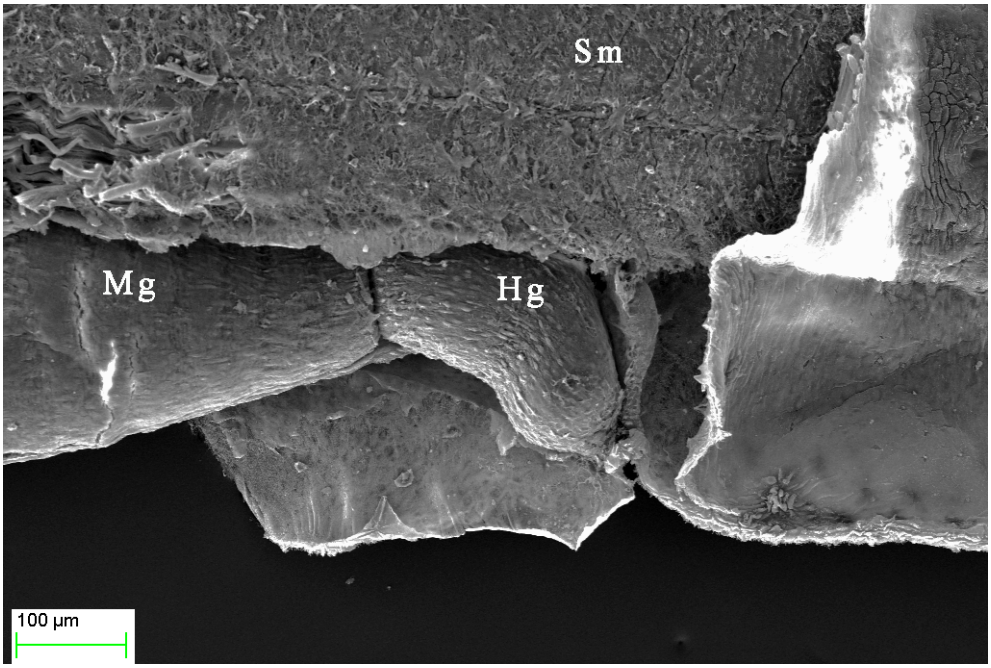

Figure 3.17 Scanning electron micrograph of the external morphology of the digestive tract in Stage 2 ballan wrasse. The midgut (*Mg*) and hindgut (*Hg*) is separated by an internal valve as well as a narrow passage seen on the organ surface. *Sm* skeletal muscle.

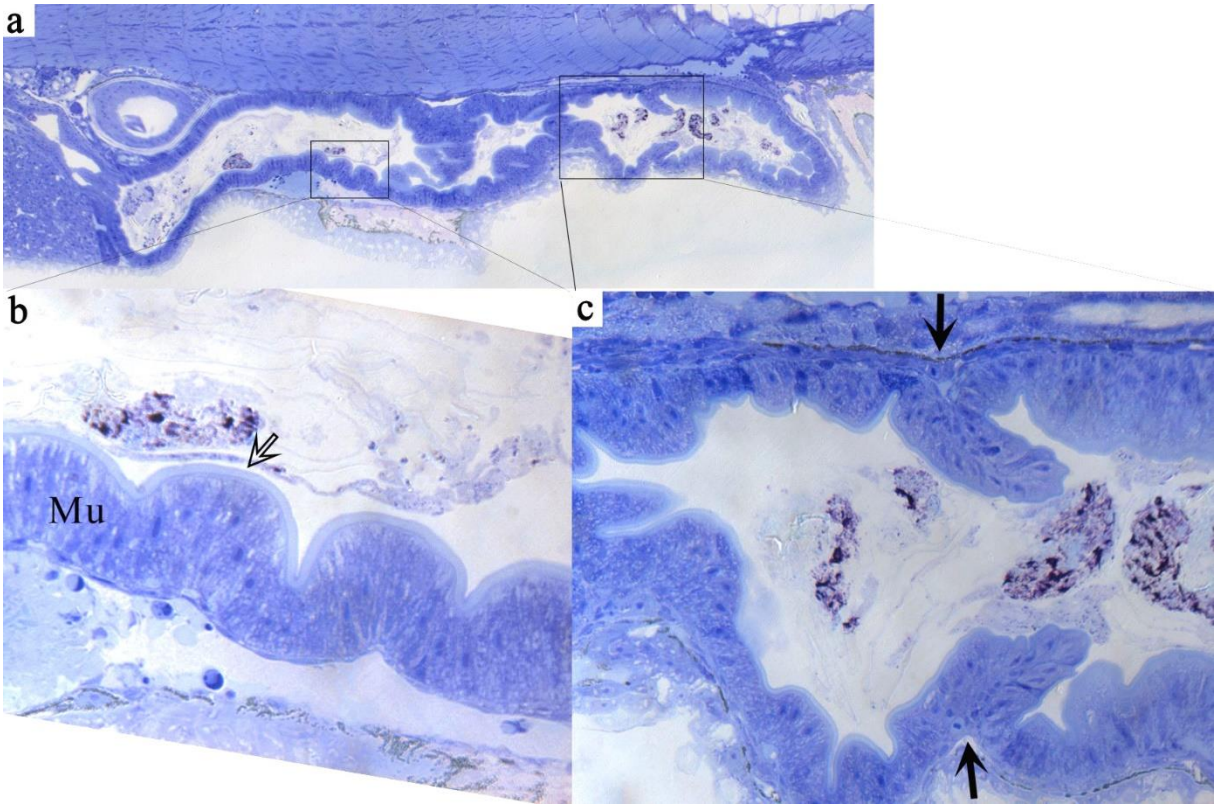

Figure 3.18 The intestine in Stage 2. a) Overview of the intestine at 10x magnification. b) Leaf-like structure of the intestinal mucosa (*Mu*) with prominent brush border (*arrow*) in the midgut at 40x magnification. c) Ileo-rectal valve (*black arrows*) seperates the midgut and hindgut. No muscular increase at the base of the valve were not observed in any section, 40x magnification.

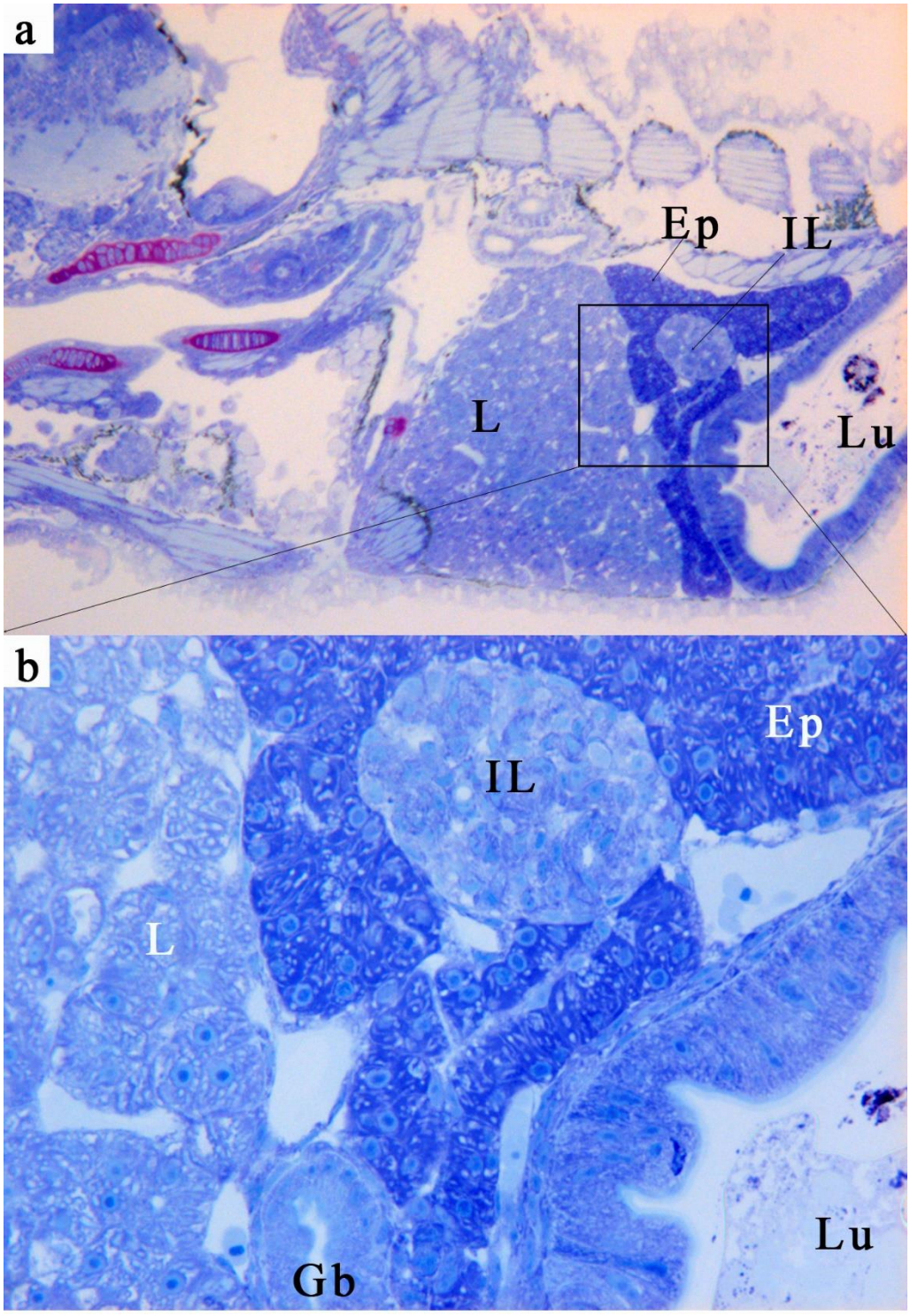

Figure 3.19 a) Anterior region of the digestive system in Stage 2 (10 DPH) ballan wrasse larva at 10x magnification and b) 40x magnification. Small fat deposits in the liver (*L*) observed as vacuoles. One primary islet of Langerhans (*IL*) was located close to the gallbladder (*Gb*). The enterocytes of the intestine hade a leaf-like structure towards the lumen (*Lu*). *Ep* exocrine pancreas. *Gb* gallbladder. *i* intestinal lumen. *Il* primary islet of Langerhans. *K* kidney. *L* liver.

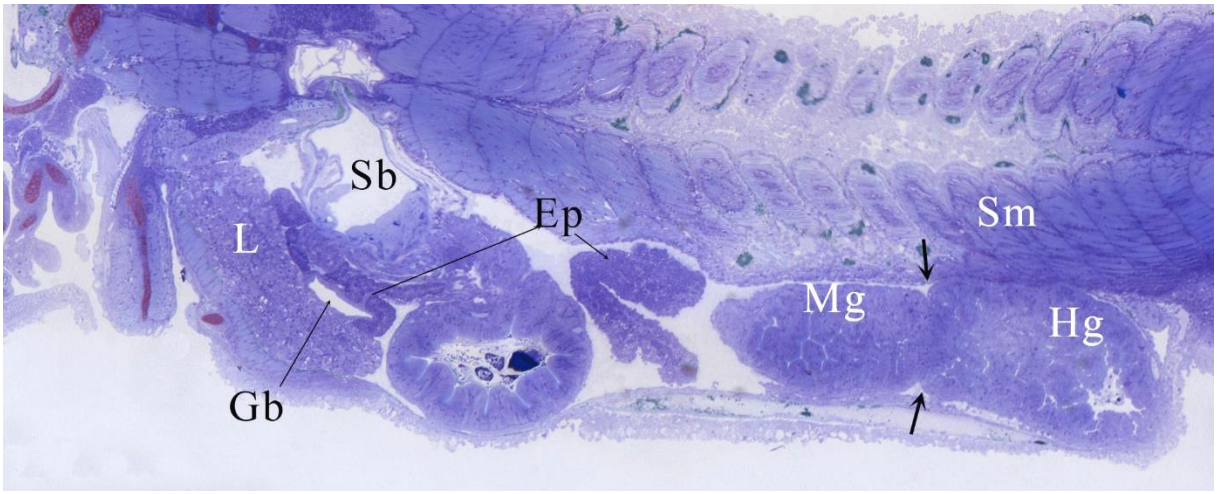

Figure 3.20 Mid-longitudinal section of Stage 3; 18 DPH. The midgut starts to rotate, and exocrine pancreatic tissue (Ep) becomes scattered along the digestive tract. E*p* endocrine pancreas. *Gb* gallbladder. *Hg* hindgut. *L* liver. *Mg* midgut. S*b* swimbladder. *Sm* skeletal muscle.

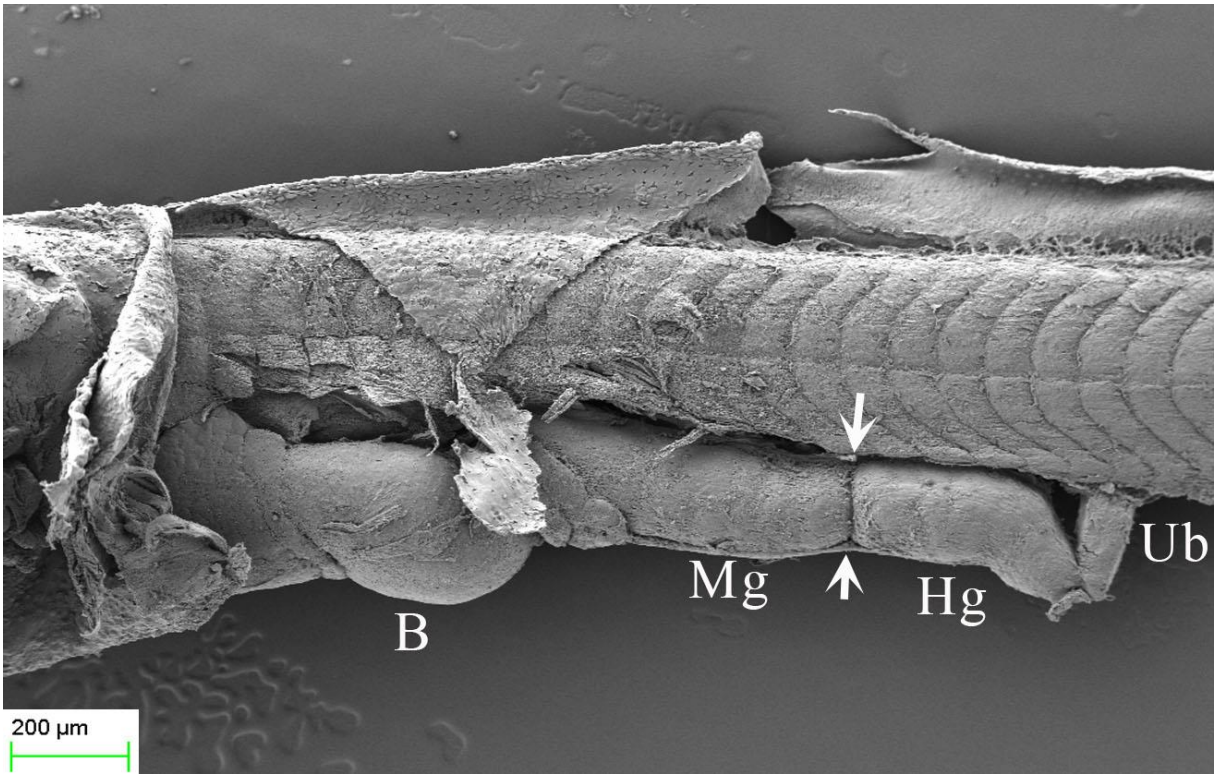

Figure 3.21 Scanning electron micrograph of the outer surface of the digestive tract, divided into bulbus (*B*), midgut (*Mg*) separated from the hindgut (*Hg*) by a valve (*black arrows*). The hindgut ends with an anus along with the opening of the urinary bladder (*Ub*).

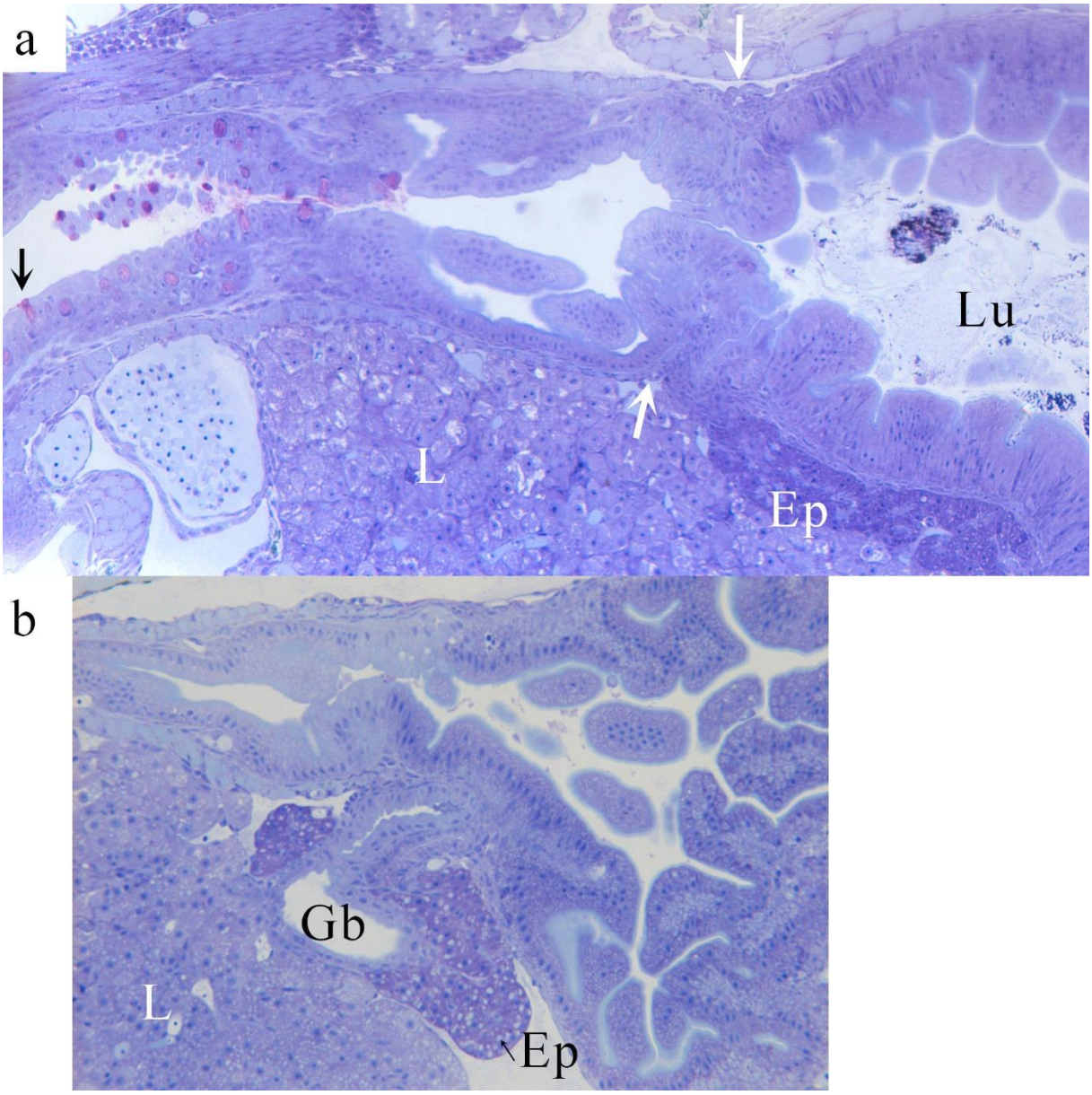

Figure 3.22 Histological section in Stage 3 (18 DPH) ballan wrasse larva at a) The esophageal mucoid mucosa (*black arrow* goblet cells) was surrounded by thick *m. externa* where the circular muscle layer was the most prominent layer. The prominent muscle layer was lost when the esophagus enters the intestinal lumen (*Lu*) just after the constriction between the esophagus and the midgut (*white arrows*). The intestine has an overall high structure of single columnar epithelium at 10x magnification and b) The gallbladder (Gb) was located between the liver tissue and exocrine pancreas (Ep) and the ductus choledochus empties the bile from the gallbladder into the intestinal lumen shorty after the end of the esophagus, 20x magnification.

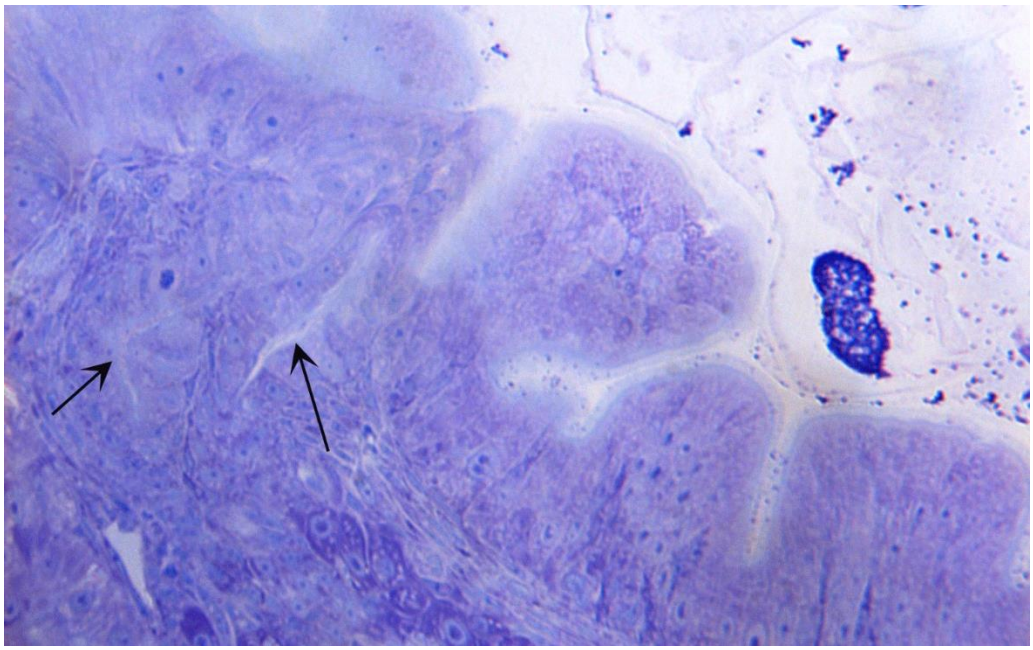

Figure 3.23 Entrance of the pancreatic duct, (*ductus hepaticus*) and common bile duct (*ductus cholechodus*) into the lumen of the bulbus in Stage 3 ballan wrasse. The ducts never merges, but end in the lumen as two separate openings.

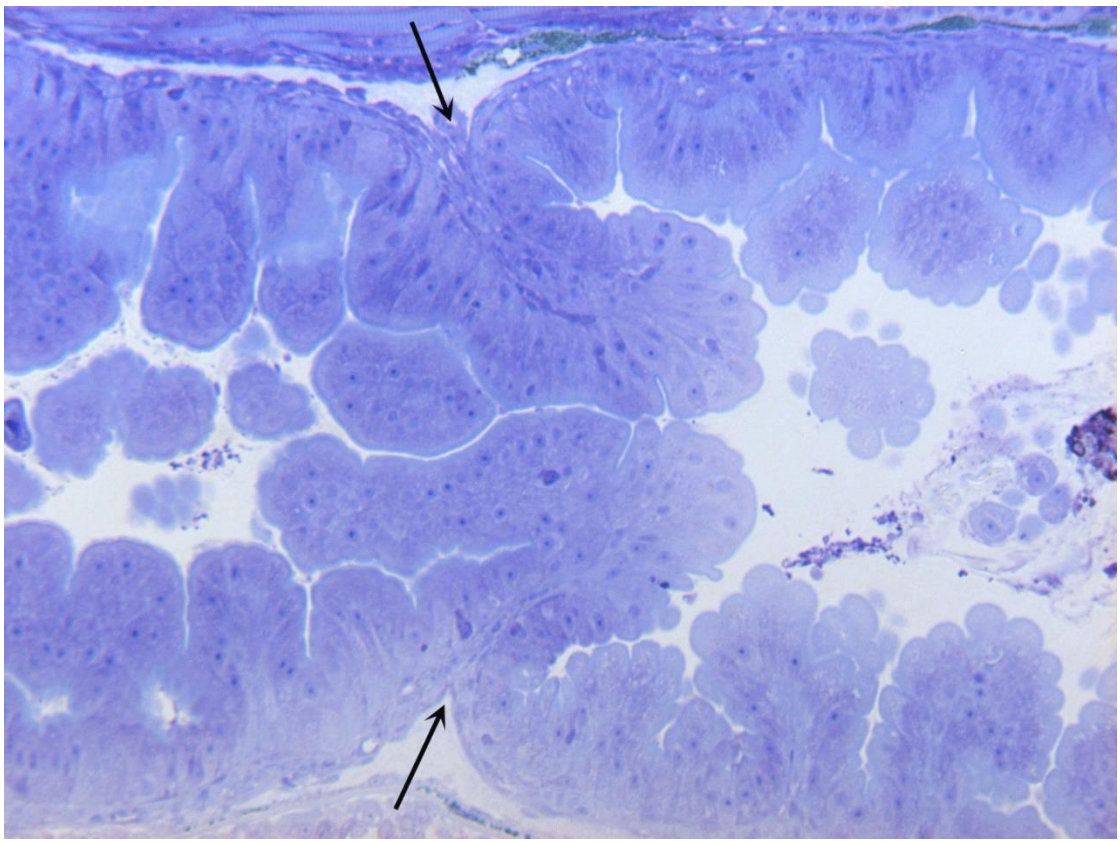

Figure 3.24 Valve (*black arrows*) between distal midgut and hindgut in Stage 3 larvae. Increased external muscle layer at the base of the valve were not observed.

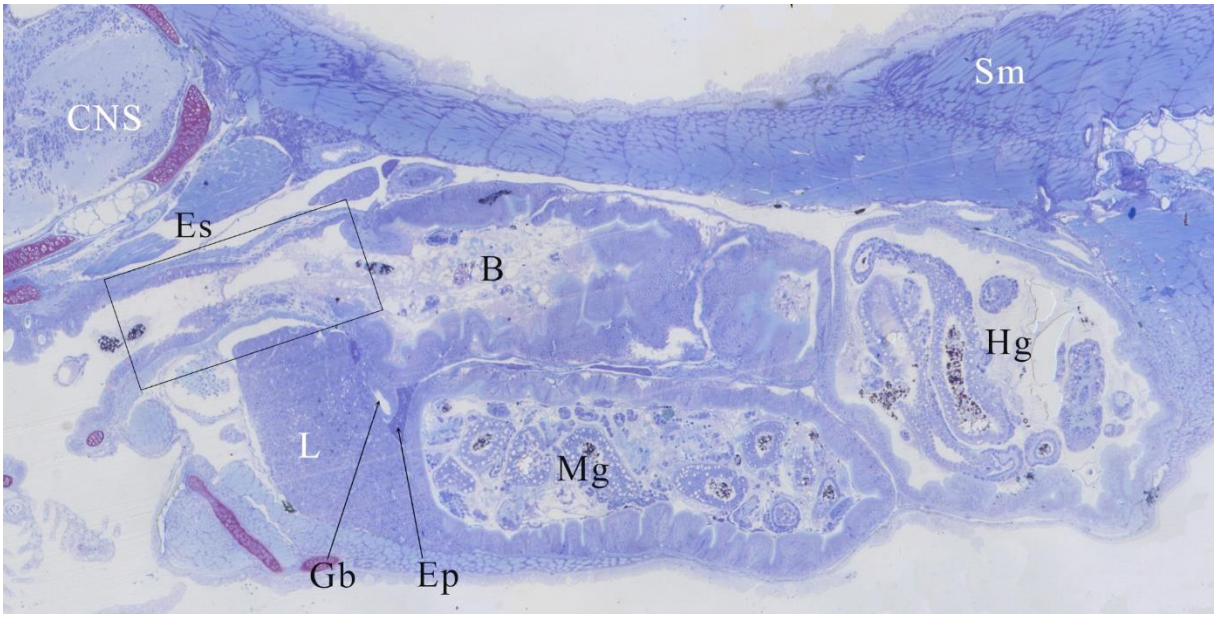

Figure 3.25 Mid-longitudinal section of the digestive system of Stage 4 ballan wrasse larva. *CNS* central nervous system. *B* bulbus. *Ep* exocrine pancreas. *Es* esophagus (length marked as a box). *Gb* gallbladder. *Hg* hindgut. *L* liver. *Mg* midgut. S*m* skeletal muscle.

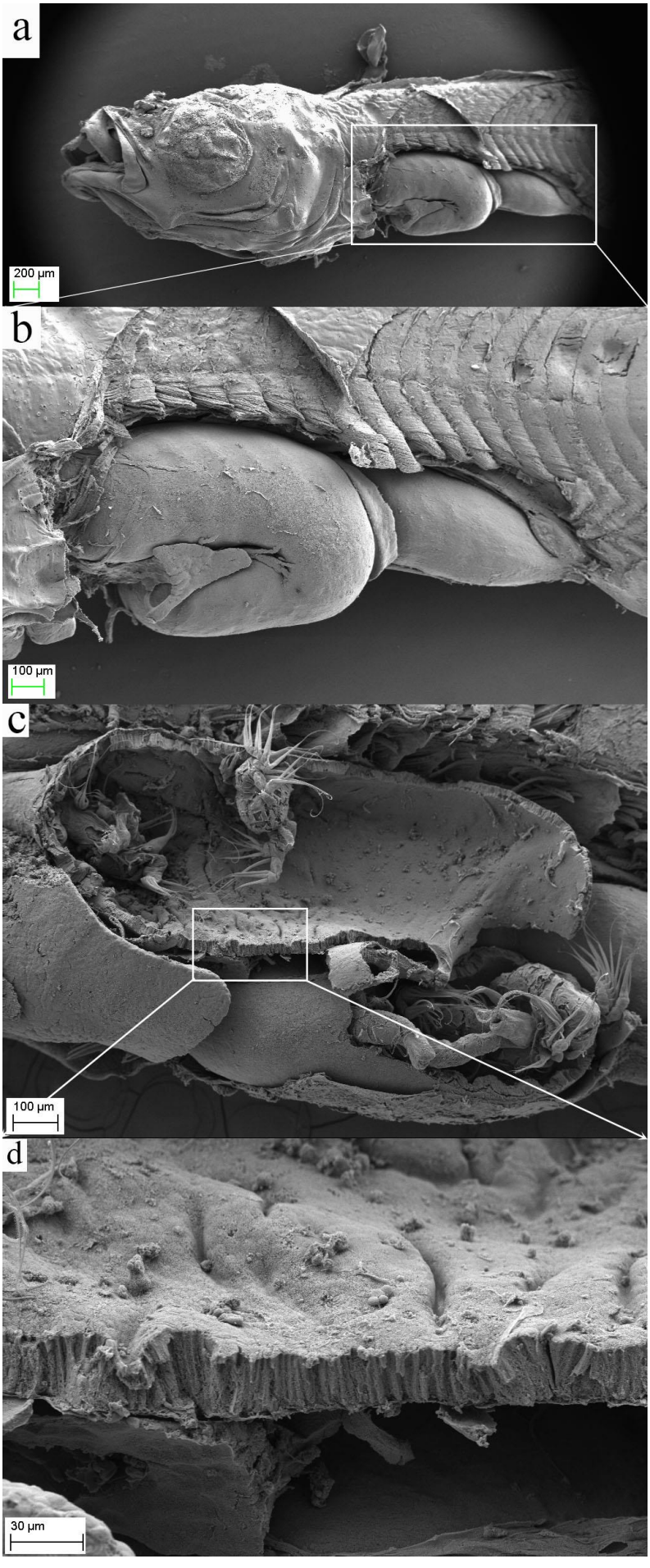

Figure 3.27 A-B) Scanning EM of the left outer surface of the digestive tract in Stage 4 (29 DPH) ballan wrasse larvae showing the bulbus, intestinal rotation and hindgut ending with the anus. c) sagittal section of the digestive tract shows digested *Artemia* in the bulbus and middle midgut. d) Mucosal folding by the enterocytes of the bulbus. Lipid droplets and or mucus droplets superficial for the enterocytes.

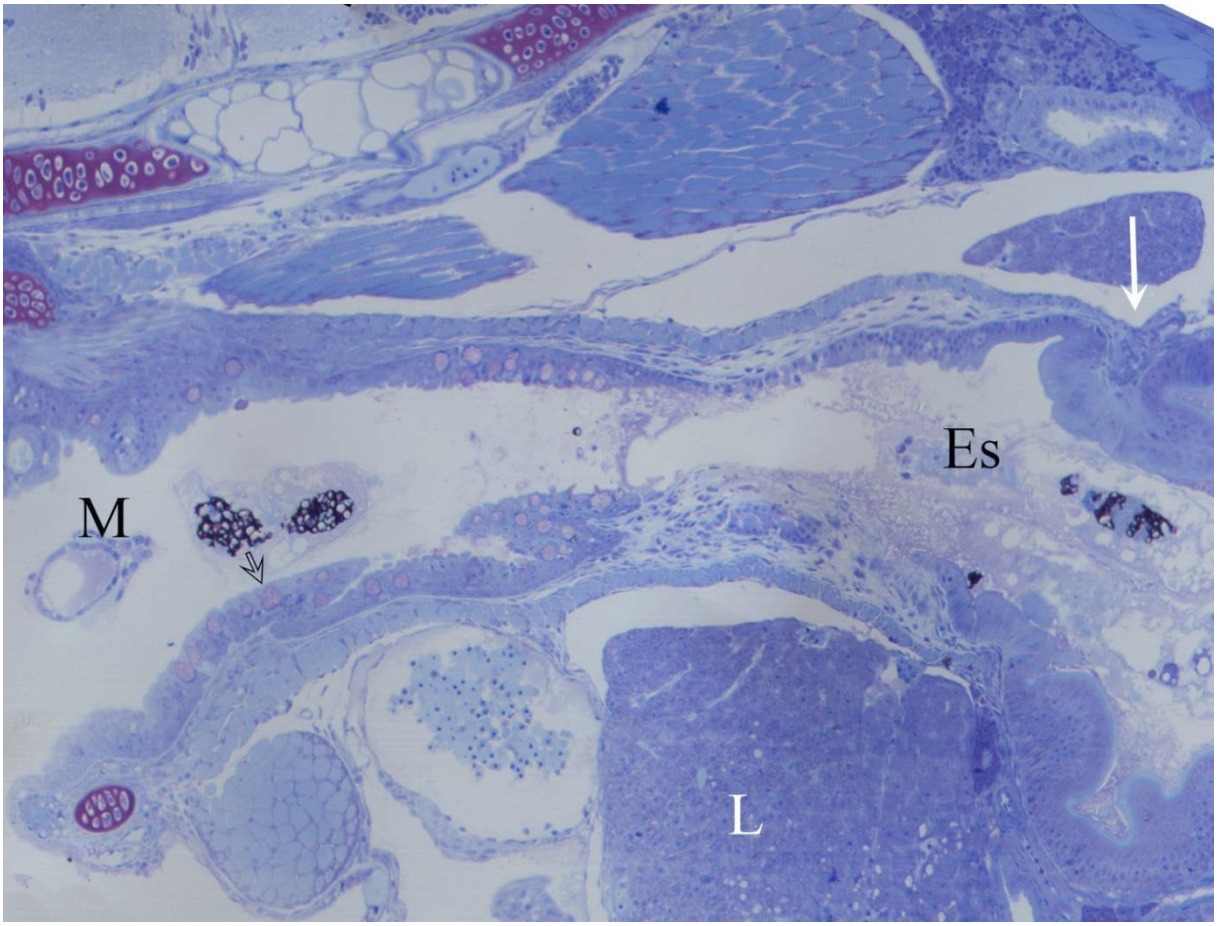

Figure 3.27 Esophagus (*Es*) in Stage 4 were located dorally for the liver (*L*). The mouth (*M*) and proximal region of the esophagus contains goblet cells (*black arrow*), which were absent in the distal region. The esophagus ended in a constriction (*white arrow*) prior to the bulbus.

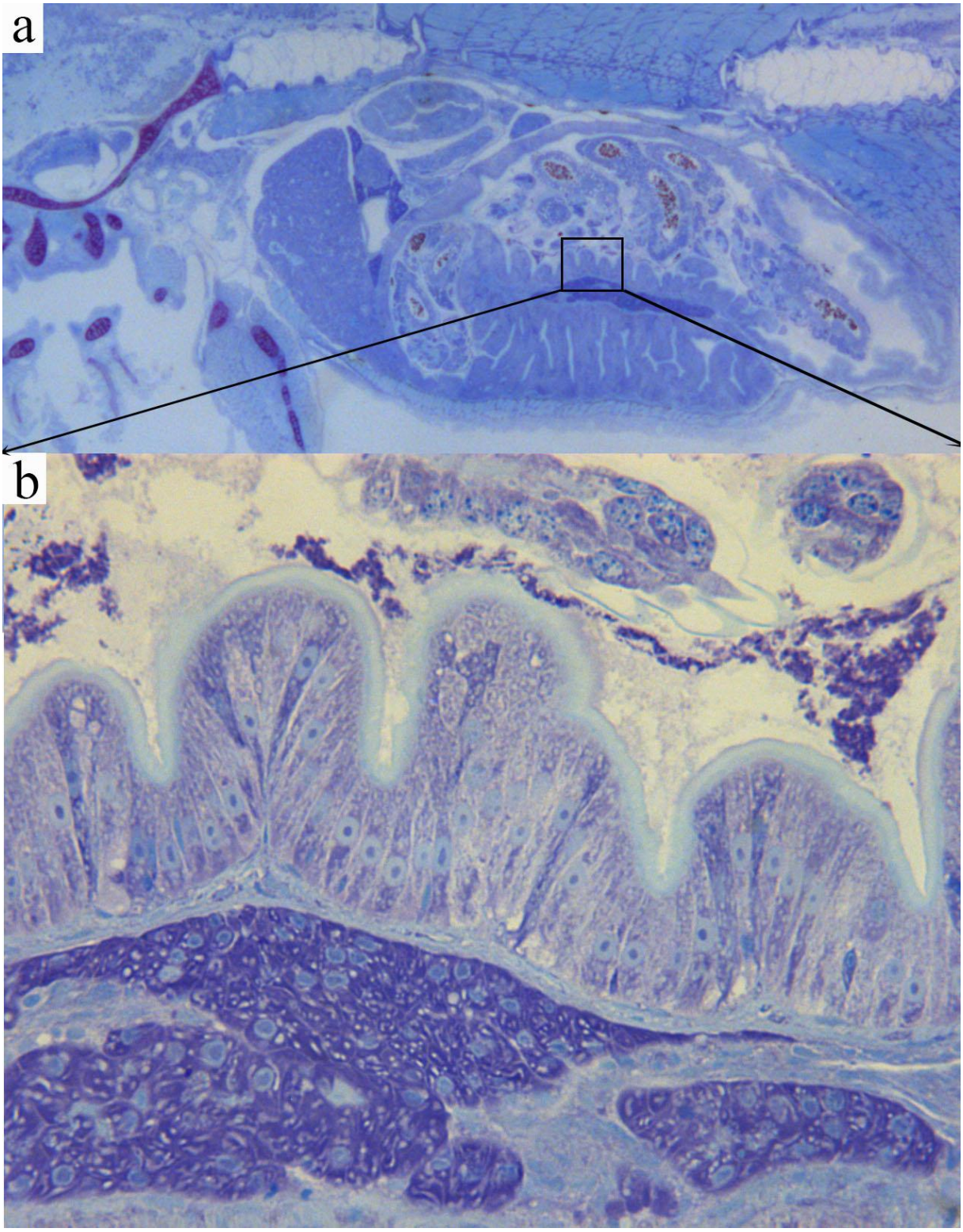

Figure 3.28 a) Midgut and hindgut in Stage 4 seperated by a valve. The mucosal folding decreased toward the anus. b) Mucosal folding of the midgut consisting of simple columnar epithelium. Enterocytes with microvilli were located on a thin *submucosa* and *m.externa*. Scattered exocrine pancreas located ventrally for the digestive tract.

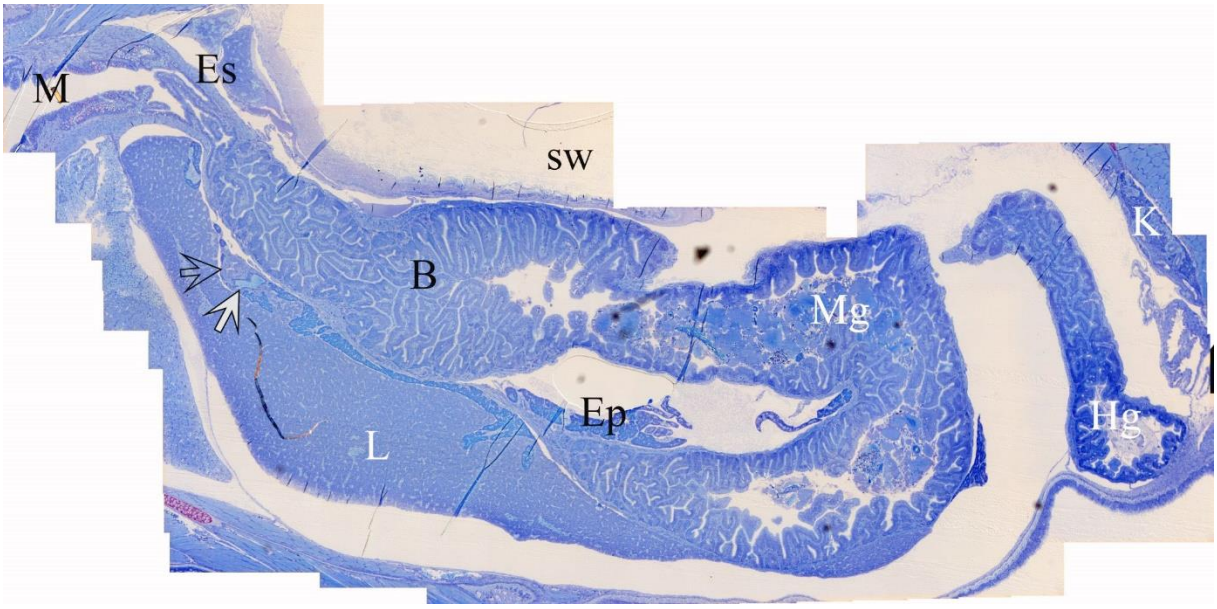

Figure 3.29 Mid-longitudinal section of the digestive system in Stage 5 ballan wrasse at 10x magnification. The esophagus (*Es*) connect the mouth (*M*) to the intestine, thus is segmented into bulbuls (*B*), midgut (Mg) and hindgut (*Hg*). The pancreatic duct (*black arrow*) and common bile duct (*white arrow*) ends in the lumen of the bulbus. *Ep* exocrine pancreas. *K* kidney. *L* liver. *Sw* swimbladder.

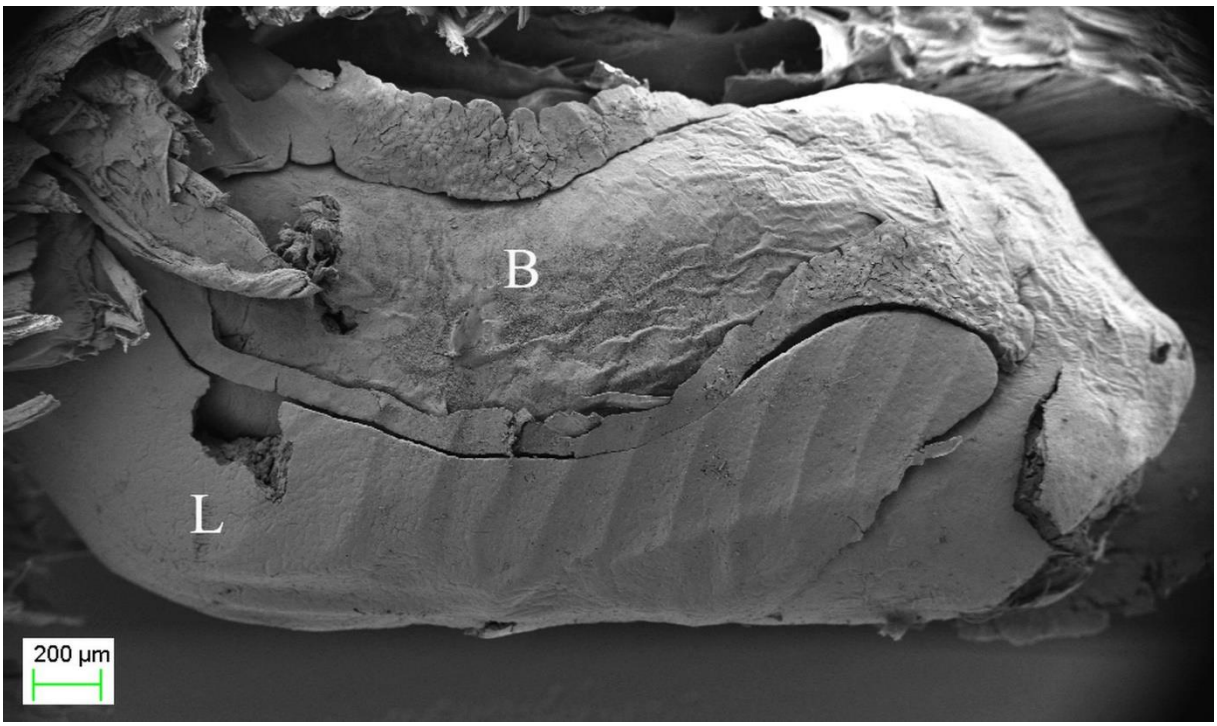

Figure 3.30 Outer surface of the left side of the digestive system using SEM of Stage 5 ballan wrasse juvenile. The massive liver (*L*) as a compact organ covering the ventral surface of the digestive tract and the exocrine pancreas was spread out to fill the empty spaces between the liver and the digestive tract. *B* bulbus.

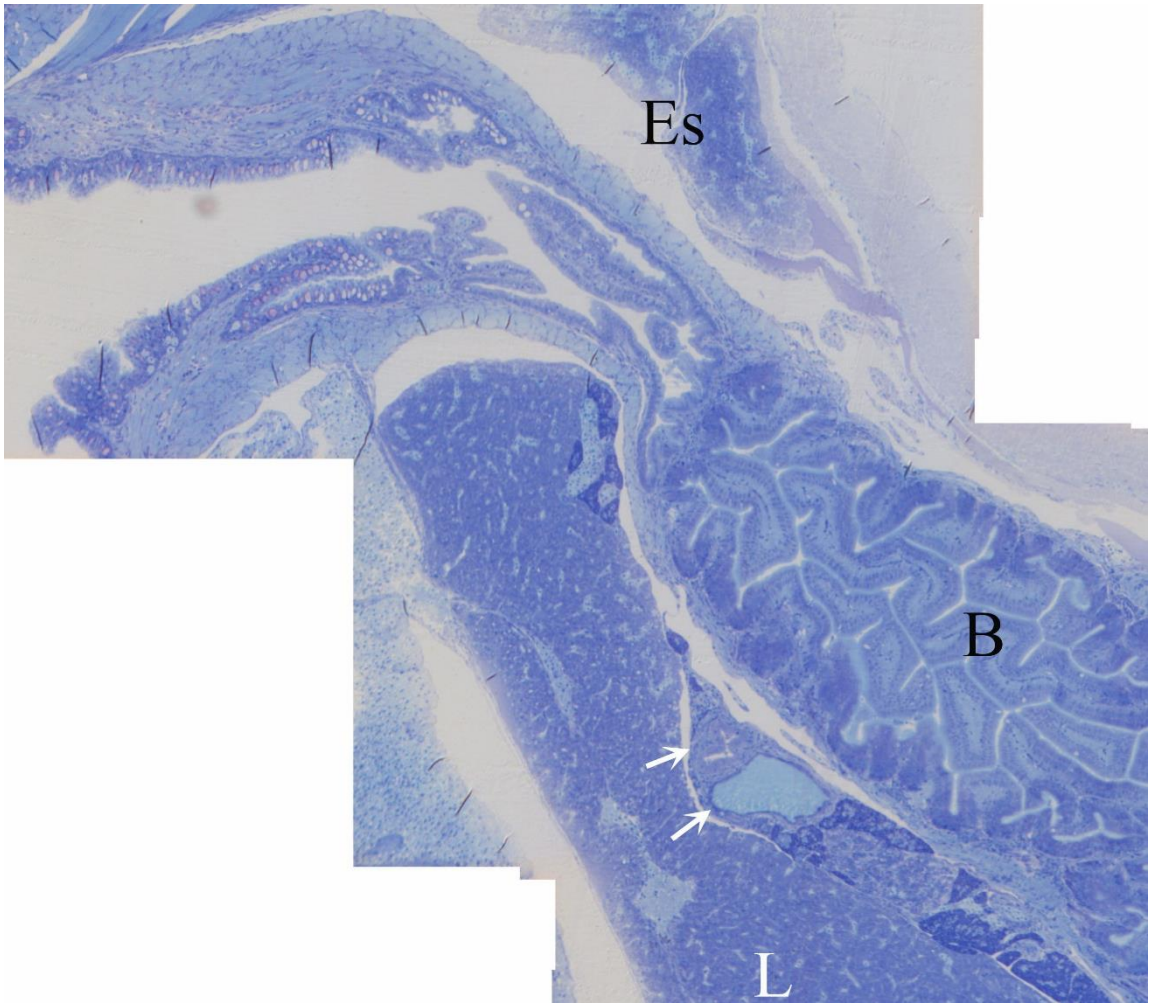

Figure 3.31 Esophagus (*Es*) in Stage 5 were short and located dorsally for the liver (*L*). Highest density of goblet cells were in the proximal region. The esophagus ended with a constriction prior to the bulbus (*B*). *White arrows* pancreatic duct (upper) and gallbladder (lower) with bile.

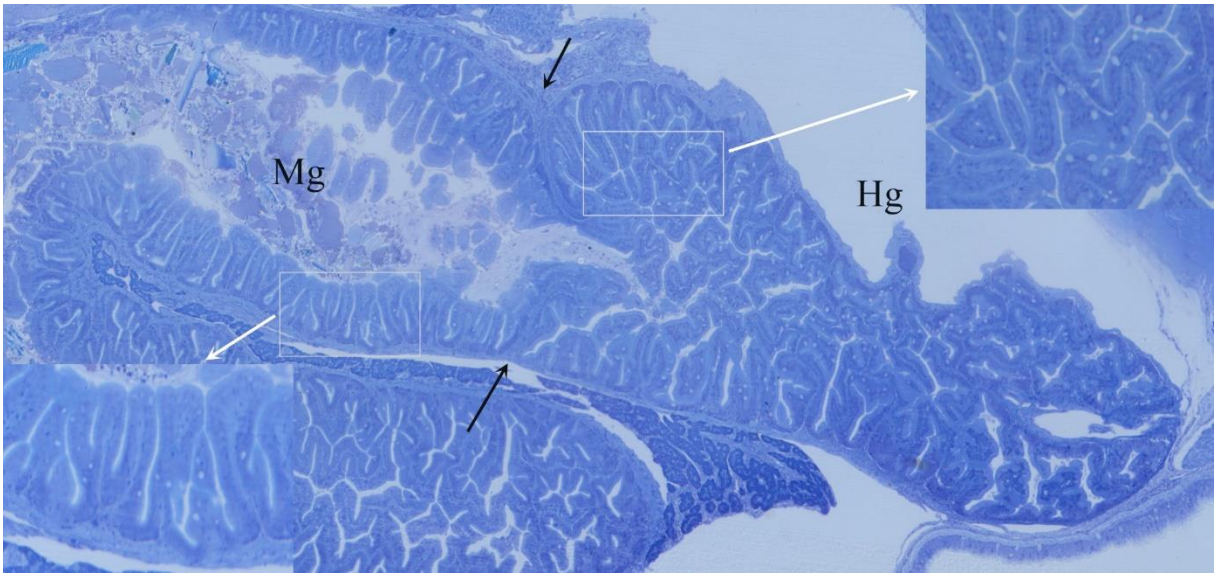

Figure 3.32 Midgut (Mg) and hindgut (Hg) in Stage 5 separated by a valve (*black arrows*). The density of goblet cells increased towards the hindgut.

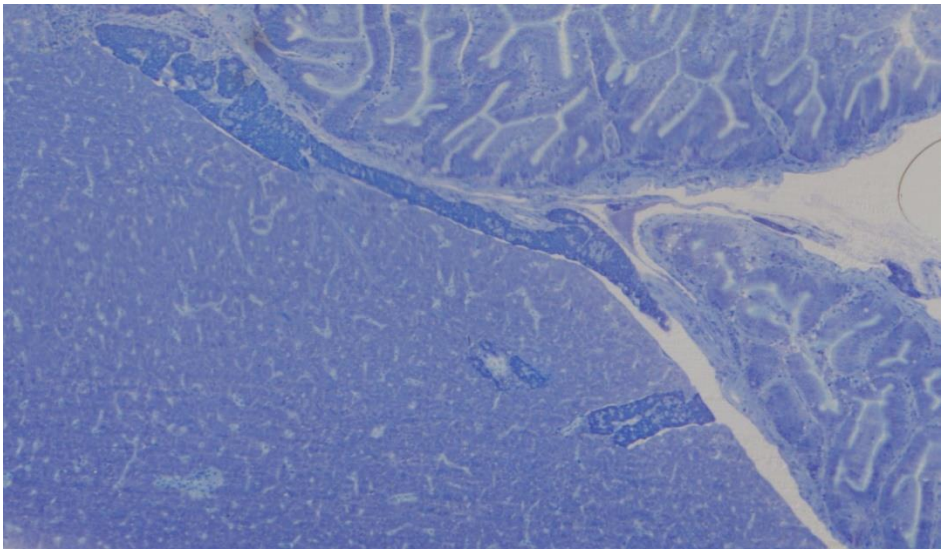

Figure 3.33 Hepatopancreas in Stage 5 (71 DPH) ballan wrasse.

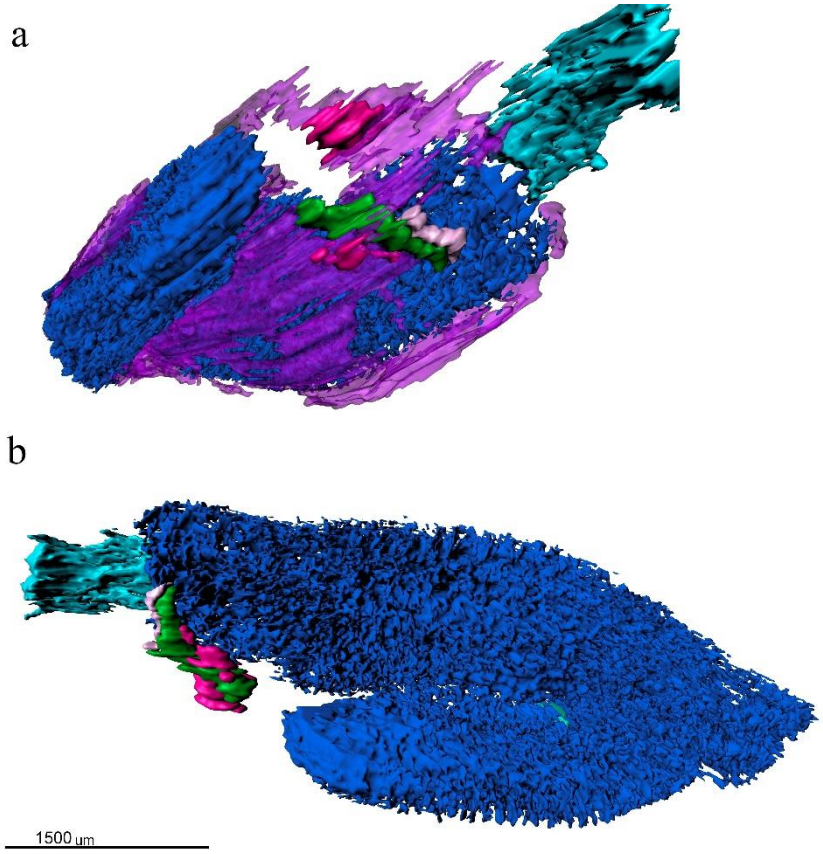

Figure 3.34 Several islets of Langerhans (*dark pink*) were observed in Stage 5. A) One larger primary islet located close to the gallbladder (*green*) and b) several smaller islets nearby. *Light blue* mucosal surface of the esophagus. *Dark blue* surface of the intestinal mucosa. *Bright pink* pancreatic duct.

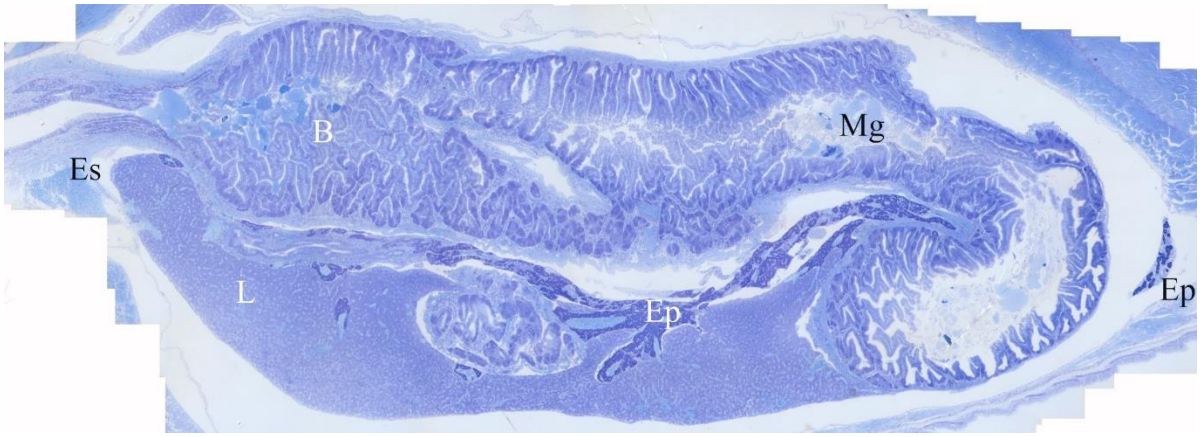

Figure 3.35 Mid-longitudinal section of the digestive system in Stage 6 ballan wrasse juvenile at 10x magnification. *B* bulbus. *Ep* exocrine pancreas. *Es* esophagus. *L* liver. *Mg* midgut.

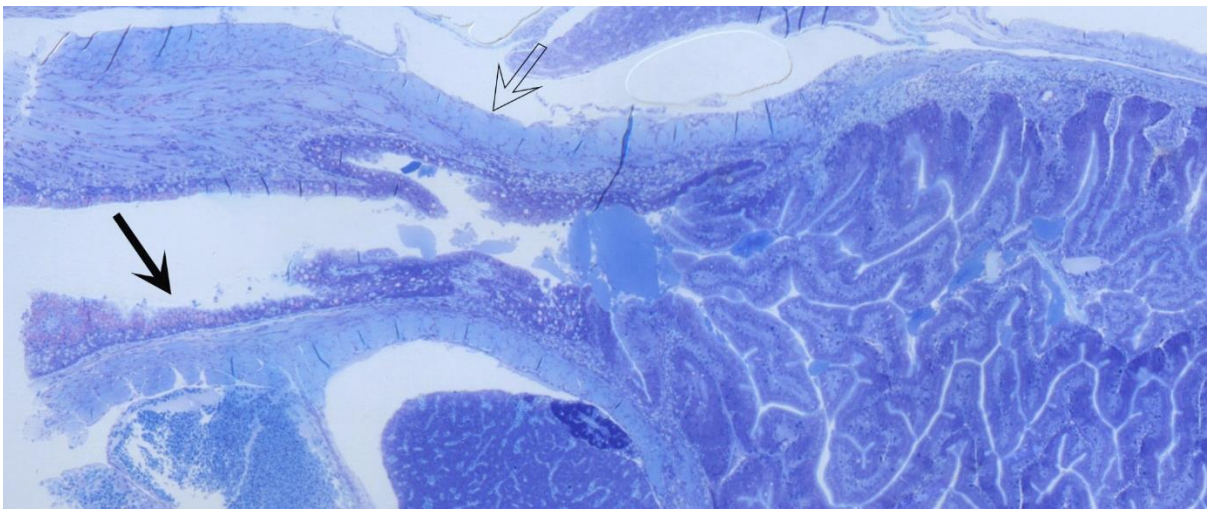

Figure 3.36 Esophagus Stage 6 with mucoid mucosa (*black arrow*) from proximal to distal region and prominent outer circular muscle layer (*transparent arrow*) which diminish in the bulbus region.

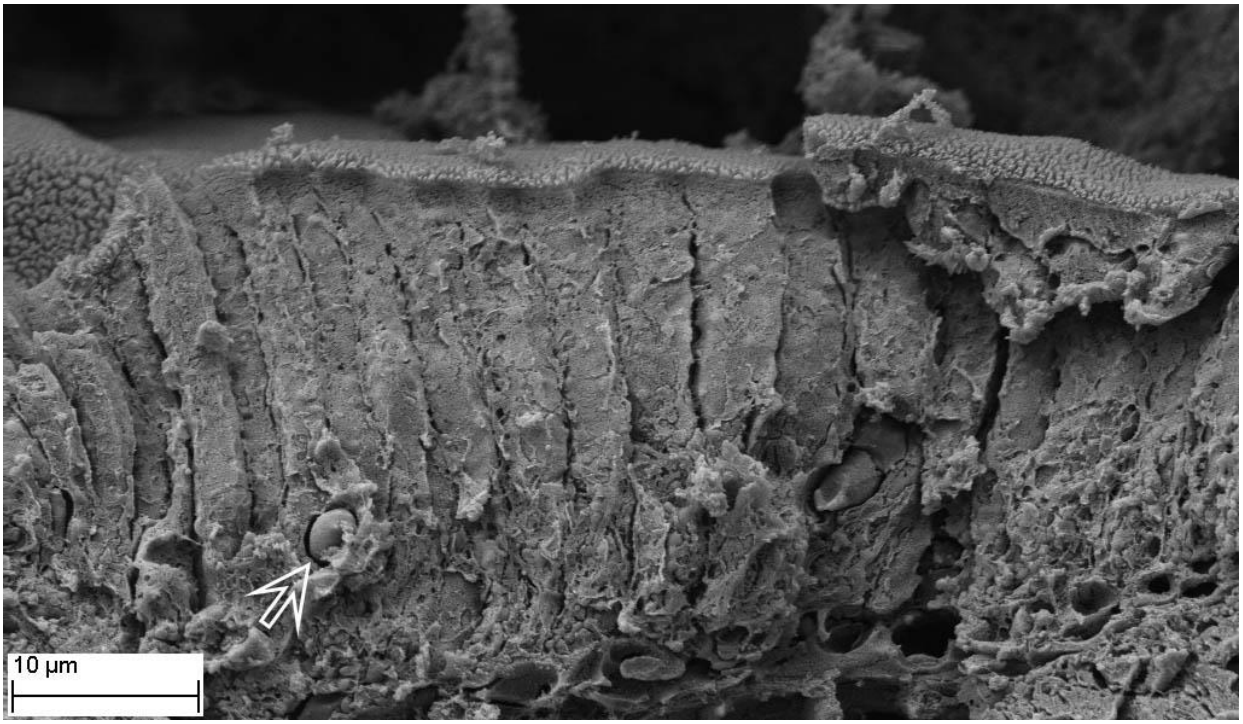

Figure 3.37 Scanning EM of mature enterocytes in the intestine (tall, hexagonal shape) in Stage 6. The apical site of the cell was covered of microvilli. The enterocytes are connected basally to a basement membrane. New enterocytes (probably the circular cell on the lower left, *white arrow*) will mature here and grow up towards the apical site into the intestinal lumen.

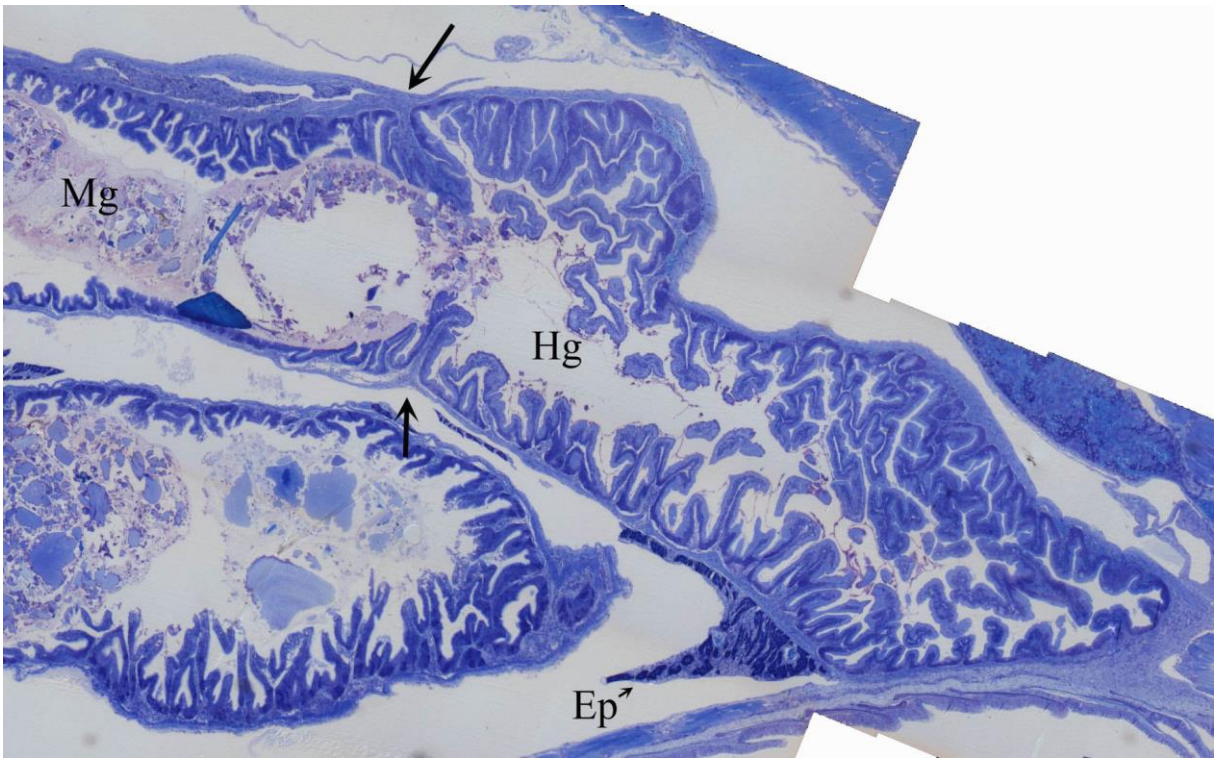

Figure 3.38 Midgut (*Mg*) and hindgut (*Hg*) is seperated by a valve with increased muscle layer (*black arrow*). *Ep* exocrine pancreas. 10x magnification.

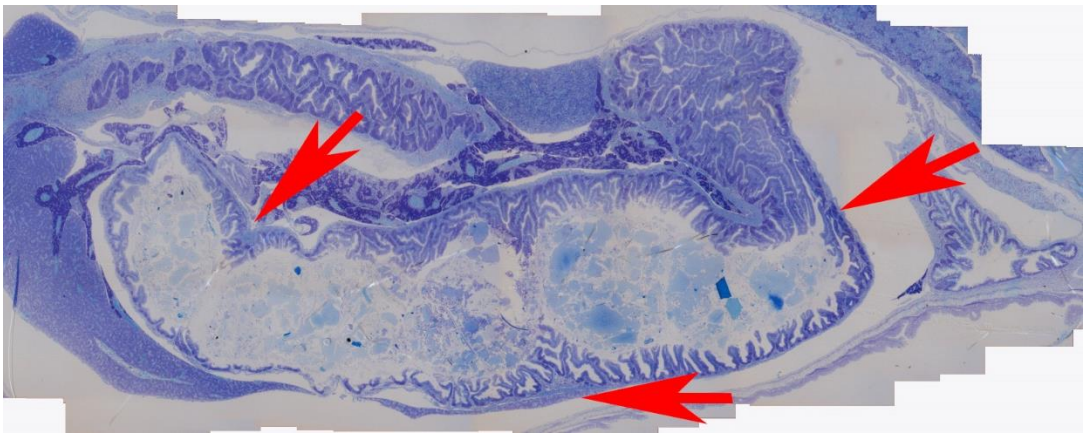

Figure 3.39 Narrow passages in the midgut (red arrows) due to muscle contractions.

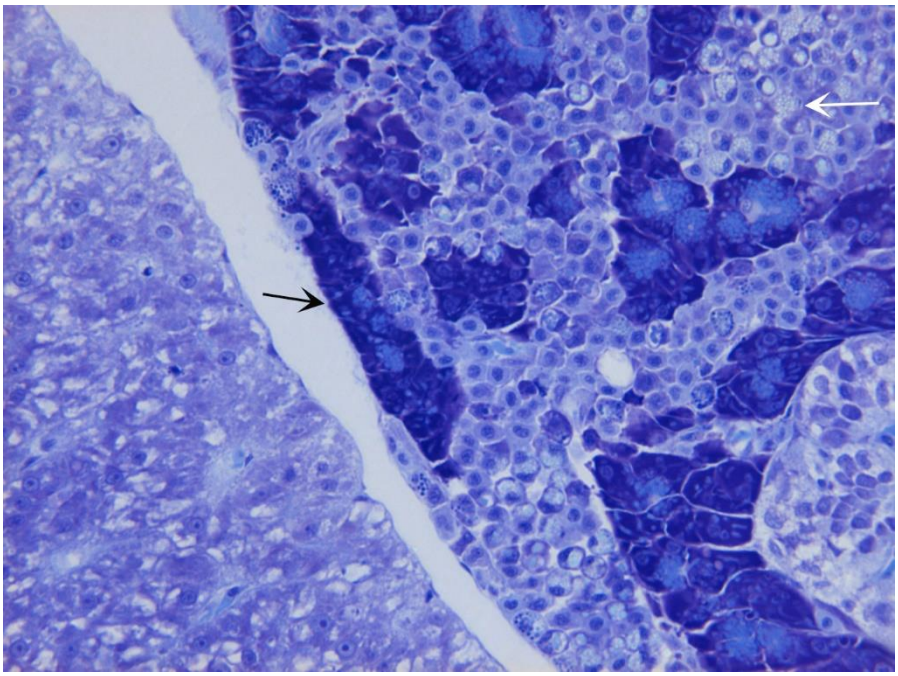

Figure 3.40 Immune cells (cells of lighter staining, often darker nucleus), particular eosinophilic granular cells (*white arrow*), within the connective tissue (tissue type on the right side) of the exocrine pancreas in Stage 6 ballan wrasse juvenile. Acinar cells (*black arrow*) of the exocrine pancreas was stained dark purple and arranged in tubules, vesicles (zymogen granules) stained light blue. Hepatocytes on the left side of the image. 20x magnification. Stained toluidine blue.

4. DISCUSSION

This is the first three-dimensional study of the development of the digestive system including the digestive tract, liver, gallbladder, exocrine and endocrine pancreatic tissue in ballan wrasse. The primary aim of this study was to establish 3D models of the digestive system at six developmental reference stages, and secondly, to describe the ontogeny and growth of the digestive system and relate morphometric scaling to functional capacity for digestion and processing. The final aim was to study morphological and histological evidence for the possible presence of an intestinal bulb.

4.1. Ontogeny of the digestive system in ballan wrasse from larvae until juvenile

4.1.1 The digestive tract

Successful digestion and absorption are key factors for survival of fish larvae. The digestive system, comprising of a digestive tube with two openings, was first observed in Annelida in an evolutionary perspective, whereas primitive multicellular animals, i.e. cnidarian (*Hydra*), only possess a gastrovascular cavity (Miller and Harley, 2010). The development of a digestive tube permits one-way passage of ingested food, and a compartmentalised specialisation of the tube for efficient digestion. The overall ontogeny of the digestive system in ballan wrasse larvae and juveniles observed in this study compares well with previous studies of the digestive system in ballan wrasse (Dunaevskaya, 2010, Gagnat, 2012, Piccinetti et al., 2017) and reports on other marine teleosts (Kjørsvik et al., 1991, Gisbert et al., 2004, Falk-Petersen, 2005, Sala et al., 2005, Kamisaka and Rønnestad, 2011, Gomes et al., 2014b). The main developmental steps that take place during the ontogeny of the digestive tract and its associated organs do not differ much between species, but there are differences in the timing and rates of development. First, the endodermal progenitor cells show a high rate of proliferation, followed by the development of a lumen of the digestive tract and polarisation of the cells controlled by binary cell fate i.e. enterocytes and goblet cells (Ng et al., 2005). Moreover, the rostral lumen expands into a bulbus while the tract continues to grow in volume and surface area and becomes a series of specialized compartments. The development of the digestive tract is also adapted to the feeding mode, where agastric fishes such as the ballan wrasse never develop gastric digestion nor pyloric caeca

and have a relatively short digestive tract, whereas herbivorous fish develop a long intestine and possible fermentation to support the digestive process (Al-Hussaini, 1949, Rimmer and Wiebe, 1987).

The ballan wrasse larvae and juveniles have a short digestive tract. At onset of exogenous feeding (Stage 1), the relative length was measured to 41% of the SL, an observation that correlates with reported short gut length (often less than 50% of the body length) at the onset of feeding in other marine fish larvae (Rønnestad et al., 2013). The relative length of the digestive tract increased to 57% of SL in Stage 3, and then gradually to 69% of the SL of juveniles (Stage 6), supporting a carnivore diet with a short intestine (Dipper et al., 1977, Figueiredo et al., 2005, Bone, 2008). The ballan wrasse follows a similar pattern as turbot larvae, with an increase in the relative length of the digestive tract early in development, and gradually declining growth close to metamorphosis (Segner et al., 1994).

The esophagus represents the transition from the mouth and the intestine and derives from the anterior foregut (Govoni et al., 1986). Ballan wrasse displayed several changes in the organisation of the esophagus during development. At first feeding (Stage 1), the esophagus had a cylindrical shape and terminated in a constriction before the intestine. No goblet cells and no folding in the *mucosa* were observed, but these features appeared between Stages 1 and 2 with goblet cells in the proximal region close to the pharynx and mucosal folding between Stages 2 and 3. In the juvenile ballan wrasse (Stage 6), the esophagus consisted of longitudinal folded mucoid single cuboidal epithelium and striated *m. externa* from the esophagus until the constriction prior to the bulbus. The amount of goblet cells increased, first only located proximally, and later throughout the esophagus. The time of appearance of goblet cells is species-specific, but is usually prior to or at the onset of exogenous feeding and is thus similar to other species (Pedersen and Falk-Petersen, 1992, Bisbal and Bengtson, 1995, Yúfera and Darías, 2007b, Zambonino Infante et al., 2008), while in some species goblet cells appear after onset of exogenous feeding (Gisbert et al., 2004, Micale et al., 2006). The esophageal mucus-producing goblet cells play an important role, since fish lack saliva glands. They help lubricate the ingested food particles and avoid abrasions from ingested feeds, i.e small crustaceans with exoskeletons with occasionally sharp spines and antennae. The mucus also provides a barrier for bacterial infections and it has been suggested that it assists in pregastric digestion with its acid properties in altricial larvae (Baglole, 1997, Gisbert et al., 2004, Yúfera and Darías, 2007b). The longitudinal folding of the esophagus, particularly between Stages 4-6, increases the surface area, and the capacity to increase the diameter and enable passage of larger feeds.

Together with efficient mucus production, this permits the ballan wrasse to adapt a new feeding mode with different and larger prey (Yúfera and Darías, 2007b).

The intestine occupied the largest percentage volume (60-80%) of the digestive system, and developed from an incipient gut at Stage 1 into a segmented gut divided into proximal midgut with a bulbus with an increased lumen diameter, middle midgut and distal midgut separated from the hindgut by a valve from Stage 2 onwards. The 3D-model indicated that a bulbus is present in Stage 2 of the ballan wrasse. Previous studies have suggested that a teleost bulbus is derived from the posterior foregut and the proximal midgut (Govoni et al., 1981). The middle and distal midgut are distinguished from the bulbus by a somewhat narrowed lumen and shorter villi as well as being part of the rotated gut, whereas the bulbus ended where the rotation started. This is coherent with other studies where the gut primordium develops into segmented regions, both in the ballan wrasse (Dunaevskaya, 2010, Gagnat, 2012, Krogdahl et al., 2014) and other fish species (Govoni et al., 1986, Kjørsvik et al., 1991, Rønnestad et al., 2003, Wallace et al., 2005, Chen et al., 2006, Sánchez-Amaya et al., 2007, Kamisaka and Rønnestad, 2011, Liu et al., 2013, Gomes et al., 2014b). The intestine became curled into one loop from Stage 3; which is well after the onset of feeding. The timing of the differentiation into a loop differs between fish. Some fish larvae such as the Atlantic halibut already have a rotated gut when they start feeding (Kamisaka et al., 2001) while the ayu *Plecoglossus altivelis* and Atlantic cod have a straight gut at the start of feeding (Kamisaka et al., 2003, Kamisaka and Rønnestad, 2011). The rotation and length of the intestine continued to increase from Stages 4 - 6.

The most prominent cell types of the ballan wrasse intestinal *mucosa* were enterocytes, followed by goblet cells. Enterocytes are the absorptive cell units in the intestinal mucosa for nutrient uptake. As the gut tissue matured during ontogeny, the *mucosa* became a mucoid columnar epithelium with microvilli. The first intestinal goblet cells appeared in the hindgut between Stages 3 and 4. In the midgut, the first goblet cells appeared at very low densities in the bulbus region and between Stages 4 and 5. The enterocytes at Stage 1 were 15.93±0.74 x 2.80±0.53 x 0.97±0.07 µm (height x width x microvilli height) and matured to larger cells at Stage 6 of 22.12±2.22 x 3.19±0.64 x 0.72±0.16 µm. Pre-feeding turbot larvae (Segner et al., 1994) and first-feeding sea bass *Dicentrarchus labrax* (Deplano et al., 1991, García Hernández et al., 2001) have “adult” enterocytes who have active lipid absorption and active brush border enzymes. This thus differ from the ballan wrasse enterocytes that became taller during ontogeny. Romundstad (2015) investigated the development of larval hepatocytes and enterocytes in ballan wrasse under different feeding regimes. For both cell types, the

mitochondrial- cristae density and outer membrane properties changed between 3 DPH and older larvae (6, 8, and 15 DPH), indicating a maturation of both the hepatocytes and enterocytes (Romundstad, 2015).

The gut tissue is the largest endocrine organ in the vertebrates in terms of widespread release of hormones and bioactive peptides. The hormones are produced in enteroendocrine cells (EEC) that are located in the *mucosa* (Ahlman and Nilsson, 2001, Rønnestad et al., 2017). Wallace et al., (2005) observed EEC in zebrafish mainly in the anterior intestine, though these cells seem to appear in the posterior intestine before the bulbus and midgut, unlike the "classic rostral-to-caudal" morphogenesis in zebrafish and mammalian intestine (Ng et al., 2005). Cholecystokinin (CCK) is one of the key gut hormones and it stimulates the secretion of bile and pancreatic enzymes, regulates the passage from stomach to the midgut, and acts as an anorectic factor (Rønnestad et al., 2017). The location of CCK-producing cells differs between species: in Atlantic halibut (with a rotated gut at the start of exogenous feeding) the CCK-producing cells were located close to the anterior midgut from 12 days after start feeding, while in the straight gut of ayu larvae CCK-producing cells were distributed along the midgut from hatching (Kamisaka et al., 2001, 2003). In Atlantic cod larvae, CCK cells were located mainly in the anterior midgut and a few cells in the posterior midgut and occasionally in the hindgut in the rotated digestive tract of from 8 DPH (Hartviksen et al., 2009). In this present study, the EEC could not be identified with the staining technique used; however, given the special features of a very short agastric digestive tract, this warrants further studies in ballan wrasse to understand how digestion is efficiently controlled to optimize efficiency.

The hindgut is a separated region from the midgut and relates to the mammalian ileum, where it plays a role in water and ion uptake as well as in the enterohepatic circulation. The purpose of the ileorectal valve is to serve as a one-way valve into the compartment, and thus to permit special processing of the remaining chyme and undigested matter in the hindgut. In ballan wrasse, an increased muscle bundle around the valve only became prominent at Stage 6, 102 DPH juveniles. The ileorectal valve between the distal midgut and the hindgut became clearly visible between Stages 1 and 2 (4-10 DPH). However, in other studies of ballan wrasse, the valve has been observed at 4 DPH (Dunaevskaya, 2010, Gagnat et al., 2016) even though these 4 DPH larvae were of smaller SL than 4 DPH larvae in this study. The ileorectal sphincter is present in Atlantic cod from 3 DPH (Falk-Petersen, 2005) and summer flounder *Paralichthys dentatus*, and in Atlantic halibut from 26 DPH (Bisbal and Bengtson, 1995). In the present study, the valve did not seem to have an increased external muscle layer in Stages 2-4. This

indicates little muscular regulation or control with the sphincter function. Earlier study have shown that longitudinal muscle does not seem to be present in the larval *m.externa* (Govoni et al., 1986). Only in the adult stage have both circular and longitudinal external muscles. In the present study, no pattern of muscular layer direction could be distinguished in the few muscle fibers that was present for the earlier stages. A reason why there is no increase in muscle fibres around the valve in Stages 2-4 could be result of circular and longitudinal smooth muscle of the *m. externa* is a characteristic for an adult digestive tract, and. There are also several special functions in the posterior midgut and hindgut that could not be studied with the present technique and staining. For instance, Wallace et al., (2005) observed a second epithelial cell type (NaPi+ enterocytes) in the distal midgut in zebrafish. These cells have supranuclear vesicles, and it has been suggested that they display pinocytosis-related digestive activity (Govoni et al., 1986, Bisbal and Bengtson, 1995, Gisbert et al., 2004). Pinocytotic activity of the intestine has been related to an immunological role (Wallace et al., 2005, Rønnestad et al., 2007). Similar pinocytotic activity by enterocytes has been observed in juvenile ballan wrasse 4th segment (Krogdahl et al., 2014). The transcriptome of the hindgut in juvenile ballan wrasse indicates its important immune-related functions, i.e. antigen recognition and immune cell activation and differentiation, as well as gene expression related to bile and vitamin B12 uptake (Kjørsvik et al., 2014). Paneth cells are present in the base of the crypts in the mammalian small intestine, but has not been observed in fish (Pack et al., 1996, Stanley Bennet et al., 1976, Ng et al., 2005, Wallace et al., 2005).

4.1.2 Associated organs

The liver was present at the anterior end of the abdominal cavity from Stage 1 (4 DPH). However, compared to many marine fish, e.g. Atlantic cod and Atlantic salmon, that maintain a compact form of the liver throughout life, the shape of the ballan wrasse liver changed substantially during ontogeny. Between Stages 4 and 5 (29 and 71 DPH) it developed from a compact form to an elongated form located anterior and also ventral to the midgut and all the way to the hindgut. Gagnat et al. (2016) observed a similar elongation pattern of the liver between 21 and 33 DPH. Compared to Gagnat et al., (2016), the 3D models developed in this study provide an improved and more detailed understanding of the shape and distribution than single 2D sections. The 3D reconstructed model of Stage 6 also demonstrated changes in liver morphology around that stage, when the liver was “pushed” to the left side of the abdomen due to the intestinal rotation. In the hepatocytes there were no apparent ontogenetic changes. There

were some small fat vesicles observed in hepatocytes from the start of exogenous feeding (Stage 1), but even during the juvenile stage there were no large fat depositions in the liver, indicating that fat is deposited in other tissues. Fat deposition in fish may occur in several organs (e.g. mesenteric fat, muscle and liver), with an annual variety in feed availability for wild fishes, and is also related to swimming performance (Sheridan, 1988, Brix et al., 2009). The slow-moving bottom-dwelling fish, i.e. Atlantic cod, have a fatty liver and little fat deposits in the skeletal muscle, whereas in salmon and trout, active surface feeders; muscles contains larger fat deposits (Sheridan, 1988, Brix et al., 2009, Kryvi and Poppe, 2016).

The gallbladder in ballan wrasse was permanently located on the right side of the digestive tract from the early stages, and the common bile duct *ductus choledochus* terminated in the lumen of the bulbus from the ventral side and up, along with the pancreatic duct *ductus pancreaticus*. This location permits the bile and the pancreatic enzymes to be secreted in the anterior part of the midgut, in the bulbus, just after the feed enters the gut, with the result that digestion can be initiated immediately. Anatomically, the two ducts ended separately at the luminal surface of the bulbus, and they are not analogous to the human papilla of Vater, where the bile duct and pancreatic duct merge and enter the lumen as a single opening (Gartner and Hiatt, 2007). The right-sided location of the gallbladder is also seen in Atlantic cod (Kamisaka and Rønnestad, 2011) and halibut (Gomes et al., 2014b), and again were clearly visualized through reconstructed 3D models of the digestive system. The surface area and volume of the gallbladder increased throughout development. However, the data do not necessarily infer an enhanced storage capacity of bile in the gallbladder, since the larvae were sampled during feeding, and the gallbladder probably contracts post-prandially. CCK stimulate gallbladder contraction to release bile into the lumen of the intestine (Silver and Morley, 1991). There are limited studies of the storage and concentration of bile in fish. Grosell et al., (2000) measured bile concentration in rainbow trout, where the gallbladder was dissected to determine the volume of the bile. The total volume of stored bile in starved rainbow trout was 0.36±0.14 ml kg^{-1} after 24h and 2.46±0.14 ml kg^{-1} 120 h after feeding, simultaneous with increased bile acid concentration (Grosell et al., 2000). Besides storing and concentrating the bile, inter-digestive changes in bile concentration of bilirubin due to gallbladder contractions have been observed in adult dogs (Itoh et al., 1982).

The exocrine pancreas was located posterior to the liver as a compact organ from first feeding (Stages 1-2). However, the 3D-models showed a change in the morphology of the exocrine

pancreatic tissue between Stage 2 and 3. The pancreas became elongated and scattered within the abdomen between the liver and the digestive tract, as well as exocrine pancreas surrounding larger blood vessels within the liver from Stage 5 onwards, also referred to as hepatopancreas. Hepatopancreas is not observed in Atlantic cod (Kamisaka and Rønnestad, 2011) and is more common in invertebrates (H. Kryvi, University of Bergen, *pers. comm*.). However, hepatopancreas has been observed in some teleosts, including catfish *Siluriformes* (Mumford et al., 2007), redbanded seabream *Pagrus auriga* (Sánchez-Amaya et al., 2007), some species of *Cyprinidae* such as mirror carp and gudgeon (Al-Hussaini, 1949), and has also previously been identified in the ballan wrasse (Kjørsvik et al., 2014, Gagnat et al., 2016).

Gagnat et al., (2016) suggested that the development of hepatopancreas occurred concurrently with metamorphosis in ballan wrasse. In their study, metamorphosis was defined as lasting from a SL of 6.0 mm until 15.0-17.0 mm [until 55 DPH; 49 DPH were suggested by Dunaevskaya et al. (2016)]. In the present study, a clear hepatopancreas was observed from Stage 5 (71 DPH; SL of 16.56 mm). At this stage, the external morphology confirms the juvenile phase and that hepatopancreas is present in the post-metamorphosis individuals in ballan wrasse

Zymogen granules within the acinar cells of the exocrine pancreas were observed from Stage 1, and compares well with other studies of ballan wrasse larva (Dunaevskaya, 2010, Gagnat, 2012). Zymogen granules often appear just before or soon after the start of exogenous feeding, indicating a functional pancreas and an actively feeding fish (Zambonino Infante and Cahu, 2001, Mitra et al., 2015).

Numerous eosinophilic granular cells (eosinophils) were observed within the connective tissue between the exocrine pancreatic cells in the juvenile ballan wrasse (Stage 6, 102 DPH). Infiltration of immune cells between the pancreatic cells and surrounding adipose tissue has also been observed in an earlier study of juvenile ballan wrasse (Helland et al., 2014). However, high levels of immune cells within the exocrine pancreas are a normal observation (non-pathological) for the ballan wrasse pancreas (H. Hellberg, Fish Vet Group, *pers. comm*.). The real function of these cells is unknown, but it has been suggested that it is related to a defense mechanism (Mumford et al., 2007). Teleost eosinophils are similar to mammalian mast cells, and they both can occur in all loose connective tissue close to blood vessels (Gartner and Hiatt, 2007, Kryvi and Poppe, 2016). In addition, eosinophils in Stage 6 were present in the intestinal *submucosa* and in between the intestinal *serosa*.

4.2 Growth of the digestive system

In terms of absolute morphologic scaling, the digestive organs generally increased both in volume and surface areas as the larvae grew. For the gut tissue, the relative growth of the volume and surface areas showed a peak in the earliest Stages (1-2), followed by a slower increase (Stage 2-4), a new peak between Stages 4-5 and then again a lower growth in juvenile ballan wrasse (Stages 5-6). Segner et al (1994) who was working with turbot suggested a possible strategy for growth of digestive organs were the fish first invested to elongate the digestive tract to increase the gut residence time for digestion, and then a second phase to increase the mucosal surface area to enhance the absorptive efficiency. To increase the mucosal surface area is also a priority for the ballan wrasse larvae. However, turbot develops a stomach during the metamorphosis and acquire a longer gut (114 % of SL at post-metamorphosis) compared to ballan wrasse (Segner et al., 1994). The ballan wrasse seems to invest in both gut length, surface area and tissue mass (volume) in the earliest Stages (1-2) while the exocrine pancreas, liver and endocrine pancreas shows a rapid volume increase in the later Stages (Stages 4-5). As juveniles, there was a decline in the liver volume, while the exocrine pancreas increased in volume (between Stages 5 and 6). This morphometric decline of the liver and small increase of the exocrine pancreas seems to be explained by the formation of the hepatopancreas. This suggestion was also supported by the data of Gagnat et al. (2016).

The total volume of the digestive organs analysed in the present study (gut tissue, liver, exocrine- and endocrine pancreas) compared well with that of Gagnat et al., (2013). However, the morphometric scaling of the relative volume of the organs differed somewhat from Gagnat et al., (2016) where they reported a lower relative volume of the gut tissue, while the liver and pancreas had higher relative volumes compared to the present study (**Appendix E**).

From larval to juvenile stage (Stages 1-6), the relative volume of the gut tissue declined (79 % at Stage 1 to 61% at Stage 6), while the exocrine pancreas increased from 7% to 11% and together with the liver increased in their total relative volume (from 21 % to 38 %). Calculation of the relative growth of digestive organs using the data of Gagnat et al (2016) shows that the liver and pancreas together increased from 31% to 47% compared to gut tissue (decreased from 67% to 52 %) in 4-55 DPH ballan wrasse larvae (**Appendix E**). An opposite pattern was observed in Atlantic cod where the relative volume of liver and pancreas decreased (from 46 % at 1 DPH until 16 % at 39 DPH) as the intestinal bulbus developed into a functional stomach, possibly resulting in a less prominent role of the pancreatic enzymes in digestion (Kamisaka and Rønnestad, 2011). In common dentex and turbot larvae at onset of exogenous feeding the

relative volume of digestive organs (intestine, liver and pancreas) shows a strong increase in gut tissue and liver tissue during the first month after hatching, while the pancreas decreases concurrent with appearance of gastric glands (Sala et al., 2005). The growth of organs from Stages 5-6 were very low, suggesting an allocation of the energy, e.g. into growth of muscles. Similarity of growth pattern between fish and avian is observed in the domesticated Pekin duck and wild mallard *Anas platyrhynchos*. Study of the digestive system with respect to the body mass shows rapid growth of the liver, grizzard and small intestine during the first 3 weeks after hatching. As the digestive tract mature, they allocate more of their energy resource into protein accumulation located in the pectoral muscles (Kenyon et al., 2004).

4.3 Morphometric scaling related to function

All organs had a strong growth rate from Stages 1-2. These larvae were fed on enriched rotifers and *Artemia* (Stages 1-4), and the endocrine pancreas, liver and gut tissue had highest specific growth rates (in declining order).

The folding of the intestine (formation of villi) started early (between Stages 2-3). The thickening and increased folding of the intestinal mucosa indicates the importance of increasing the surface area for absorption in the first period after hatching where the larvae transfer from endogenous to exogenous feeding to maximize the nutrient absorption in the food together with enhanced activity of membrane enzymes in the brush border (Zambonino Infante and Cahu, 2001).

The increased processing performed by the digestive tract are likely to require enhanced capacity to process the absorbed nutrients (Pelletier et al., 1994). Since liver has a key role in handling the post-absorptive flow of incoming nutrients from the digestive tract, liver seems to respond to the growth requirement with a strong specific growth rate. The ratio of volume of the liver compared to the volume of the gut tissue at Stage 1 were 0.166 and had a stable increase until Stage 6 at 0.429 (**Table 4.1**). A small decrease from Stages 5-6 can be due to formation of the hepatopancreas.

Table 4.1 Ratio of liver volume compared to the gut tissue in Ballan wrasse from Stage 1; 4 DPH until Stage 6; 102 DPH.

Stage	$\frac{\text{Volume of the liver}}{\text{Volume of the gut tissue}}$	DPH
1	0.16	4
2	0.23	10
3	0.30	18
4	0.33	29
5	0.543	71
6	0.429	102

Liver is the major metabolic organ and important energy storage, and produce bile, which is important to digest lipids. In larval cod, the liver increases in both in size (hypertrophy) and number (hyperplasia) from hatching until 30 DPH (Wold, 2007). Further, Pelletier et al., (1994) studied the Atlantic cod for 8 months with initial size of 40-50 cm to study aerobic capacity and growth rates of white muscle, liver and digestive tract. As the fatty cod liver grew, the protein:DNA ratio only changed slightly, suggesting that as the liver increases, the number of hepatocytes increases while the amount of proteins per cell remains stable (Pelletier et al., 1994). This might be true for the ballan wrasse liver as well; thus while hypertrophy and hyperplasia takes place in the growing liver; the amount of protein in the remains stable. The early growth of the liver may be correlated with the finding of expression of Cyp7 A1 in ballan wrasse larva, which were upregulated from 10 DPH, suggesting a response to the feed (Hansen et al., 2013). Increased liver size can also increase the bile acids production by the hepatocytes. However, mammalian cholesterol homeostasis is highly regulated by bile acids, which plays a key role in absorption of lipids and fat-soluble vitamins. 22-day-old rat liver shows increased level of hepatocytes and increased level of Cyp7 in the individual cells (Massimi et al., 1998), suggesting amplified protein content per cell. Limited studies have been conducted on Cyp7 in fish (Uno et al., 2012).

When the larvae fed on formulated feed (Stages 5-6); the exocrine pancreas, endocrine pancreas and liver showed strongest specific growth.

The growth of pancreas and liver in ballan wrasse might emphasize the importance of their position in agastric fish with regards to digestion. The pancreas was always located posterior

of the liver until it began to be scattered between the digestive tract and within the liver tissue. The neuronal and hormonal regulation of the digestion and appetite is crucial for the survival. The elongated parts of the exocrine pancreas around the digestive tract, especially in the juvenile ballan wrasse, can help to minimize the distance for transporting signals (e.g. CCK) between the two tissues for releasing the digestive enzymes stored in the zymogen granules. Few zymogen granules were observed within the acinar cells at Stage 1, 5.1 mm SL, similar to previous observations in relation to SL (Dunaevskaya, 2010, Gagnat, 2012) though no food were present in the incipient gut. Zymogen granules often appear before or soon after the start of exogenous feeding, indicating an active feeding fish (Zambonino Infante and Cahu, 2001, Mitra et al., 2015). The volume of the pancreas compared to the gut tissue remained variable until the larvae were weaned on formulated feed (Stages 1-4), where the pancreas showed a rapid increase (Stage 5) in relative volume which can be correlated with the enzyme production (**Table 4.2**).

Table 4.2 The ratio of the volume of exocrine pancreas compared to the gut tissue during the ontogeny of ballan wrasse from Stage 1; 4 DPH until Stage 6; 102 DPH.

Stage	$\frac{\text{Volume of the exocrine pancreas}}{\text{Volume of the gut tissue}}$	DPH
1	0.09	4
2	0.06	10
3	0.09	18
4	0.06	29
5	0.13	71
6	0.19	102

Trypsin is considered the key digestive enzyme in fish (Zambonino Infante and Cahu, 1994). In ballan wrasse larvae, trypsin expression (mRNA) is age-related; it is very low in the yolk-sac stage, and peaks around weaning (24-27 DPH) and decrease again in older larva (Hansen et al., 2013). A similar trend of trypsin expression is seen in larval Atlantic cod with a peak at 17 DPH and decreasing level throughout metamorphosis, presumably due to formation of gastric glands (Kortner et al., 2011). Ballan wrasse lacks gastric glands, and the decrease might indicate an inadequate amount and/or quality of proteins in the diet, or an intracellular starvation-induced degradation (Rønnestad and Hamre, 2001, Hansen et al., 2013). It could also indicate important roles for other alkaline proteolytic enzymes (i.e. chymotrypsin and elastase)

and that they play a bigger part in digestion and that there also is a low new-synthesis of trypsin (Hansen et al., 2013). Hansen et al (2013) suggested that a cause for the decrease could be increased lipid and carbohydrate digestion, where the endocrine regulation of blood glucose is important for homeostasis. BAL mRNA increased gradually after 31 DPH and pancreatic chitinase peaked around 27 DPH (Hansen et al., 2013).

Islet of Langerhans (endocrine pancreas) appeared between Stage1 and 2 (4-10 DPH). Because of the number of sections for a larva, and limited time for the project, not all the sections was included in the 3D reconstruction. Therefore, some details regarding scattered tissues and small structures might have been lost, e.g. number of clusters of islets of Langerhans. There is a previous observation of islets already at 4 DPH in some larvae (Gagnat, 2012), indicating that these cells appear between 4 and 10 DPH in ballan wrasse. A small cluster of endocrine cells within the exocrine pancreas may have been present at 4 DPH, as well as several smaller clusters; islet neogenesis, for the older larva and juvenile (Stages 5 and 6). After the appearance of islets in ballan wrasse larvae, the 3D reconstruction revealed a morphometric scaling and growth rate of the endocrine pancreas grew 201% day^{-1} between Stages 1 and 2, and leveled out to 16.93 % day^{-1} from Stages 1-6; about twice the rate of the other organs.

Assuming there is no methodical errors, there is a strong difference in the growth rate of endocrine pancreatic cells compared to exocrine pancreas. This may suggest an altered postabsorptive hormonal and metabolic state in ballan wrasse during the ontogeny of the digestive system from larval to juvenile stage. Further studies should explore this relation, using molecular on biochemical methods. The change from post-prandial state to postabsorptive state alters the metabolic activity to maintain of the plasma glucose levels in homeostasis by involving pancreatic glucose-lowering insulin and glucose-raising glucagon, where both of insulin and glucagon are regulated after a meal (Rønnestad et al., 2017).

4.4 Presence of an intestinal bulb

One of the key aims of this study was to explore histological and morphological evidence for the presence of an intestinal bulb in the anterior midgut. Histologically there was no marked difference between the proximal and the middle midgut, i.e. the enterocytes with microvilli continued throughout the intestine. No prominent muscular layer was observed around the

bulbus or at the end of the bulbus at any stages during this study. The 3D models showed a luminal diameter increase in the hypothesized bulbus region at Stage 2 and there was also a narrow passage prior to distal midgut and the ileorectal valve. However, the narrow passage was not very prominent as the gut became rotated from Stage 3. The 3D models indicates that a dissected digestive tract outside the abdominal cavity from a Ballan wrasse larva older than 18 DPH may show a hint of a bulb of the proximal midgut. Similarly did a dissected digestive tract 18 DPH only show a tendency of a bulb of the proximal midgut (Ø. Sæle, *pers. comm*). Observations by by Ø. Sæle and H Le (NIFES, Norway, *pers. comm*) on the dissected digestive tract of ballan wrasse juveniles mounted in a Ringer solution indicated only minor hints of a bulbus based on gut diameters and motility patterns. Taken together, the histological and morphological evidence lend some support to the presence of a bulbus in the ballan wrasse from first feeding to the juvenile stage. However, it does not appear to have a pseudogaster function with an increased capacity to retain food in this compartment.

In vitro studies of the post-prandial effect on the passage rate of the digestive tract in juvenile ballan wrasse supports that there is no functional pseudogaster in this species H. Le (Nifes, pers. comm.). However, video records of dissected and mounted intestine show strong muscular contractions of the intestinal segments, thus region-specific peristalsis. The muscular contractions after a meal is strong in the proximal and middle midgut, until the digested food is gradually passing downstream to the distal midgut and hindgut. 3D models verified a constriction (sphincter) between the esophagus and the bulbus. This sphincter might prevent reflux of chyme into the esophagus during the strong contractions in the first segments. Similar organization is observed in agastric Chinese sucker, which also have a sphincter separating the esophagus and the intestine (Liu et al., 2013).

The bile and the pancreatic secretions are emptied into the bulbus from Stage 3. Whether there is a pronounced bulbus or not, one of the main function of the proximal midgut is to ensure efficient food mixing between the ingested feed and secretions (bile and enzymes) in an alkaline environment (pH). A bulbus might increase the efficiency of the mixing, while retrograde peristalsis (Rønnestad et al., 2000b) is a complementary way to enhance the mixing efficiency. Such mixing function was observed for a bulbus in altricial species such as the Atlantic cod (Kamisaka and Rønnestad, 2011), Japanese flounder *Paralichthys olivaceaus* (Rønnestad et al., 2000b), Atlantic halibut (Gomes et al., 2014), which all are larvae with a presumptive stomach that fully develops during metamorphosis.

The functional intestinal bulb of goldfish *Carassius auratus* shows prominent folding of the mucosa and striated external muscles of the esophagus and intestinal bulb, and the circular muscle layer is enlarged and forms the intestinal sphincter (Mcvay and Kaan, 1940, Caceci, 1984) which can provide increased residence time for food passing through the digestive tract.

Although a functional bulbus where not observed, the rotation of the gut might slow down the chyme passage rate and increase the residence time of the digested food to enhance digestive and absorptive efficiency. If there were no food retention and no valves, the gut transit would be faster and food would pass right through the digestive tract. Shao (2016) reported that juvenile ballan wrasse has a high feed passage rate compared to other fish species. Juveniles fed on formulated feed shows a total residence time in the digestive system of only 14 hours. The fast transit was suggested to be due to the lack of stomach and the short intestine relative to the SL (Shao, 2016). However, there must be some hold back for the food passage, where motility patterns of muscle contractions of the intestinal wall and the ileorectal valve, can play a role together with to increase the residence time and help in the absorption of nutrients.

The 3D-model of Stage 6 (102 DPH) juvenile ballan wrasse revealed several narrow passages in the midgut prior to the ileorectal valve. Based on the observations of H. Le (Nifes, *pers. comm.*), these narrow passages were most likely the results of muscular contractions. The mechanism for smooth muscular contraction are similar to striated muscles in vertebrates with actin-activated myosin motor proteins but instead of responding to the neurotransmitter acetylcholine as in striated muscles, the smooth muscle responds to hormones and neurotransmitters starting a signal transduction cascade (Somlyo and Somlyo, 1994). As discussed by Rønnestad et al (2000b), and Gomes et al (2014a), prolonged and static contractions of the circular smooth muscle will increase the resistance to chyme flow, and may thus be regarded as a physiological sphincter that results in increased residence time in the section cranial to the constriction. Contractions can be initiated by the muscle itself, by interstitial cells of Cajal (ICC), neurotransmitters or hormones (Holmberg et al., 2003).

4.5 Discussion of Materials and methods

Over the past years, technological advances have led to a breakthrough in microscopic techniques with new data analysis through 3D reconstructions. 3D visualisation has been applied in a diverse range of scientific fields and scale, from reconstruction of the *Drosophila melanogaster* gastrulation (Khairy and Keller, 2011) to whole reconstruction of nine day old mouse embryo (Brune et al., 1999) and barnacle *Anelasma squalicola* (Bergum, 2016). 3D visualisation are also applied to magnetic resonance imaging from mapping fat deposit in fish (Brix et al., 2009) to measuring consciousness in the living human brain (Lundervold, 2010).

The 3D models reconstructed in this study are based on serial sections of the larvae. This approach for creating models is can be based on different histological methods. In the present study resin was used, while other alternatives are paraffin sections or cryosections. However, some artefacts and deformities on serial sections are unavoidable. This challenge is a contributing factor to the rugged shape of the surface for some models. Due to the workload and technical challenges of creating the model, particularly the older stages, only one 3D-model was created for each stage. This larva was carefully selected based on size and visual appearance, and is believed to be typical representation for each stage. Thus, since the basis of the morphometric scaling is based on one larvae, care should be made when interpreting the data and statistical analysis cannot be performed. However, the data presented in this thesis compares well with previous reports, based on other methodological approaches on the same species (Gagnat et al., 2016).

4.5.1 Comparing growth data to previous studies

Compared to previous growth data of ballan wrasse larva, the larva sampled for this study was somewhat larger (SL) than expected based on the earlier classification of developmental stages (**Table 2.1**). Ottesen et al. (2012) classified Stage 1 yolk sac larvae within 0-108 day degrees, and Stage 2 within 122-341 day degrees (exclusively on exogenous feed); Stage 3 within 355-456 and Stage 4 at 471-686 day degrees. The calculated age based on day degrees for each stage in the present study compares well with that reported for each stage by Ottesen et al. (2012). In the present study, the Stage 1 was at 53, Stage 2 at 138, Stage 3 at 248, Stage 4 at 417, Stage 5 at 1101 and Stage 6 at 1606 day degrees, respectively.

Differences between SL in the present and previous studies could in part be due to the bias in sampling where sampling date was selected based on the presumed growth. There is typically a variation in SL within a batch, or within a tank, that will be larger with increased age. Differences in SL can be explained if the larvae in the previous studies were fixated prior to the measuring the SL of the larva, which causes shrinkage of tissues (Rolls, 2017). However, SL of the larva in the present study were measured in fresh samples. Other causes of the growth differences can be rearing temperature, parental effect on the egg quality, egg size and size of the larva at hatching (Hunter, 1981) and also nutrition (Karlsen et al., 2015). Ottesen et al. (2012) reared the studied larvae at a water temperature of 11-14℃, which is 2℃ lower compared to the conditions for rearing of the batch of larvae collected at Marine Harvest Labrus.

Earlier studies have demonstrated that the larval developmental status is better correlated with size than age (Sæle and Pittman, 2010). This has also been reported for ballan wrasse larvae. In an experiment, the larvae were fed two types of feeds (rotifers or copepods) that resulted in very different growth rates (Gagnat, 2012). However, as noted previously when the larvae were fed the two diets and were compared at the same size, the size of different organs was the same. Thus, Gagnat (2012) did not observe a dietary effect on the volume of different digestive organs. Assuming that the allometric growth patterns and size of organs is similar between ballan wrasse larvae at the same SL, the larval SL and volume of organs can be compared to Gagnat (2012) and Gagnat et al., (2016) data. The present data on ballan wrasse compares well with wrasse fed enriched rotifers (RotMG) with regards to volumetric development of the gut tissue, liver and pancreas. The minor differences in volume may relate to the different applied methods for morphometric scaling analysis.

Gagnat et al. (2016) estimated the volume of different organs on cross sections by the Cavalieri method by using CAST 2 to a point grid. The cross sections were studied by applying pointed grids systematically on the sections. The volume of an organ in one slide is calculated by (number of points hitting the tissue) x (area of one point) x (4 μm; the section thickness) x (Z-distance between the two sections). The number of sections used by Gagnat et al. (2016) were kept to a level were all tissue types of interest (if developed) appeared in at least five sections, hence an average of 24-34 number of sections per larvae. The Cavalieri method is an unbiased estimation using a rectangular approximation of the area under the curve (AUC) (Rosen and Harry, 1990), whereas the 3D rendering software Imaris calculates the volume of tissue of interest as a triangular surface within a grid set by the voxel size (referring to section 2.4 in this

thesis). As a follow-up to this work it could be interesting to compare the two methods on the same image stacks. Within the timeframe of this thesis this was not possible.

4.5.2 Light microscopy

Some of the sections had artefacts that are visible after staining (**Figure 4.1**). A cause of such artefacts is the room temperature where the histological sections are processed, which in the laboratory at HIB to some extent depends on the outside temperature. Especially on colder days, the sections easily folded and was hard to unfold. This was especially the case when sectioning Stage 5 in December 2015. Artefacts may also result from applying a blunt knife on the microtome, which works as a plough through the sections. This was corrected by moving the knife to use a different part of it, or to change the knife. Dirt on the sections may follow from the embedding process (if the tissue was not cleaned well enough in PBS before infiltration, or use of an unclean tube or cast), sectioning process (e.g. use of dirty water when putting the sections on glass slides) or the staining process (e.g. use of unfiltered staining). Such technical problems were reduced to a minimum by strict procedures including to keep the equipment and water clean (fresh water in the morning and after lunch) and filter the staining before use to avoid excess particles on the sections.

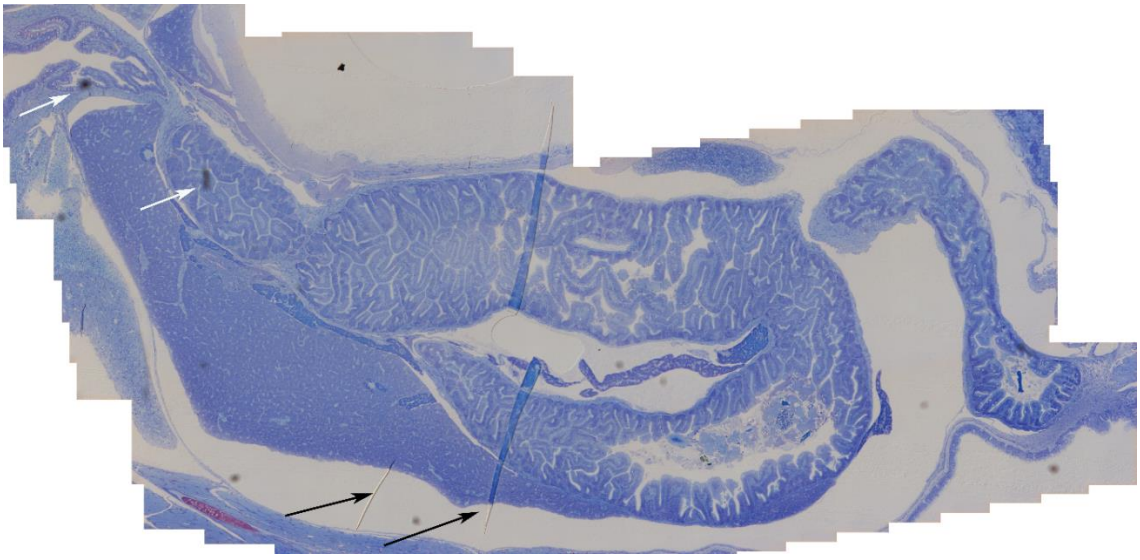

Figure 4.1 Artefacts on a histological section of Stage 5 71 DPH ballan wrasse larvae. *Black arrows*: folding of the section. *White arrows*: dirt on the section (dust particles). This section passed the selection criteria and was used in the 3D modelling.

Due to the artefacts on the some of the sections, there was an adjustment in which sections were used in the 3D-models. Using the 3D reconstruction of Stage 6 (and similar for Stages 1-5) as an example, where every 13th section was photographed and used in the model. However, if the 13th section had artefacts, section before or after were used instead, i.e. the 12th or 14th section were used. On average in Stage 6, the image stack had the average distance of 26 μm (2 μm section thickness) between the sections.

4.5.3 The 3D rendering software (Imaris)

The geometry settings in Imaris was manually set by the operator as XYZ voxel sizes (3D pixels). The X/Y dimensions are normally detected automatically by the Imaris software based on the image stack format, while the Z voxel size is the number of slides times the thickness of the slides (e.g. Z-voxel size for Stage 6: every 13th x 2μm = 26 μm, **Appendix C, Table C.1**).

For Stage 5, the X/Y voxel size was set manually wrong. The voxel size should have been 3.52 but was set to 2.49. Therefore, the retrieved statistical parameters (area and volume) was mathematically corrected afterwards. This correction factor was calculated as follows: the area and volume of a dice (side length = 2.49) and a ball (r = 2.49) was compared to the area and volume of a dice (side length =3.52) and a ball (r = 3.52) (**Appendix C, Table C.2**). This gave an "area factor" correcting factor of 1.998419 and a "volume factor" correcting factor of 2.825074 which was used for multiplying statistical parameters (area and volume) retrieved from the 3D model to calculate the correct area and volume of organs. Correction of the scale bar on images of the 3D model for Stage 5 was performed in Adobe Photoshop.

The software tended to crash frequently when the models rendered detailed and complexly folded surfaces (e.g. lumen intestine). To prevent too frequent crashes, the polygons with nodes for different surfaces should not be too close. Therefore, the regions where the outer surface of digestive tract, gallbladder, exocrine- and endocrine pancreas and liver was close, some local adjustments were necessary for Stage 3-6. When working with models with highly detailed surfaces in Imaris (in Stages 5 and 6 in particular) there were frequent software crashes (2-3 times daily). There was no apparent specific pattern, or working mode corresponding to when the Imaris software crashed. This may indicate bugs in in the software or hardware issues (e.g. RAM), or other technical problems unknown to the operator.

The mucosal surface of the intestine was somewhat modified to prevent such crashes by making complicate villi to simpler surfaces with less details. All the details around the mucosa of the intestine are as close to true as possible, though some details (the smallest details of the villi) was not possible to draw in Stages 5-6. GPU-deconvolution AutoQuant X3.1 software (AutoQuant, Media Cypernetics) were considered for faster processing of the datasets, but was not applied because of economic considerations (about £5000).

The reconstructed 3D models were modified when the images were not perfectly aligned. Underlying causes for this could be small artifacts on the sections, or imperfect alignment in AutoAligner, or a combination of several factors. The 3D models were modified by deleting the surfaces on the slide. When drawing a surface of an organ over 3 slides and delete the surface on slide 2, Imaris will still generate the surface from the information given in slide 1 and 3 and connect them together. This was only done when the surface of the organ was familiar, i.e. the ducts from the gallbladder and from the pancreas are expected to the hollow tubes that could be followed through the serial sections (**Table 4.3**).

Table 4.3 Modification of the 3D models in Stage 6 juvenile ballan wrasse.

Stage	Organ surface	Deleted surface on slide no.
6	Outer surface	49
6	Gallbladder and pancreatic duct	58, 63
6	Esophagus	46, 48, 63

4.5.4 Histology

There was some challenges to identify and separate between *ductus choledochus* and *ductus pancreaticus* in Stage 6. The two ducts were separated based on tracing the duct openings in the intestine through the serial sections. If there were indications of bile in the duct, it was assumed to be the gallbladder (bile will be stained blue in toluidine blue; H. Kryvi, University of Bergen, *pers.comm*.). However, the bile was only present in some of the sections. If there were no bile, it was more challenging to separate these two ducts. However, the volumes and surface areas of the gallbladder and the pancreatic duct seems to be correct in Stage 6 when

compared to morphometric scaling of other organs at Stage 6 and comparing the scaling of the pancreatic duct and common bile duct in Stage 5.

5. CONCLUSION

Six reconstructed 3D models supplemented with micrographs of the digestive system in ballan wrasse were established to show and describe the ontogeny of the digestive system as it develops from a yolk-sac larva until juvenile stage. Stage 1; 4 DPH showed an incipient intestine along with liver, pancreas and gallbladder located dorsally for the yolk sac. Segmentation of the digestive tract with folding (villi) of the mucosa together with islet of Langerhans appeared at Stage 2. The villi continued to develop in Stage 3 and onwards to Stage 6 and together with a rotation of the gut that extended the length, this considerably increased the mucosal surface area. The exocrine pancreas became scattered along the digestive tract from Stage 3, and an elongated liver developed from Stage 5 along with formation of hepatopancreas.

This study indicated presence of a morphological bulbus of the proximal midgut for some of the stages in the micrographs and 3D models. The bulbus had a histology resembling to the rest of the midgut, except for more pronounced folding of the *mucosa* (villi). However, due to the lack of increased muscle layer around or after the bulbus, it does not resemble a functional pseudogaster. There was a tendency for increased luminal volume in the bulbus at the entry site of bile and pancreatic secretions along with a constriction between the esophagus and bulbus. A narrow passage after the bulbus might increase the digestive process in the bulbus by efficient mixing of food with secreta to help to improve the digestive efficiency.

Morphometric scaling analysis revealed different allometric growth of digestive organs and tissues. The digestive system grew rapidly (in surface area, volume and SGR) in the earliest Stages (1-2), but the growth declined and came to a halt between Stages 5 and 6, suggesting that the digestive system had matured, and that the juveniles redirected their energy towards growth other organs, like muscles. As the digestive system grew, the relation between the volume mass of gut tissue declined compared to the increasing relative volumes of liver and pancreas. The latter may indicate an increased capacity for pancreatic enzyme secretion that could be a compensation for the lack of gastric hydrolysis in this species. The relative increase in liver size may indicate altered postabsorptive metabolism in this agastric species. A strong and positive morphometric scaling was observed for endocrine pancreas. This may indicate an altered postabsorptive handling of absorbed nutrients during the ontogeny.

6. FUTURE PERSPECTIVES

This study was initiated in the autumn of 2015. Since then another study have been published on the volumetric mass of the digestive system by Gagnat et al. (2016) on the similar larval stages, but by applying another method. The method used by Gagnat et al. (2016) permitted several replicates of each age. However, it would be interesting to apply the two different methods on the image stacks to verify the morphometric scaling, particularly in the later stages.

Agastric fish lacks a functional stomach with gastric glands. Since gastric digestion also serve as an important barrier for pathogens, it would be interesting to compare the microbiota between gastric and agastric species and also their effect on the digestion and homeostasis of the fish. This study show little regional specialization of the short digestive tract in ballan wrasse. The digestive process strongly relies on pancreatic enzymes for hydrolysis of ingested nutrients in alkaline environment. Hence, it will be important to know the characterization of dietary ingredients that are easily digested under such conditions in order to formulate optimal feed for this species.

The 3D models displayed pancreatic distribution around the digestive tract in the later stages, which could reduce the distance for signaling between the two tissues. In relation to appetite regulation and pancreatic secretions, a natural step further in this study could be to analyse the distribution of enteroendocrine cells in the digestive tract, i.e. CCK-cells which can be identified by immunohistochemistry. Several studies have shown a major role of the stomach in signaling satiety and hunger in vertebrates, including teleosts. However, there is limited knowledge on how the digestive system affect the appetite control in agastric fish. Further studies should focus on exploring the signaling pathways in the gut-brain axis.

The strong growth of Islet of Langerhans in ballan wrasse larva and juvenile would be interesting to study further, particularly regarding carbohydrate nutrition and glucose homeostasis. On one side, there is a rapid SGR of the endocrine pancreas compared to the other organs which could indicate an important change in endocrine regulation related to postaborptive metabolism and homeostasis of the fish. On the other side, if there were no methodical errors made in this study, and despite its strong growth rate, the distribution among exocrine and endocrine pancreas remained stable throughout the ontogeny (roughly 95 and 5%) which could indicate a high turnover of the endocrine cells. Turnover of cells can be measured by radiolabeling the RNA of the cells and study the half-life of the labeling ($t_{½}$).

7. REFERENCES

Ahlman, H. & Nilsson, O. 2001. The gut as the largest endocrine organ in the body. *Annals of Oncology,* **12** *(Suppl. 2),* S63-S68.

Al-Hussaini, A. H. 1949. On the Functional morphology of the alimentary tract of some fish in relation to differences in their feeding habits: anatomy and histology. *Journal of cell Science,* **3**(10), pp.109-139**.**

Alami-Durante, H. 1990. Growth of Organs and Tissues in Carp (*Cyprinus caprio* L.) Larvae. *Growth, Development & Aging,* **54,** pp.109-116.

Almada, F., Casas, L., Francisco, S. M., Villegas-Ríos, D., Saborido-Rey, F., Irigoien, X. & Robalo, J. I. 2016. On the absence of genetic differentiation between morphotypes of the ballan wrasse *Labrus bergylta* (Labridae). *Marine Biology,* **163**(4), 86.

Artüz, M. L. 2005. Embryonic and larval development of the ballan wrasse *Labrus berggylta* Ascanius 1767. *Hidrobiologica,* **10,** pp.98-101.

Assouline, B., Nguyen, V., Mahé, S., Bourrat, F. & Scharfmann, R. 2002. Development of the pancreas in medaka. *Mechanisms of Development,* **117**(1)**,** pp.299-302.

Baglole, C. J. 1997. *Development of the digestive system in larval yellowtail (Pleuronectes ferruginea) and winter flounder (Pleurnectes americanus).* Master thesis, University of Prince Edward Island.

Bakke, A. M., Glover, K. A. & Krogdahl, Å. 2010. Feeding, Digestion and Absorption of Nutrients. *In:* Grosell, M., Farrell, A. & Brauner, C. (eds.) *Fish Physiology: The Multifunctional Gut of Fish.* Academic Press.

Barstad, S. 2017. *Dette er våpenet som skal ta knekken på lakselusa* [Online]. Aftenposten. Available: https://www.aftenposten.no/okonomi/i/aMVE5/Dette-er-vapenet-som-skal-ta-knekken-pa-lakselusa [Accessed 13.08. 2017].

Bergum, H. O. T. 2016. *A morphological study of the parasitic barnacle, Anelasma squalicola (Lovén, 1844).* Master Thesis, Department of Biology, University of Bergen.

Bisbal, G. A. & Bengtson, D. A. 1995. Development of the digestive tract in larval summer flounder. *Journal of Fish Biology,* **47**(2)**,** pp.277-291.

Bjordal, Å. 1988. Cleaning symbiosis between wrasse (Labridae) and lice infested salmon (*Salmo salar*) in mariculture. *International Council for the Expolation of the Sea,* F:17.

Bjordal, Å. 1991. Wrasse as cleaner-fish for farmed salmon. *Prog. Underwater Sci.,* **16,** pp.17-28.

Bjordal, Å. 1992. Cleaning symbiosis as an alternative to chemical control of sea lice infestation of Atlantic salmon. *World Aquaculture Nutrition,* 4, pp.53-60.

Bone, Q., Moore, R.H 2008. *Biology of Fishes,* New York, Taylor & Francis Group.

Boxaspen, K. 2009. Lakselus - biologi og spredning. *Norsk Fiskeoppdrett,* 6a**,** pp 10-12.

Brix, O., Gruner, R., Rønnestad, I. & Gemballa, S. 2009. Whether depositing fat or losing weight, fish maintain a balance. *Proc Biol Sci,* **276**(1674), pp.3777-3782.

Brune, R. M., Bard, J. B., Dubreuil, C., Guest, E., Hill, W., Kaufman, M., Stark, M., Davidson, D. & Baldock, R. A. 1999. A Three-Dimensional Model of a Mouse at Embryonic Day 9. *Developmental Biology,* **216**(2)**,** pp.457-468.

Caceci, T. 1984. Scanning electron microscopy of goldfish, *Carassius auratus,* intestinal mucosa. *J. Fish Biol.,* **25**(1)**,** pp.1-12.

Cahu, C., Rønnestad, I., Grangier, V. & Zambonino Infante, J. L. 2004. Expression and activities of pancreatic enzymes in developing sea bass larvae (*Dicentrarchus labrax*) in relation to intact and hydrolyzed dietary protein; involvement of cholecystokinin. *Aquaculture,* **238**(1)**,** pp.295-308.

Chen, B. N., Qin, J. G., Kumar, M. S., Hutchinson, W. & Clarke, S. 2006. Ontogenetic development of the digestive system in yellowtail kingfish *Seriola lalandi* larvae. *Aquaculture,* **256**(1)**,** pp.489-501.

Costello, M. J. 1993. Review of methods to control sea lice (Caligidae: Crustacea) infections on salmon (*Salmo salar*) farms. *In:* Boxshall, G. A. & Defaye, D. (eds.) *Pathogens of wild and farmed fish: sea lice.* Ellis HorwoodLimited.

Costello, M. J. 2006. Ecology of sea lice parasitic on farmed and wild fish. *Trends Parasitol,* **22**(10)**,** pp.475-83.

Costello, M. J. 2009. The global economic cost of sea lice to the salmonid farming industry. *J Fish Dis,* **32**(1)**,** pp.115-8.

D'arcy, J., Dunaevskaya, E., Treasurer, J. W., Ottesen, O., Maguire, J., Zhuravleva, N., Karlsen, A., Rebours, C. & Fitzgerald, R. D. 2012. Embryonic development in ballan wrasse *Labrus bergylta*. *J Fish Biol,* **81**(3)**,** pp.1101-1110.

Darwall, W. R., Costello, M. J., Donnelly, R. & Lysaght, S. 1992. Implications of life-history strategies for a new wrasse fishery. *Journal of Fish Biology,* **41** (Supplement B)**,** pp.111-123.

Das, S. L., Kennedy, J. I., Murphy, R., Phillips, A. R., Windsor, J. A. & Petrov, M. S. 2014. Relationship between the exocrine and endocrine pancreas after acute pancreatitis. *World J Gastroenterol,* **20**(45)**,** pp.17196-17205.

Deplano, M., Diaz, J. P., Connes, R., Kentouri-Divanach, M. & Cavalier, F. 1991. Appearance of lipid-absorption capacities in larvae of the sea bass *Dicentrachus labrax* during transition to exotrophic phase. *Marine Biology,* **108**(3)**,** pp.361-371.

Dipper, F. A., Bridges, C. R. & Menz, A. 1977. Age, growth and feeding in the ballan wrasse *Labrus bergylta* Ascanius 1767. *Journal of Fish Biology,* **11**(2)**,** pp.105-120.

Dunaevskaya, E. 2010. *Histological investigations of organs and tissues development of ballan wrasse larvae during ontogenesis.* Master Thesis, Faculty of Bioscience and Aquaculture, Bodø University College.

Dunaevskaya, E., Amin, A. B., Ottesen, O. H. 2012. Organogenesis of Ballan Wrasse *Labrus Bergylta* (Ascanius 1767) Larvae. *Journal of Aquaculture Research & Development,* **3**(5):142.

Espe, M., Berge, G. E. & Lied, E. 2001. Protein Og Aminosyrer. *In:* Waagbø, R., Espe, M., Hamre, K. & Lie, Ø. (eds.) *Fiskeernæring.* Bergen: Kystnæringen Forlag & bokklubb AS, pp.37-56.

Espeland, S. H., Nedeaas, K., Mortensen, S., Agnalt, A.-L., Skiftesvik, A., Harkestad, L., Karlsbakk, E., Knutsen, H., Thangstad, T., Jørstad, K., Bjordal, Å. & Gjøsæter, J. 2010. Kunnskapsstatus leppefisk. Utfordringer i et økende fiskeri. *Fisken og Havet. Foreløpig utgave pr 15.11.10,* 7**,** pp.1-34.

Falk-Petersen, I. B. 2005. Comparative organ differentiation during early life stages of marine fish. *Fish Shellfish Immunol,* **19**(5)**,** pp.397-412.

Field, H. A., Dong, P. D. S., Beis, D. & Stainier, D. Y. R. 2003a. Formation of the digestive system in zebrafish. ii. pancreas morphogenesis☆. *Developmental Biology,* **261**(1)**,** pp.197-208.

Field, H. A., Ober, E. A., Roeser, T. & Stainier, D. Y. R. 2003b. Formation of the digestive system in zebrafish. I. Liver morphogenesis. *Developmental Biology,* **253**(2)**,** pp.279-290.

Figueiredo, M., Morato, T., Barreiros, J. P., Afonso, P. & Santos, R. S. 2005. Feeding ecology of the white seabream, *Diplodus sargus*, and the ballan wrasse *Labrus bergylta*, in the Azores. *Fisheries Research,* **75**(1)**,** pp.107-119.

Fiskeridirektoratet. 2017a. *Laks, regnbueørret og ørret - matfiskproduksjon. Utsett av smolt 1994-2016* [Online]. Norway: Fiskeridirektoratet. Available: https://www.fiskeridir.no/content/download/7617/95498/version/22/file/sta-laks-mat-05-kjop.xlsx [Accessed 06.08 2017].

Fiskeridirektoratet. 2017b. *Rensefisk - utsett av rensefisk 1998-2006* [Online]. Norway: Fiskeridirektoratet. Available: https://www.fiskeridir.no/content/download/7623/95528/version/39/file/sta-laks-mat-10-rensefisk.xlsx [Accessed 06.08. 2017].

Fiskeridirektoratet & Mattilsynet 2010. For stor merd eller for mange fisk? Avaliable: https://www.fiskeridir.no/content/download/15237/221726/version/1/file/anbefalinger-utredning-fdir-mattilsynet-for-stor-merd-eller-for-mange-fisk.pdf. [Accessed 08.08.17]

Froese, R. & Pauly, M. 2017. *Labrus bergylta Ascanius, 1767 Ballan wrasse* [Online]. Available: www.fishbase.org [Accessed 24.07.2017 2017].

Fuiman, L. A., Poling, K. R. & Higgs, D. M. 1998. Quantifying Developmental Progress for Comparative Studies of Larval Fishes. *Copeia,* 3**,** pp.602-611.

Gagnat, M. R. 2012. *The effect of different live feed on the early growth and development of ballan wrasse (Labrus bergylta Ascanius, 1767) larvae and its organs.* Master Thesis, Department of Biology, NTNU - Norwegian University of Science and Technology.

Gagnat, M. R., Wold, P. A., Bardal, T., Øie, G. & Kjorsvik, E. 2016. Allometric growth and development of organs in ballan wrasse (*Labrus bergylta* Ascanius, 1767) larvae in relation to different prey diets and growth rates. *Biology Open* **5**(9), pp.1241-1251.

García Hernández, M. P., Lozano, M. T., Elbal, M. T. & Agulleiro, B. 2001. Development of the digestive tract of sea bass (*Dicentrarchus labrax L.*). Light and electron microscopic studies. *Anat Embryol* **204**(1)**,** pp.39-57.

Gartner, L. P. & Hiatt, J. L. 2007. *Color textbook of histology,* (3rd. ed.). Philadelphia, PA. USA, Saunders Elsevier.

Gilbert, S. F. 2014. *Developmental Biology,* (10th. ed.). Sunderland, MA USA, Sinauer Associates, Inc.

Gisbert, E., Piedrahita, R. H. & Conklin, D. E. 2004. Ontogenetic development of the digestive system in California halibut (*Paralichthys californicus*) with notes on feeding practices. *Aquaculture,* **232**(1)**,** pp.455-470.

Gomes, A. S., Alves, R. N., Rønnestad, I. & Power, D. M. 2014a. Orchestrating change: The thyroid hormones and GI-tract development in flatfish metamorphosis. *Gen Comp Endocrinol* **20**, pp.2-12.

Gomes, A. S., Jordal, A. E. O., Olsen, K., Harboe, T., Power, D. M. & Rønnestad, I. 2015. Neuroendocrine control of appetite in Atlantic halibut (*Hippoglossus hippoglossus*): Changes during metamorphosis and effects of feeding. *Comparative Biochemistry and Physiology a-Molecular & Integrative Physiology,* **183,** pp.116-125.

Gomes, A. S., Kamisaka, Y., Harboe, T., Power, D. M. & Rønnestad, I. 2014b. Functional modifications associated with gastrointestinal tract organogenesis during metamorphosis in Atlantic halibut (*Hippoglossus hippoglossus*). *Bmc Developmental Biology,* **14**(1)**,** 11.

Govoni, J. J., Boehlert, G. W. & Watanabe, Y. 1986. The physiology of digestion in fish larvae. *Environmental Biology of Fishes,* **16**(1-3)**,** pp.59-77.

Grosell, M., O'donnell, M. J. & Wood, C. M. 2000. Hepatic versus gallbladder bile composition: in vivo transport physiology of the gallbladder in rainbow trout. *Am J Physiol Regulatory Intergrative Comp Physiol,* **287**(6)**,** R1674-R1684.

Hamre, G. I. 2001. Karbohydrat i fiskeernæring. *In:* Waagbø, R., Espe, M., Hamre, K. & Lie, Ø. (Eds.) *Fiskeernæring.* Bergen: Kystnæringen Forlag & Bokklubb AS, pp.77-92.

Hamre, K., Nordgreen, A., Grotan, E. & Breck, O. 2013. A holistic approach to development of diets for Ballan wrasse (*Labrus berggylta*) - a new species in aquaculture. *PeerJ,* **1,** e99.

Hamre, K. & Sæle, Ø. 2011. Oppdrett av leppefisk til lakselusbekjempelse: Hva står på menyen? *Norsk Fiskeoppdrett,* **9**, pp.70-72.

Hansen, T. W., Folkvord, A., Grotan, E. & Sæle, O. 2013. Genetic ontogeny of pancreatic enzymes in *Labrus bergylta* larvae and the effect of feed type on enzyme activities and gene expression. *Comp Biochem Physiol B Biochem Mol Biol,* **164**(3)**,** pp.176-84.

Hartviksen, M. B., Kamisaka, Y., Jordal, A. E., Koedijk, R. M. & Ronnestad, I. 2009. Distribution of cholecystokinin-immunoreactive cells in the gut of developing Atlantic cod *Gadus morhua* L. larvae fed zooplankton or rotifers. *J Fish Biol,* **75**(4)**,** pp.834-44.

Heath, M. R. 1992. Field Investigations of the Early Life Stages of Marine Fish. *Advances in marine biology,* **28,** pp.1-174.

Helland, S., Lein, I., Sæle, O., Lie, K., Kousoulaki, K. K., Van Dalen, S. C. M., Klaren, P. H. M., Bakke, A. M. & Krogdahl, Å. 2014. Effects of feeding frequency on growth and gut health of ballan wrasse juveniles. *Production of ballan wrasse (Labrus brgylta). Science and practice.* www.rensefisk.no.

Heuch, P. A., Bjørn, P. A., Finstad, B., Holst, J. C., Asplin, L. & Nilsen, F. 2005. A review of the Norwegian 'National Action Plan Against Salmon Lice on Salmonids': The effect on wild salmonids. *Aquaculture,* **246**(1)**,** pp.79-92.

Hjeltnes, B., Bornø, G., Jansen, M. D., Haukaas, A. & Walde, C. 2017. Fiskehelserapporten 2016. Veterinærinstituttet 2017.

Holmberg, A., Schwerte, T., Fritsche, R., Pelster, B. & Holmgren, S. 2003. Ontogeny of intestinal motility in correlation to neuronal development in zebrafish embryos and larvae. *Journal of Fish Biology,* **63**(2)**,** pp.318-331.

Hunter, J. R. 1981. Feeding ecology and predation of Marine Fish Larvae. *In:* Lasker, R. (Ed.) *Marine Fish Larvae. Morphology, Ecology, and Relation to Fisheries.* University of Washington Press, Seattle: Washington Sea Grant program.

Islam, M. S. (Ed.) 2010. *Islets of Langerhans,* The Netherlands: Springer Science.

Itoh, Z., Takahashi, I., Nakaya, M., Suzuki, T., Arai, H. & Wakabayashi, K. 1982. Interdigestive Gallbladder Bile Concentration in Relation to Periodic Concentration of Gallbladder in the Dog. *Gastroenterology,* **83**(3)**,** pp.645-651.

Iwama, G. K., Afonso, L. O. B. & Vijayan, M. M. 2006. Stress In Fish. *In:* Evan, D. H. & Clairborne, J. B. (Eds.) *The Physiology of Fishes.* 3rd ed.: Taylor and Francis.

Jobling, M. 1994. Digestion and absorption. *In: Environmental Biology of Fishes,* Chapman & Hall, Fish and Fisheries Series 16, Springer Netherlands, pp.175-209.

Kalat, T. M. & Shabanipour, N. 2010. Internal Anatomy of Common Carp (*Cyprinus carpio*) as Revealed by Magnetic Resonance Imaging. *Applied Magnetic Resonance,* **38**(3)**,** pp.361-369.

Kamisaka, Y., Fujii, Y., Yamamoto, S., Kurokawa, T., Rønnestad, I., Totland, G. K., Tagawa, M. & Tanaka, M. 2003. Distribution of cholecystokinin-immunoreactive cells in the digestive tract of the larval teleost, ayu, *Plecoglossus altivel*is. *General and Comparative Endocrinology,* **134**(1)**,** pp.116-121.

Kamisaka, Y. & Rønnestad, I. 2011. Reconstructed 3D models of digestive organs of developing Atlantic cod (*Gadus morhua*) larvae. *Marine Biology,* **158**(1)**,** pp.233-243.

Kamisaka, Y., Totland, G. K., Tagawa, M., Kurokawa, T., Suzuki, T., Tanaka, M. & Rønnestad, I. 2001. Ontogeny of cholecystokinin-immunoreactive cells in the

digestive tract of Atlantic halibut, *Hippoglossus hippoglossus*, larvae. *Gen Comp Endocrinol,* **123**(1)**,** pp.31-7.

Karlsen, O., van der Meeren, T., Ronnestad, I., Mangor-Jensen, A., Galloway, T. F., Kjorsvik, E., & Hamre, K. (2015). Copepods enhance nutritional status, growth and development in Atlantic cod (*Gadus morhua* L.) larvae - can we identify the underlying factors? *PeerJ,* **3**, e902. doi:10.7717/peerj.902

Kenyon, B. P., Watkins, E. J. & Butler, P. J. 2004. Posthatch growth of the digestive system in wild and domesticated ducks. *Br Poult Sci,* **45**(3)**,** pp.331-41.

Khairy, K. & Keller, P. J. 2011. Reconstructing embryonic development. *Genesis,* **49**(7)**,** pp.488-513.

Kjørsvik, E., Flaten, S., Bardal, T. & Wold, P. A. 2014. The digestive system of juvenile ballan wrasse. *Production of Ballan Wrasse (Labrus bergylta). Science and practice.* www.rensefisk.no [28.09.16].

Kjørsvik, E., Van Der Meeren, T., Kryvi, H., Arnfinnson, J. & Kvenseth, P. G. 1991. Early development of the digestive tract of cod larvae, *Gadus morhua* L., during start-feeding and starvation. *Journal of Fish Biology,* **38**(1)**,** pp.1-15.

Koelz, H. R. 2009. Gastric Acid in Vertebrates. *Scandinavian Journal of Gastroenterology,* **27**;sup193**,** pp.2-6.

Kortner, T. M., Overrein, I., Oie, G., Kjorsvik, E., Bardal, T., Wold, P. A. & Arukwe, A. 2011. Molecular ontogenesis of digestive capability and associated endocrine control in Atlantic cod (*Gadus morhua*) larvae. *Comp Biochem Physiol A Mol Integr Physiol,* **160**(2)**,** 190-9.

Kousoulaki, K., Bogevik, A. S., Skiftesvik, A. B., Jensen, P. A. & Opstad, I. 2015. Marine raw material choice, quality and weaning performance of Ballan wrasse (*Labrus bergylta*) larvae. *Aquaculture Nutrition,* **21**(5)**,** pp.644-654.

Krogdahl, Å. 2001. Fordøyelsessystemet hos kaldtvannsfisk - oppbygging og funksjon. *In:* Waagbø, R., Espe, M., Hamre, K. & Lie, Ø. (Eds.) *Fiskeernæring.* Bergen: Kystnæringen Forlag & Bokklubb AS, pp.11-36.

Krogdahl, Å., Sæle, Ø., Lie, K., Kousoulaki, K., Hamre, K., Helland, S. & Lein, S. 2014. Characteristics of the digestive functions in ballan wrasse fed dry and moist diets *Production of ballan wrasse - science and practice.*

Kryvi, H. & Poppe, T. 2016. *Fiskeanatomi,* Bergen, Fagbokforlaget.

Liu, C. X., Luo, Z., Tan, X. Y. & Gomg, S. Y. 2013. Ontogenetic Development of the Digestive System in Agastric Chinese Sucker, *Myxocyprinus asiaticus,* Larvae. *Journal of the world aquaculture society,* **44**(3)**,** pp.350-362.

Lobel, P. S. 1981. Trophic biology of herbivorous reef fishes: alimentary pH and digestive capabilities. *J. Fish Biol.,* **19**(4)**,** pp.365-397.

Luizi, F. S., Gara, B., Shields, R. J. & Bromage, N. R. 1999. Further description of the development of the digestive organs in Atlantic halibut (*Hippoglossus hippoglossus*)

larvae, with notes on differentail absorption of copepod and *Artemia* prey. *Aquaculture,* **176**(1)**,** pp.101-116.

Lundervold, A. 2010. On consciousness, resting state fMRI, and neurodynamics. *Nonlinear Biomed Phys,* **4** Suppl 1**,** S9.

Lusedata. 2017. *Veileder for bruk og hold av leppefisk* [Online]. Available: http://lusedata.no/wp-content/uploads/2012/05/Veileder-for-bruk-og-hold-av-leppefisk-oppdatert-v%C3%A5r-2017.pdf [Accessed 06.08. 2017].

Martinsen, T. C., Bergh, K. & Waldum, H. L. 2005. Gastric juice: A Barrier Against Infectious Diseases. *Basic & Clinical Pharmacology & Toxicology,* **96**(2)**,** pp.94-102.

Massimi, M., Lear, S. R., Huling, S. L., Jones, A. L. & Erickson, S. K. 1998. Cholesterol 7A-Hydroxylase (CYP7A): Patterns of Messenger RNA Expression During Rat Liver Development. *Hepatology,* **28**(4)**,** pp.064-1072.

Mazurais, D., Darias, M., Zambonino-Infante, J. L. & Cahu, C. L. 2011. Transcriptomics for understanding marine fish larval development 1 1 This review is part of a virtual symposium on current topics in aquaculture of marine fish and shellfish. *Canadian Journal of Zoology,* **89**(7)**,** pp.599-611.

Mcvay, J. A. & Kaan, H. W. 1940. The digestive tract of *Carassius auratus*. *The Biological Bulletin,* **78,** pp.53-67.

Micale, V., Garaffo, M., Genovese, L., Spedicato, M. T. & Muglia, U. 2006. The ontogeny of the alimentary tract during larval development in common pandora *Pagellus erythrinus* L. *Aquaculture,* **251**(2)**,** pp.354-365.

Miller, S. A. & Harley, J. P. 2010. Nutrition and digestion, in *Zoology.* 8th ed. US, NY, McGraw-Hill Companies, pp. 481-502.

Mitra, A., Mukhopadhyay, P. K. & Homechaudhuri, S. 2015. Histomorphological study of the gut developmental pattern in early life history stages of featherback, *Chitala chitala* (Hamilton). *Archives of Polish Fisheries,* **23**(1), pp.25-35.

Mumford, S., Heidel, J., Smith, C., Morrison, J., Macconnell, B. & Blazer, V. 2007. *Fish Histology and Histopathology,* US Fish and Wildlife Service's National Conservation Training Center.

Ng, A. N., De Jong-Curtain, T. A., Mawdsley, D. J., White, S. J., Shin, J., Appel, B., Dong, P. D., Stainier, D. Y. & Heath, J. K. 2005. Formation of the digestive system in zebrafish: III. Intestinal epithelium morphogenesis. *Dev Biol,* **286**(1)**,** pp.114-35.

Osse, J. W. M. & Van Den Boogaart, J. G. M. 1995. Fish larvae, development, allometric growth, and the aquatic environment. *ICES mar. Sci. Symp.,* **201,** 21-34. Copenhagen, Denmark: International Council for the Exploration of the Sea, 1991-.

Otterlei, E., Nyhammer, G., Folkvord, A. & Stefansson, S. O. 1999. Temperature- and size-devependent growth of larval and early juvenile Atlantic cod (*Gadus morhua):* a comparative study of Norwegian costal cod and northeast Arctic cod. *Can. J. Fish. Aquat. Sci. ,* **56**(11)**,** pp.2099-2111.

Ottesen, O., Karlsen, Å., Treasurer, J. W., Fitzgerald, R., Maguire, J., Rebours, C. & Zhuravleva, N. 2008. Ballan wrasse offer efficient, environmentally friendly sea lice control. *Global aquaculture advocate,* **11,** pp. 44-45.

Ottesen, O. H., Dunaevskaya, E. & Arcy, J. 2012. Development of *Labrus Bergylta* (Ascanius 1767) Larvae from Hatching to Metamorphosis. *Journal of Aquaculture Research & Development,* 03.

Pack, M., Solnica-Krezel, L., J., M., Neuhauss, S. C. F., Schier, A. F., Stemple, D. L., Driever, W. & Fishman, M. C. 1996. Mutations affecting development of zebrafish digestive organs. *Development,* **123**(1)**,** pp.321-328.

Pedersen, T. & Falk-Petersen, I. B. 1992. Morphological changes during metamorphosis in cod (*Gadus morhua* L.) with particular reference to the development of the stomach and pyloric caeca. *Journal of Fish Biology,* **41**(3)**,** pp.449-461.

Pelletier, D., Dutil, J. D., Blier, P. & Guderly, H. 1994. Relation between growth rate and metabolic organization of white muscle, liver and digestive tract in cod, *Gadus morhua*. *J Comp Physiol B,* **164**(3)**,** pp.179-190.

Philpott, D. E. 1966. A rapid method for staining plastic embedded tissues for light microscope. *Sci. Instrum,* **11,** pp.11-12.

Piccinetti, C. C., Grasso, L., Maradonna, F., Radaelli, G., Ballarin, C., Chemello, G., Evjemo, J. O., Carnevali, O. & Olivotto, I. 2017. Growth and stress factors in ballan wrasse (*Labrus bergylta*) larval development. *Aquaculture Research,* **48**(5)**,** pp.2567-2580.

Quintela, M., Danielsen, E. A., Lopez, L., Barreiro, R., Svasand, T., Knutsen, H., Skiftesvik, A. B. & Glover, K. A. 2016. Is the ballan wrasse (*Labrus bergylta*) two species? Genetic analysis reveals within-species divergence associated with plain and spotted morphotype frequencies. *Integr Zool,* **11**(2)**,** pp.162-72.

Ray, A. K. & Ringø, E. 2014. The Gastrointestinal Tract of Fish. *In:* Merrifield, D. & Ringø, E. (Eds.) *Aquaculture Nutrition: Gut health, Probiotics and Prebiotics.* First ed. West Sussex: John Wiley and Sons, Ltd.

Rimmer, D. W. & Wiebe, W. J. 1987. Fermentative microbial digestion in herbivorous fishes. *J. Fish Biol.,* **31**(2)**,** pp.229-236.

Rolls, G. 2017. *Process of Fixation and the Nature of Fixatives* [Online]. Leica biosystems > Education > Fixation and Fixatives: Leica biosystems. Available: http://www.leicabiosystems.com/pathologyleaders/fixation-and-fixatives-1-the-process-of-fixation-and-the-nature-of-fixatives/ [Accessed 10.08. 2017].

Rombough, P. J. 1997. The effect of temperature on embryonic and larval development. In: *Seminar Series-Society For Experimental Biology,* **61,** pp.177-224.

Rombout, J. H. W. M., Lamers, C. H. J., Helfrich, M. J., Dekker, A. & Taverne-Thiele, J. J. 1985. Uptake and transport of intact macromolecules in the intestinal epithelium of carp (*Cyprinus carpio* L.) and the possible immunological implications. *Cell Tissue Res,* **239**(3)**,** pp.519-530.

Romundstad, M. 2015. *Effects of different live feed on ballan wrasse (Labrus bergylta) larval hepatocyte and enterocyte development.* Master Thesis, Department of Biology, NTNU - Norwegian University of Science and Technology.

Rosen, G. D. & Harry, J. D. 1990. Brain volume estimation from serial section measurements: a comparison of methodologies. *Journal of Neuroscience Methods,* **35**(2)**,** pp.115-124.

Rønnestad, I., Dominguez, P. & Tanaka, M. 2000a. Ontogeny of digestive tract functionality in Japanese flounder, *Paralichthys olivaceus* studied by *in vivo* microinjection: pH and assimilation of free amino acids. *Fish Physiology and Biochemistry,* **22**(3)**,** pp.225-235.

Rønnestad, I., Gomes, A. S., Murashita, K., Angotzi, R., Jonsson, E. & Volkoff, H. 2017. Appetite-Controlling Endocrine Systems in Teleosts. *Front Endocrinol (Lausanne),* **8,** 73.

Rønnestad, I. & Hamre, K. 2001. Marine larver - spesielle ernæringskrav. *In:* Waagbø, R., Espe, M., Hamre, K. & Lie, Ø. (Eds.) *Fiskeernæring.* Bergen: Kystnæringen Forlag & bokklubb AS, pp.297-312.

Rønnestad, I., Kamisaka, Y., Conceição, L. E. C., Morais, S. & Tonheim, S. K. 2007. Digestive physiology of marine fish larvae: Hormonal control and processing capacity for proteins, peptides and amino acids. *Aquaculture,* **268**(1)**,** pp.82-97.

Rønnestad, I., Rojas-García, C. R. & Skadal, J. 2000b. Retrograde peristalsis; a possible mechanism for filling the pyloric caeca? *Journal of Fish Biology,* **56**(1)**,** pp.216-218.

Rønnestad, I., Tonheim, S. K., Fyhn, H. J., Rojas-García, C. R., Kamisaka, Y., Koven, W., Finn, R. N., Terjesen, B. F., Barr, Y. & Conceição, L. E. C. 2003. The supply of amino acids during early feeding stages of marine fish larvae: a review of recent findings. *Aquaculture,* **227**(1)**,** pp.147-164.

Rønnestad, I., Yúfera, M., Ueberschär, B., Ribeiro, L., Sæle, Ø. & Boglione, C. 2013. Feeding behaviour and digestive physiology in larval fish: current knowledge, and gaps and bottlenecks in research. *Reviews in Aquaculture,* **5,** S59-S98.

Sala, R., Santamaría, C. A. & Crespo, S. 2005. Growth of organ systems of *Dentex dentex* (L) and *Psetta maxima* (L) during larval development. *J Fish Biol,* **66**(2)**,** pp.315-326.

Sánchez-Amaya, M. I., Ortiz-Delgado, J. B., García-López, Á., Cárdenas, S. & Sarasquete, C. 2007. Larval ontogeny of redbanded seabream *Pagrus auriga* Valenciennes, 1843 with special reference to the digestive system. A histological and histochemical approach. *Aquaculture,* **263**(1)**,** pp.259-279.

Segner, H., Storch, V., Reinecke, M., Kloas, W. & Hanke, W. 1994. The development of functional digestive and metabolic organs in turbot, *Scophthalmus maximus*. *Marine Biology,* **119**(3)**,** pp.471-486.

Shao, X. 2016. *The feed passage rate and nutrient digestibility in Ballan wrasse juveniles (Labrus bergylta Ascanius, 1767).* Master Thesis, Department of Biology, University of Bergen.

Sheridan, M. A. 1988. Lipid dynamics in fish: aspects of absorption, transportation, deposition and mobilization. *Comp Biochem Physiol,* **90**(4)**,** pp.679-690.

Silver, A. J. & Morley, J. E. 1991. Role of CCK in regulation of food intake. *Progress in Neurobiology,* **36**(1)**,** pp.23-34.

Skiftesvik, A. B., Bjelland, R. M., Durif, C. M. F., Johansen, I. S. & Browman, H. I. 2013. Delousing of Atlantic salmon (*Salmo salar)* by cultured vs. wild ballan wrasse (*Labrus bergylta*). *Aquaculture,* **402,** pp.113-118.

Skiftesvik, A. B., & Bjelland, R. M. 2003. Oppdrett av berggylt (*Labrus bergylta*). *Norsk Fiskeoppdrett,* **28**(5).

Smith, D. M., Grasty, R. C., Theodosiou, N. A., Tabin, C. J. & Nascone-Yoder, N. M. 2000. Evolutionary relationships between amphibian, avian and mammalian stomachs. *Evol Dev,* **2**(6)**,** pp.348-359.

Smith, D. M. & Tabin, C. J. 1999. Developmental biology: BMP signalling specifies the pyloric sphincter. *Nature,* **402**(6763)**,** pp.748-749.

Somlyo, A. P. & Somlyo, A. V. 1994. Signal transduction and regulation in smooth muscle. *Nature,* **372,** pp.231-236.

Stanley Bennet, H., Dean Wyrick, A., Lee, S. W. & Mcneil, J. H. 1976. Science and art in preparing tissues for light mucroscopy, with special reference to glycol methacrylate, glass knives and simple stains. *Staining Technology* **51**(1), pp.71-79.

Sæle, Ø., Haugen, T., Karlsen, Ø., Van Der Meeren, T., Bæverfjord, G., Hamre, K., Rønnestad, I., Moren, M. & Lie, K. K. 2017. Ossification of Atlantic cod (*Gadus morhua*) – Developmental stages revisited. *Aquaculture,* **468,** pp.524-533.

Sæle, Ø. & Pittman, K. A. 2010. Looking closer at the determining of a phenotype? Compare by stages or size, not age. *Journal of Applied Ichthyology,* **26**(2)**,** pp.294-297.

Sæle, Ø., Solbakken, J. S., Watanabe, K., Hamre, K., Power, D. & Pittman, K. 2004. Staging of Atlantic halibut (*Hippoglossus hippoglossus L*.) from first feeding through metamorphosis, including cranial ossification independent of eye migration. *Aquaculture,* **239**(1)**,** pp.445-465.

Torstensen, B. E., Frøyland, L. & Lie, Ø. 2001. Lipider. *In:* Waagbø, R., Espe, M., Hamre, K. & Lie, Ø. (Eds.) *Fiskeernæring.* Bergen: Kystnæringen Forlag & bokklubb AS, pp.57-76.

Uno, T., Ishizuka, M. & Itakura, T. 2012. Cytochrome P450 (CYP) in fish. *Environmental Toxicology and Pharmacology,* **34**(1)**,** pp.1-13.

Villegas-Rios, D., Alonso-Fernandez, A., Fabeiro, M., Banon, R. & Saborido-Rey, F. 2013. Demographic variation between colour patterns in a temperate protogynous hermaphrodite, the ballan wrasse *Labrus bergylta*. *PLoS One,* **8**(8)**,** e71591.

Wagner, G. N., Fast, M. D. & Johnson, S. C. 2008. Physiology and immunology of *Lepeophtheirus salmonis* infections of salmonids. *Trends Parasitol,* **24**(4)**,** pp.176-83.

Walford, J. & Lam, T. J. 1993. Development of digestive tract and proteolytic enzyme activity in seabass (*Lates calcarifer*) larvae and juveniles. *Aquaculture,* **109**(2)**,** pp.187-205.

Wallace, K. N., Akhter, S., Smith, E. M., Lorent, K. & Pack, M. 2005. Intestinal growth and differentiation in zebrafish. *Mech Dev,* **122**(2)**,** pp.157-73.

Wallace, K. N. & Pack, M. 2003. Unique and conserved aspects of gut development in zebrafish. *Developmental Biology,* **255**(1)**,** pp.12-29.

Wilson, R. W., Wilson, J. M. & Grosell, M. 2002. Intestinal bicarbonate secretion by marine teleost fish - why and how? *Biochimica et Biophysica Acta (BBA)-Biomembranes,* **1566**(1)**,** pp.182-193.

Wold, P. A. 2007. *Functional development and response to dietary treatment in larval Atlantic cod (Gadus morhua L.).* Doctoral thesis, NTNU Norwegian University of Science and Technology.

Yee, N. S., Lorent, K. & Pack, M. 2005. Exocrine pancreas development in zebrafish. *Dev Biol,* **284**(1)**,** pp.84-101.

Yúfera, M. & Darías, M. J. 2007a. Changes in the gastrointestinal pH from larvae to adult in Senegal sole (*Solea senegalensis*). *Aquaculture,* **267**(1)**,** pp.94-99.

Yúfera, M. & Darías, M. J. 2007b. The onset of exogenous feeding in marine fish larvae. *Aquaculture,* **268**(1)**,** pp.53-63.

Zambonino Infante, J. L. & Cahu, C. 2001. Ontogeny of the gastrointestinal tract of marine fish larvae. *Comparative Biochemistry and Physiology Part C,* **130**(4)**,** pp.477-487.

Zambonino Infante, J. L. & Cahu, C. L. 1994. Influence of diet on pepsin and some pancreatic enzymes in sea bass (*Dicentrarchus labrax*) larvae. *Comp. Biochem. Physiol.,* **109**(2)**,** pp.209-212.

Zambonino Infante, J. L., Gisbert, E., Sarasquete, C., Navarro, I., Gutierrez, J. & Cahu, C. L. 2008. Ontogeny and physiology of th digestive system of marine fish larvae. *Feeding and digestive functions of fishes***,** pp.281-348.

Zelditch, M. L., Swiderski, D. L. & Sheets, H. D. 2012. *Geometric Morphometrics for Biologist: A Primer,* USA, Academic Press.

Øie, G., Galloway, T., Sørøy, M., Holmvaag Hansen, M., Norheim, I. A., Halseth, C. K., Almli, M., Berg, M., Gagnat, M. R., Wold, P. A., Attramadal, K., Hagemann, A., Evjemo, J. O. & Kjørsvik, E. 2017. Effect of cultivated copepods (Acartia tonsa) in first-feeding of Atlantic cod (*Gadus morhua*) and ballan wrasse (*Labrus bergylta*) larvae. *Aquaculture Nutrition,* **23**(1), pp.3-17.

APPENDIX A: FORMULAS (CHRONOLOGICAL AFTER APPEARANCE IN MATERIALS AND METHODS)

A.1 Teleost fixation

Fixative

- 300 ml PBS (phosphate buffered saline water) pH 7.2
- 100 ml 0.2 M cacodylate buffer pH 7.2
- 50 ml 25% glutaraldehyde
- 50 ml 20% formaldehyde from paraformaldehyde

1X PBS (phosphate buffered saline water)

- 8.0 g NaCl Sodium chloride
- 0.2 g KCl Potassium chloride
- 14.4 g $Na_2HPO_4 \cdot H_2O$
- 2.3 g $Na_2H_2PO_4$

  Dissolved in 1000 ml distilled water. pH adjusted to 7.2 by adding base (10 M NaOH) or acid (10M HCl). Stored in a refrigerator (4˚C).

0.2 M cacodylate buffer

- 42.8 g $C_2H_6AsNaO_2 – 3H_2O$ (Sodium-cacodylate-3-hydrate)
- 6.9 ml 1.0M HCl Hydrochloric acid

  Dissolved in distilled water into 1000 ml. pH adjusted to 7.2 by adding base (1N NaOH) or acid (1N HCl).

25% Glutaraldehyde

Finished from producer

20% Formaldehyde

Paraformaldehyde dissolved in distilled water and heated up to 80˚C. Some drops of NaOH added before cooled down and filtrated.

A.2 Agar gel

- 0.5 g Agarose

- 50 ml distilled water

Shake during heating. Embed into petri dishes and solidify in RT for 30 min. Agarose gel can be reused when it is packed in biofilm and stored in a refrigerator.

A.3 Embedding in Technovit ® 7100 (Herau Kulzer GmbH & Co, Germany)

Pre-infiltration

- 1:1 96% Ethanol and Technovit 7100

  Preinfiltration of tissue for 2 hours under gentle shaking (120/min)

Infiltration

- 100 ml Technovit 7100 with hardener I (one bag of 0.1 g Hardener 1)

  Infiltration of tissue overnight under gentle shaking (120/min)

Embedding

- 15 ml Technovit 7100
- 1 ml hardener II

  Mix thoroughly and fill up the embedding cast. Add the tissue and cover with a knob. Let it polymerize in RT. Stored in airtight bags.

A.4 Toluidine blue (Philpott, 1966)

- 2.0 g borax (sodium tetraborate decahydrate)
- 1.0 g toluidine blue
- 100 ml distilled water

Borax is dissolved in 100 ml distilled water before toluidine blue is added. The solution is filtered through a paper filter before use. Glass slides (with sections) are colored with toluidine blue for 60 seconds before excessive color is washed away with temperate water. Glass slides are air dried before cover slips was mounted. Tissues were stained depending on its concentration of polyanions. Polyanions-rich tissue (e.g cartilage matrix) were stained purple.

A.5 1 % Osmium tetroxide (Merck KGaA, Germany)

- 1 ampulla (0.1 g) osmium tetroxide OsO_4
- 10 ml distilled water

Mixed thoroughly under gentle shaking.

APPENDIX B: LARVAL DATA

Table B.1 Larval data from sampling

#	Date	Tank	Age (dph)	Stage	SL (mm)	Food	Mean ± SEM	Comments
1	09.09.2015	2	4	1	5.123	Enriched rotifers		Startfeeding
2	09.09.2015	2	4	1	5.184	Enriched rotifers		Startfeeding
3	09.09.2015	2	4	1	4.849	Enriched rotifers		Startfeeding
4	09.09.2015	2	4	1	5.122	Enriched rotifers		Startfeeding
5	09.09.2015	2	4	1	5.068	Enriched rotifers		Startfeeding
6	09.09.2015	2	4	1	5.486	Enriched rotifers		Startfeeding
7	09.09.2015	2	4	1	5.243	Enriched rotifers		Startfeeding
8	09.09.2015	2	4	1	5.232	Enriched rotifers		Startfeeding
9	09.09.2015	2	4	1	5.408	Enriched rotifers	5.19 ± 0.17	Startfeeding
10	09.09.2015	2	4	1	x	Enriched rotifers		The rest of the larva from the sample
11	09.09.2015	7	10	2	8.027	Enriched rotifers		
12	09.09.2015	7	10	2	7.954	Enriched rotifers		
13	09.09.2015	7	10	2	6.685	Enriched rotifers		
14	09.09.2015	7	10	2	6.596	Enriched rotifers		
15	09.09.2015	7	10	2	6.461	Enriched rotifers		
16	09.09.2015	7	10	2	5.194	Enriched rotifers		
17	09.09.2015	7	10	2	5.526	Enriched rotifers		
18	09.09.2015	7	10	2	5.279	Enriched rotifers		
19	09.09.2015	7	10	2	4.423	Enriched rotifers		
20	09.09.2015	7	10	2	5.069	Enriched rotifers	6,12 ± 1.16	
21	17.09.2015	2	12		4.959	Enriched rotifers		
22	17.09.2015	2	12		4.944	Enriched rotifers		
23	17.09.2015	2	12		5.497	Enriched rotifers		

24	17.09.2015	2	12		4.909	Enriched rotifers		
25	17.09.2015	2	12		6.143	Enriched rotifers		
26	17.09.2015	2	12		6.009	Enriched rotifers		
27	17.09.2015	2	12		7.502	Enriched rotifers		
28	17.09.2015	2	12		5.684	Enriched rotifers		
29	17.09.2015	2	12		7.11	Enriched rotifers		
30	17.09.2015	2	12		5.374	Enriched rotifers		
31	17.09.2015	7	18	3	6.876	Enriched rotifers		
32	17.09.2015	7	18	3	7.13	Enriched rotifers		
33	17.09.2015	7	18	3	9.263	Enriched rotifers		
34	17.09.2015	7	18	3	5.021	Enriched rotifers		
35	17.09.2015	7	18	3	6.709	Enriched rotifers		
36	17.09.2015	7	18	3	6.909	Enriched rotifers		
37	17.09.2015	7	18	3	8.171	Enriched rotifers		
38	17.09.2015	7	18	3	5.549	Enriched rotifers		
39	17.09.2015	7	18	3	8.565	Enriched rotifers		
40	17.09.2015	7	18	3	6.575	Enriched rotifers	7,07 ± 1.30	
41	28.09.2015	2	23		5.227	Enriched rotifers		
42	28.09.2015	2	23		6.285	Enriched rotifers		
43	28.09.2015	2	23		7.274	Enriched rotifers		
44	28.09.2015	2	23		6.851	Enriched rotifers		
45	28.09.2015	2	23		5.709	Enriched rotifers		
46	28.09.2015	2	23		5.776	Enriched rotifers		
47	28.09.2015	2	23		6.18	Enriched rotifers		
48	28.09.2015	2	23		6.564	Enriched rotifers		
49	28.09.2015	2	23		7.187	Enriched rotifers		
50	28.09.2015	2	23		6.385	Enriched rotifers		

51	28.09.2015	7	29	4	9.131	*Artemia*		
52	28.09.2015	7	29	4	8.34	*Artemia*		
53	28.09.2015	7	29	4	8.967	*Artemia*		
54	28.09.2015	7	29	4	10.358	*Artemia*		
55	28.09.2015	7	29	4	7.681	*Artemia*		
56	28.09.2015	7	29	4	8.373	*Artemia*		
57	28.09.2015	7	29	4	10.197	*Artemia*		
58	28.09.2015	7	29	4	8.579	*Artemia*		
59	28.09.2015	7	29	4	9.848	*Artemia*		
60	28.09.2015	7	29	4	NA	*Artemia*	9,05 ± 0.91	
61	09.11.2015	2	66		10.504	*Artemia*		Too small
62	09.11.2015	2	66		9.884	*Artemia*		Too small
63	09.11.2015	2	66		11.981	*Artemia*		Too small
64	09.11.2015	2	66		10.892	*Artemia*		Too small
65	09.11.2015	2	66		12.397	*Artemia*		Too small
66	09.11.2015	2	66		12.453	*Artemia*		Too small
67	09.11.2015	2	66		10.888	*Artemia*		Too small
68	09.11.2015	2	66		12.376	*Artemia*		Too small
69	09.11.2015	2	66		13.935	*Artemia*		Too small
70	09.11.2015	2	66		10.956	*Artemia*		Too small
71	09.11.2015	2	66		15.749	*Artemia*		OK
72	09.11.2015	2	66		14.223	*Artemia*		OK
73	09.11.2015	2	66		14.734	*Artemia*		OK
74	09.11.2015	2	66		15.043	*Artemia*		OK
75	09.11.2015	2	66		17.914	*Artemia*		OK
76	09.11.2015	2	66		17.643	*Artemia*		OK
77	09.11.2015	2	66		18.202	*Artemia*		OK
78	09.11.2015	7	71		13.626	Weaned food		Too small
79	09.11.2015	7	71		15.213	Weaned food		Too small
80	09.11.2015	7	71		13.881	Weaned food		Too small
81	09.11.2015	7	71		13.399	Weaned food		Too small
82	09.11.2015	7	71		13.176	Weaned food		Too small
83	09.11.2015	7	71		13.289	Weaned food		Too small
84	09.11.2015	7	71		12.28	Weaned food		Too small
85	09.11.2015	7	71		12.079	Weaned food		Too small
86	09.11.2015	7	71		12.146	Weaned food		Too small
87	09.11.2015	7	71		11.552	Weaned food		Too small
88	09.11.2015	7	71	5	16.566	Weaned food		OK
89	09.11.2015	7	71	5	17.522	Weaned food		OK
90	09.11.2015	7	71	5	15.311	Weaned food	16,46 ± 1.10	OK
91	15.12.2015	2	102	6	23.31	Weaned food		
92	15.12.2015	2	102	6	25.442	Weaned food		
93	15.12.2015	2	102	6	25.959	Weaned food		
94	15.12.2015	2	102	6	27.866	Weaned food		
95	15.12.2015	2	102	6	20.784	Weaned food		
96	15.12.2015	2	102	6	24.845	Weaned food		
97	15.12.2015	2	102		28.995	Weaned food		too big
98	15.12.2015	2	102		29.651	Weaned food		too big
99	15.12.2015	2	102	6	23.038	Weaned food	25.85 ± 2.90	
100	15.12.2015	2	102		29.213	Weaned food		Too big

101	15.12.2015	2	102		27.773	Weaned food		Too big
102	15.12.2015	7	108		37.241	Weaned food		Too big
103	15.12.2015	7	108		32.955	Weaned food		Too big
104	15.12.2015	7	108		39.35	Weaned food		Too big
105	15.12.2015	7	108		41.732	Weaned food		Too big

Table B.2 Standard length (SL) of larva in Imaris and scanning EM for Stages 1-6.
Standard length of larvae used in Imaris and SEM were SEM 1 are larvae where the skin and muscle have been dissected away to investigate the surface of the GI-tract. SEM 2 larvae have been cut medially to investigate the lumen of the GI tract.

Stage	Age (DPH)	SL Imaris	SL SEM 1	SL SEM 2	SL of the sample (mean ± SEM)
1	4	5.123	5.184	5.122	5.19 ± 0.17
2	10	6.027	6.461	6.596	6.12 ± 1.16
3	18	7.209	7.13	7.263	7.07 ± 1.30
4	29	9.131	8.967	10.356	9.05 ± 0.91
5	71	16.566	17.522	15.311	16.46 ± 1.10
6	102	23.31	23.038	25.422	25.85 ± 2.90

Table B.3 Size of enterocytes measured on scanning electron micrographs; Stages 1-2 and 6.

Stage	#	Height enterocytes (µm)	Width enterocytes (um)	brush border (µm)	Mean surface area ([height+brush border]*width)
1	1	17.045	2.9	1.033	52.4262
1	2	16.514	2.945	1.087	51.834945
1	3	15.423	2.665	0.934	43.591405
1	4	15.871	2.615	1.023	44.17781
1	5	14.651	3.533	0.841	54.733236
1	6	15.409	3.177	1.03	52.226703
1	7	16.707	1.563	0.996	27.669789
1	8	15.894	2.248	1.02	38.022672
1	9	16.631	3.158	0.892	55.337634
1	10	15.091	3.217	0.892	51.417311
1	**Mean**	**15.9236 ± 0.74511948**	**2.8021 ± 0.53849558**	**0.9748 ± 0.07557619**	**47.3510066**
2	1	17.27	3.168	1.555	59.6376
2	2	19.103	3.648	2.068	77.231808
2	3	17.41	2.331	1.883	44.971983
2	4	17.115	4.632	1.998	88.531416
2	5	13.645	3.143	2.041	49.301098
2	6	16.105	3.042	2.086	55.337022
2	7	19.966	2.939	2.011	64.590403
2	8	18.402	2.542	2.239	52.469422

2	9	10.937	2.43	2.071	31.60944
2	10	19.538	2.43	1.865	52.00929
2	**Mean**	**16.9491 ± 2.65842338**	**3.0305 ± 0.66598112**	**1.9817 ± 0.17394772**	**57.3697894**
6	1	20.131	4.235	0.648	87.999065
6	2	18.464	3.938	0.912	76.302688
6	3	18.549	3.331	1.041	65.25429
6	4	22.095	3.416	0.523	77.263088
6	5	22.304	3.377	0.604	77.360316
6	6	22.99	3.321	0.731	78.777441
6	7	24.14	3.037	0.8	75.74278
6	8	23.618	2.834	0.865	69.384822
6	9	25.237	1.761	0.518	45.354555
6	10	23.77	2.734	0.645	66.75061
6	**Mean**	**22.1298 ± 2.22772331**	**3.1984 ± 0.64606752**	**0.7287 ± 0.16449076**	**73.1106264**

APPENDIX C: IMARIS DATA

Table C.1 Photo information and Imaris settings (x, y and z voxel size).

Stage	Total # sections *	# sections of interest	# Sections used in AA, Imaris	Every # used in AA, Imaris	z-voxel size	Photo system	Image magnification	x- and y-voxel size
1	163	120	60	2	4	Leica M420	16x	2.00
2	293	264	88	3	6	Leica M420	12.5x	2.49
3	454	288	94	3	6	Leica M420	12.5x	2.49
4	408	408	92	4	8	Leica M420	12.5x	2.49
5	1050	768	87	9	18	Leica DMLB	10x	2.52
6	1204	1042	84	13	26	Leica DMLB	10x	3.52

** not all of the total # sections contained did not contain digestive organs, therefore not of interest.*

Table C.2 Incorrect XY voxel size in Stage 5

	Dice	**Ball**	
Area (A)	Area=$6a^2$ $A_{2.49}$=37.2006 $A_{3.52}$=74.3424	Area=$4\pi r^2$ $A_{2.49}$=77.91275445 $A_{3.52}$=155.7023585	
$A_{3.52}/A_{2.49}$	**1.99841938**	**1.99841938**	**Factor of Area (A)**
Volume (V)	Volume=a3 $V_{2.49}$=15.438249 $V_{3.52}$=43.614208	Volume=$4/3\pi r^3$ $V_{2.49}$=64.6675819 $V_{3.52}$=182.6907673	
$V_{3.52}/ V_{2.49}$	**2.825074**	**2.825074**	**Factor of Volume (V)**

Table C.3 Surface area of digestive organs (mm^2) in ballan wrasse Stages 1-6.

Developmental stage	**1**	**2**	**3**	**4**	**5**	**6**
SL (mm)	5.184	6.461	7.13	8.967	17.522	23.038
Age (DPH)	4	10	18	29	71	102
Total area	2.288602	7.6799696	9.86661018	34.9321043	233.473239	236.091646
Outer surface digestive tract	0.997549	3.71525	3.88686	12.945	56.3026682	58.4082
Esophageal lumen	0.027152	0.238787	0.152995	0.432091	3.26255953	3.64476
Intestinal lumen	0.232488	2.52926	3.10048	13.4767	102.860644	106.758
Liver	0.209993	0.664379	1.37392	5.18986	38.8101037	30.6709
Exocrine pancreas	0.156773	0.42689	1.18352	2.29243	30.497478	34.4798
Endocrine pancreas		0.0244109	0.0414182	0.136205	0.889140747	0.656696
Gallbladder	0.015763	0.0314247	0.122749	0.444797	0.634146431	1.23106
Ductus pancreaticus			0.00466798	0.0150213	0.216498764	0.24223
Yolk	0.648884	0.049568				

Table C.4 Volume of organs (mm^3) in ballan wrasse Stages 1-6.

Developmental stage	**1**	**2**	**3**	**4**	**5**	**6**
SL (mm)	5.184	6.461	7.13	8.967	17.522	23.038
DPH	4	10	18	29	71	102
Total volume	0.02436247	0.16647646	0.292322	1.19706921	15.0202114	15.5908363
Outer surface digestive tract	0.012164	0.105996	0.19616301	0.69600998	8.39685472	8.6994698
Esophageal lumen	5.9795E-05	0.00151012	0.00073336	0.00356547	0.0546762	0.0687876
Intestinal lumen	0.0006858	0.0386402	0.0282904	0.35790499	2.6346217	3.7602298
Gut tissue (surface – lumen)	0.0114183	0.06584568	0.16713925	0.33453925	5.7075568	4.8704523
Liver	0.0019509	0.0154326	0.050458	0.113282	3.10447373	2.0923000
Exocrine pancreas	0.0011018	0.00427495	0.0153312	0.0223121	0.79245586	0.9283569
Endocrine pancreas		0.00017932	0.00026612	0.00076898	0.01964709	0.0161596
Gallbladder	6.4558E-05	0.00016857	0.00107031	0.00316957	0.0137871	0.0218975
Ductus pancreaticus			9.5977E-06	5.611E-05	0.00369497	0.0036348
Yolk	0.0083354	0.0002747				

APPENDIX D: NUTRIENT COMPOSITION OF FEED AT MARINE HARVEST

Table D1 Larviva Multigain enrichment diet for rotifers and Artemia analysis.

Crude proteins	13 %
Crude lipids	44 %
Crude ash	8.50 %
Crude cellulose	2.60 %
VitC added	33 3000 mg kg^{-1}
VitE added	6 6000 mg kg^{-1}
VitA added	150 000 IU kg^{-1}
VitD3	50 000 IU kg^{-1}
E4-Cu	24 mg kg^{-1}
n-3 HUFA	11.90 %
DHA	11.10 %
EPA	0.25 %
ARA	0.06 %

Table D2 Otohime larval fish diet analysis and composition.

Analysis	**Otohime B1/B2 (B1: 250-360 um; B2: 360-650 um)**	**Otohime C1 (580-840 um)**
Moisture	6.3 %	6.3 %
Crude protein	56.3 %	58.3 %
Crude fat	15.9 %	12.9 %
Crude fiber	2.6 %	1.6 %
Crude ash	13.5 %	15.0 %
Calcium	2.5 %	2.7 %
Phosphorus	2.3 %	2.5 %

VitA	10 000 IU kg^{-1}	10 000 IU kg^{-1}
VitD3	2 000 IU kg^{-1}	2 000 IU kg^{-1}
VitE (a-tocopherol)	1 250 mg kg^{-1}	1250 mg kg^{-1}
Cu	7.0 mg kg^{-1}	7.0 mg kg^{-1}
Mn	31.8 mg kg^{-1}	31.8 mg kg^{-1}
Dioxin total count	<1 pg TEQ g^{-1}	
Composition		
Fish meal	>20%	>20 %
Krill meal	>35 %	>35 %
Squid meal	>15 %	>10 %
Wheat flour	<5 %	<5 %
Potato starch	<5 %	<5 %
Fish oil	<5 %	<5 %
Brewer's yeast	<5 %	<5 %
Vitamin and mineral premix	<5 %	<5 %
Inorganic calcium phosphate	<5 %	<5 %
Plant gum (soylecithin)	<5 %	<5 %
Guar gum	<5 %	<5 %
Betaine	<5 %	<5 %
Paracoccus bacterial cell powder	<5 %	<5 %
Cell powder	<5 %	<5 %
Calcium carbonate	<5 %	<5 %

APPENDIX E: COMPARATIVE STUDY OF SELECTED DIGESTIVE ORGANS

Table E.1 Volume of digestive organs (mm^3) and their relative volume (%) compared to the RotMG fed larvae in the study performed by Gagnat et al., (2016).

		Volume of digestive organs (mm^3)				**Mean relative volume of digestive organs (%)**					
Age (DPH)	**SL (mm)**	**Gut tissue**	**Liver**	**(exo-crine) pancreas***	**Endo-crine pancreas**	**Gut tissue**	**Liver**	**(exo-crine) Pancreas***	**Endo-crine pancreas**	**Day degree**	**Reference**
4	3.91	0.0038	0.0012	0.0006		68	21	11		48	RotMG fed larvae Gagnat et al. (2016)
8	3.90	0.0059	0.0025	0.006		66	28	7		96	RotMG fed larvae Gagnat et al. (2016)
4	5.12	0.011	0.0019	0.0011	NA	79	13	8		54	
21	5.14	0.045	0.017	0.006		66	25	9		252	RotMG fed larvae Gagnat et al. (2016)
10	6.02	0.06	0.015	0.004	0.0001	77	18	5	0.2	138	
18	7.20	0.167	0.050	0.01	0.0002	71	22	7	0.1	248	
33	8.48	0.164	0.149	0.023		49	44	7		440	RotMG fed larvae Gagnat et al. (2016)
29	9.13	0.33	0.113	0.022	0.0007	71	24	5	0.2	417	
55	12.35	0.25	0.186	0.038		53	39	8		792	RotMG fed larvae Gagnat et al. (2016)
71	16.56	5.70	3.10	0.79	0.019	59	32	8	0.2	1101	
102	23.31	4.87	2.09	0.92	0.016	62	26	12	0.2	1606	

** Gagnat et al., 2016 did not differentiate between exocrine and endocrine pancreas.*

Table E.2 Correlation coefficient (R^2) between volume of different digestive organs compared to the SL of the present study compared to RotMG fed larvae by Gagnat et al. (2016).

Volume of tissue related to SL	**R^2**	**Rerefence**
Gut tissue	0.9904	RotMG fed larvae Gagnat et al. (2016)
Gut tissue	0.8276	
Liver	0.9402	RotMG fed larvae Gagnat et al. (2016)
Liver	0.7148	
Pancreas	0.9963	RotMG fed larvae Gagnat et al. (2016)
Exocrine pancreas	0.9298	
Endocrine pancreas	0.8083	

Figure E.1 Total volume of digestive organs (mm^3) compared to the SL (mm) between the present study and RotMG fed larvae by Gagnat et al. (2016).